



Taxonomy, phylogeny and divergence times of *Polyporus* (Basidiomycota) and related genera

Ji X^{1,#}, Zhou JL^{1,3,#}, Song CG¹, Xu TM¹, Wu DM^{2,*} and Cui BK^{1,*}

¹Institute of Microbiology, School of Ecology and Nature Conservation, Beijing Forestry University, Beijing 100083, China

²Biotechnology Research Institute, Xinjiang Academy of Agricultural and Reclamation Sciences / Xinjiang Production and Construction Group Key Laboratory of Crop Germplasm Enhancement and Gene Resources Utilization, Shihezi, Xinjiang 832000, China

³International Exchange and Cooperation Department, Kunming University, Kunming, Yunnan 650214, China

Ji X, Zhou JL, Song CG, Xu TM, Wu DM, Cui BK 2022 – Taxonomy, phylogeny and divergence times of *Polyporus* (Basidiomycota) and related genera. *Mycosphere* 13(1), 1–52, Doi 10.5943/mycosphe/13/1/1

Abstract

Polyporus is a taxonomically controversial genus which includes species belonging to six infrageneric groups. Recently, many species of *Polyporus* have been transferred into other related genera viz. *Cerioporus*, *Favolus*, *Lentinus*, *Neofavolus* and *Picipes* based on the phylogenetic and morphological analyses. To ascertain the relationships of *Polyporus* and its allied genera, eight DNA fragments viz. the internal transcribed spacers 1 and 2 with the 5.8S rDNA (ITS), the nuclear ribosomal large subunit (nLSU), partial translation elongation factor 1- α gene (EF1- α), the mitochondrial small-subunit (mtSSU), the β -tubulin gene (TUB), the gene for RNA polymerase II largest subunit (RPB1), the gene for RNA polymerase II second largest subunit (RPB2) and the nuclear ribosomal small subunit (nSSU), are used in the molecular systematic studies. Phylogenetic analyses were carried out based on two combined datasets (ITS+nLSU) and (ITS+nLSU+EF1- α +mtSSU+RPB1+RPB2+nSSU+TUB), and the results indicated that species of *Polyporus* and its related genera fell into six well supported clades: the picipes clade, the favolus clade, the neofavolus clade, the lentinus clade, the core polyporus clade and the squamosus clade. Moreover, the conserved regions of six DNA fragments (5.8S, nLSU, EF1- α , RPB1, RPB2 and nSSU) were used to analyze the divergence times and evolutionary relationships of *Polyporus* and its related genera by using BEAST v1.8. Bayesian evolutionary analysis revealed that the ancestor of Polyporales split at about 141.81 Mya, while the mean stem ages of the six major clades of *Polyporus* and its allied genera were 49–63 Mya. Based on the combined analyses of morphology, phylogenies and divergence times, species in the picipes clade formed the genus *Picipes* by the coriaceous (fresh) to hard (dry) basidiomata and strongly branched skeleto-binding hyphae; species nested in the favolus clade and the neofavolus clade were separately treated as two distinct genera *Favolus* and *Neofavolus*; the polyporoid species in the lentinus clade with central and light-colored stipe and inflated hyphae were transferred into *Lentinus*, and the core polyporus clade was treated as *Polyporus* s. str. The squamosus clade contained species belonging to several different genera viz. *Datronia*, *Datroniella*, *Echinochaete*, *Mycobonia*, *Neodatronia*, *Polyporus* s. lat. and *Pseudofavolus*, but there are no enough efficient morphological evidence to combine all species in the squamosus

Submitted 16 November 2021, Accepted 21 January 2022, Published 26 January 2022

These two authors contributed equally to this work and shared the first author

Corresponding Author: Dong-Mei Wu – e-mail – wdm0999123@sina.com,

Bao-Kai Cui – e-mail – cuibaikai@bjfu.edu.cn

clade into a specific genus. In addition, three new species of *Polyporus* and seven new species of *Picipes* are described and illustrated.

Key words – molecular clock – morphology – multi-gene phylogenies – new species – Polyporaceae

Introduction

Polyporus P. Micheli ex Adans. was firstly used by Micheli (1729) to define 14 polypores with pore layers can hardly be peeled off from the context. But the name was invalid until Adanson (1763) restored Micheli's concept. Linnaeus (1753) treated *Polyporus* as a synonym of *Boletus* L., while Fries (1821) accommodated most polyporoid species into *Polyporus*. After that, many mycologists revised the definition of *Polyporus*, and the definition provided by Gilbertson & Ryvarden (1987) was widely accepted. They characterized *Polyporus* by the features of annual stipitate basidiomata, a dimitic hyphal system with generative hyphae and skeleto-binding hyphae, hyaline, thin-walled, and cylindric basidiospores, and causing white rot.

Most *Polyporus* species grow on different kinds of dead woods, especially on dead hardwoods. But several species can also grow on living hardwoods or other substrates, for examples, *P. squamosus* (Huds.) Fr. always grows on living hardwoods and causes stem rot (Schwarze et al. 2000), *P. rhizophilus* Pat. grows with the grass roots, *P. umbellatus* (Pers.) Fr. only rises on the ground from sclerotia, and *P. phyllostachydis* Sotome, T. Hatt. & Kakish. is limited to bamboo roots (Ryvarden & Gilbertson 1994, Núñez & Ryvarden 1995a, Sotome et al. 2007, Sotome et al. 2008). Several species of *Polyporus* are known as medicinal fungi (Dai et al. 2009), and the most famous one is *P. umbellatus*.

Because Micheli (1729) initially did not select the type species of *Polyporus*, there is no consensus on the type selection. Murrill (1903, 1904) first selected *P. ulmi* Paulet, which is the synonym of *P. squamosus*, as the nomenclatorial type of *Polyporus*, but it was rejected by others according to the "First Species Rule" (Krüger & Gargas 2004). The first acceptable type for *Polyporus* is *P. brumalis* (Pers.) Fr., proposed by Clements & Shear (1931) who argued that the best known or important one should be selected as the correct lectotype. This selection was supported by Krüger & Gargas (2004), but, this lectotypification was refused by Donk (1933) and ICBN (Greuter et al. 2000) because it was not identified by Micheli. In addition, *P. arcularius* (Batsch) Fr. is another candidate which is supported by Cunningham (1948). Since Donk (1933) chosen *P. tuberaster* (Jacq. ex Pers.) Fr. as the type species, this lectotype has been followed by most succeeding researchers (Cunningham 1965, Singer 1986, Niemelä & Kotiranta 1991, Ryvarden 1991, Núñez & Ryvarden 1995a, Sotome et al. 2008, Dai et al. 2014, Zhou et al. 2016a).

Polyporus is a widespread genus that includes many species belonging to six morphological groups, *Polyporus* group, *Favolus* group (= *Favolus* Fr.), *Melanopus* group (= *Melanopus* Pat.), *Polyporellus* group (= *Polyporellus* Karst.), *Admirabilis* group and *Dendropolyporus* group (= *Dendropolyporus* (Pouz.) Jülich) described by Núñez & Ryvarden (1995a). According to the morphological analyses, 32 species were divided into those groups, although several of them had been removed and many other species were added (Dai 1996, 1999, Buchanan & Ryvarden 1998, Popoff & Wright 1998, Hattori 2000, Thorn 2000, Dai et al. 2003, 2007, 2009, 2014, Ryvarden & Iturriaga 2003, Zheng & Liu 2005, Sotome et al. 2007, 2013, 2016, Drechsler-Santos et al. 2008, Xue & Zhou 2012, 2014, Hyde et al. 2016, Runnel & Ryvarden 2016, Zhou et al. 2016a, Palacio et al. 2017, Tibpromma et al. 2017, Zhou & Cui 2017, Zmitrovich et al. 2017, Cui et al. 2019, Xing et al. 2020).

Phylogenetically, *Polyporus* was proved to be a polyphyletic genus according to the mtSSU analysis (Ko & Jung 2002), and this attitude has been demonstrated by others (Krüger & Gargas 2004, Krüger et al. 2006, Sotome et al. 2008, Dai et al. 2014, Zmitrovich & Kovalenko 2016, Zhou et al. 2016a, Tibpromma et al. 2017). The phylogenetic analyses of basidiomycetes revealed that *Polyporus* clusters in the core polyporoid clade with *Echinochaete* Reid, *Pseudofavolus* Pat., *Datronia* Donk, *Lentinus* Fr., *Dichomitus* D.A. Reid and several other genera (Binder et al. 2005,

2013, Garcia-Sandoval et al. 2011, Tibpromma et al. 2017). Based on molecular analyses, *Polyporus* was mainly divided into six major clades, but these clades did not conform to the six morphological groups (Sotome et al. 2008, Zhou et al. 2016a). Species of *Polyporellus* always clusters with *Lentinus* (Krüger & Gargas 2004, Sotome et al. 2008, Binder et al. 2013, Dai et al. 2014, Seelan et al. 2015, Tibpromma et al. 2017), while several species of *Polyporus* and *Melanopus* always gather together with *Datronia*, *Echinochaete*, *Mycobonia* Pat. and *Pseudofavolus* (Krüger & Gargas 2004, Sotome et al. 2008, Binder et al. 2013). When studying group *Favolus*, species of this group were divided into two genera viz. *Neofavolus* Sotome & T. Hatt. typified by *N. alveolaris* (DC.) Sotome & T. Hatt. and *Favolus* typified by *F. brasiliensis* (Fr.) Fr. (Sotome et al. 2013). Based on multi-gene phylogenetic analyses, species in *Melanopus* were proved to be distributed in two different clades viz. picipes clade and squamosus clade (Zhou et al. 2016a). The picipes clade has been described as *Picipes* Zmitr. et Kovalenko (Zmitrovich & Kovalenko 2016), and sixteen species with hard basidiomata in dried condition, brownish to black stipes and strongly branched skeleto-binding hyphae were included in this genus (Zhou et al. 2016a). While the *Polyporus* and *Datronia* species in the squamosus clade were combined into *Ceriporus* Qué. by Zmitrovich & Kovalenko (2016). Moreover, species of *Polyporellus* were recently treated as members of *Lentinus* (Krüger 2002, Seelan et al. 2015, Zhou et al. 2016a, Zmitrovich & Kovalenko 2016). Although the above opinions have been phylogenetically supported, species in the squamosus clade and the lentinus clade are morphologically diversified. More valuable information to confirm the above taxonomic researches are needed.

To recognize different taxonomic ranks, Hennig (1966) proposed the divergence time that can be used as a universally standardized criterion in the systematics of all known organisms. This conception was firstly used in the study of fishes, anthropoid primates and fruit flies at the end of 20th century (Avice & John 1999). For fungi, Zhao et al. (2017) confirmed that the mean stem ages of Basidiomycota and Entorrhizomycota are ca. 530 million years ago (Mya), subphyla of Basidiomycota are 406–490Mya, while the most classes and orders of Agaricomycotina are separately about 358–393Mya and 120–290Mya.

Nowadays, as more fungal fossil specimens being found and DNA fragments being used in analyzing the relationships between different fungal groups, molecular divergence time analyzing has been widely used in estimating evolutionary times of different fungi, for example, mycorrhizal fungi (Hibbett & Matheny 2009, Kohler et al. 2015), white and brown rot lineages (Eastwood et al. 2011, Garcia-Sandoval et al. 2011), porcino (Feng et al. 2012), amanitas (Cai et al. 2014, Sánchez-Ramírez et al. 2014), *Heterobasidion* Bref. (Chen et al. 2015), Caliciaceae Chevall. (Prieto & Wedin 2017), *Bondarzewia* Singer (Song et al. 2016), *Agaricus* L. (Zhao et al. 2016), *Laetiporus* Murrill (Song & Cui 2017), Basidiomycota (Zhao et al. 2017) and *Sanghuangporus* Sheng H. Wu, L.W. Zhou, and Y.C. Dai (Zhou et al. 2019). However, there is no study focused on the evolutionary times of *Polyporus* and its allied genera.

In the present study, we investigated the taxonomy and phylogeny of *Polyporus* and related genera (including *Favolus*, *Lentinus*, *Neofavolus* and *Picipes*). Six DNA fragments viz. the 5.8S, nLSU, EF1- α , RPB1, RPB2 and nSSU, were used to estimate the evolutionary time of *Polyporus* and its related genera. Besides the above genes, ITS, mtSSU and TUB were also used in the phylogenetic analyses. Multigene phylogenetic analyses of ITS+nLSU and ITS+nLSU+EF1- α +mtSSU+RPB1+RPB2+nSSU+TUB were provided to reveal the phylogenetic relationships between *Polyporus* and its allied genera.

Materials & Methods

Morphological studies

All specimens tested in this study are deposited in the herbaria of the Institute of Microbiology, Beijing Forestry University (BJFC, Beijing, China) and the Institute of Applied Ecology, Chinese Academy of Sciences (IFP, Shenyang, China). Macro-morphological characteristics were described based on the field notes and the herbarium specimens. Color

descriptions were based on Petersen (1996). Micro-morphological features were obtained from dried specimens under light microscopes, the proceedings were followed previous studies (Zhou et al. 2016a, b, Zhou & Cui 2017). Free-hand sections were observed and measured in 5% potassium hydroxide solution after staining with 1% Congo Red solution. Cotton Blue and Melzer's reagents were respectively used to examine whether the tissues have cyanophilous and amyloid reactions or not. All the microscopic characteristics were inspected and photographed at a magnification of up to $\times 1000$ by Nikon Eclipse Ni microscope (Nikon Corporation, Tokyo, Japan). All the sizes of basidiospores, basidia, cystidioles and hyphae were measured using the Image-Pro Plus 6.0 software (Media Cybernetics, Silver Spring, USA). To represent variation in the size, no less than 30 basidiospores were measured from each specimen. The following abbreviations were used in this study: IKI- = neither amyloid nor dextrinoid, KOH = 5 % potassium hydroxide, CB = Cotton Blue, CB+ = cyanophilous, CB- = acyanophilous, L = mean spore length \pm standard deviation, W = mean spore width \pm standard deviation, Q = variation in the L/W ratios between the specimens studied, Qm = mean L/W ratio \pm standard deviation, n (a/b) = number of spores (a) measured from given number (b) of specimens.

DNA extraction and amplification

Total DNA were extracted from dried specimens using CTAB rapid plant genome extraction kit-DN14 (Aidlab Biotechnologies Co., Ltd., Beijing, China) and FH plant DNA kit II (Demeter Biotech Co., Ltd., Beijing, China) according to the manufacturer's procedures. The primer pair ITS4 and ITS5 (White et al. 1990) was used to amplified ITS regions while LR0R/LR7 (Vilgalys & Hester 1990), EF1-983F/EF1-1567R (Rehner & Buckley 2005), Bt-1a/Bt-1b (Glass & Donaldson 1995), PNS1/NS41 (Hibbett 1996), MS1/MS2 (White et al. 1990), RPB1-Af/RPB1-Cr (Matheny et al. 2002) and fRPB2-5F/bRPB2-7.1R (Liu et al. 1999, Matheny 2005) were used to amplified nLSU, EF1- α , TUB, nSSU, mtSSU, RPB1 and RPB2 regions, respectively. The primers RPB1-2.2f (Binder et al. 2010) and bRPB2-6F (Matheny 2005) sometimes were separately used as alternatives to RPB1-Af and fRPB2-5F. 50 μ l PCR volume with 2×1.5 μ l primers (10 pM), 2 μ l DNA extract, 20 μ l ddH₂O and 25 μ l $2 \times$ EasyTaq PCR Supermix (TransGen Biotech Co., Ltd., Beijing, China) was used each tube. All the polymerase chain reactions (PCRs) were performed on S1000TM Thermal Cycler (Bio-Rad Laboratories, California, USA). The PCR procedures for different genes were as Zhou et al. (2016a):

a) PCR conditions for mtSSU, ITS, nSSU, TUB and EF1- α were (i) 2 min initial denaturation at 94°C, (ii) 36 cycles of 45 s denaturation at 94°C, 45 s annealing at 52°C (for mtSSU)/53°C (for ITS, nSSU and TUB)/54°C (for EF1- α) and 1 min extension at 72°C, (iii) 10 min final extension at 72°C.

b) PCR condition for nLSU was (i) 5 min initial denaturation at 94°C, (ii) 36 cycles of 1 min denaturation at 94°C, 1min 20 s annealing at 50°C and 1 min 30 s extension at 72°C, (iii) 10 min final extension at 72°C.

c) PCR condition for RPB1 and RPB2 was (i) 2 min initial denaturation 94°C, (ii) 9 cycles of 45 s denaturation at 94°C, 45 s (minus 1°C per cycle) annealing at 60°C and 1min 30 s extension at 72°C, (iii) 36 cycles of 45 s denaturation at 94°C, 1 min annealing at 53°C and 90 s extension at 72°C for, (iv) 10 min final extension at 72°C.

All PCR products were directly purified and sequenced in the Beijing Genomics Institute (BGI), China, with the same primers. Newly generated sequences were submitted to GenBank and listed in Table 1.

Divergence time estimation of *Polyporus* and related genera

Two fossil calibrations, *Archaeomarasmius leggetti* Hibbett, D. Grimaldi & Donoghue and *Quatsinoporites cranhamii* S.Y. Sm., Currah & Stockey, were used in the divergence time estimating. *Archaeomarasmius leggetti*, an agaricoid fungus dated to 94–90 Mya (Hibbett et al. 1997), was treated as the representative of the minimum age of Agaricales. While the other fossil,

Q. cranhamii, was considered to be the minimum divergence time of Hymenochaetales at 113 Mya (Smith et al. 2004).

Table 1 Names, voucher codes, locations and corresponding GenBank accession numbers of the taxa used in this study.

Species	Specimen No.	Country	GenBank accession No.							
			ITS	nLSU	EF1- α	mtSSU	TUB	RPB1	RPB2	nSSU
<i>Agaricus campestris</i>	LAPAG370	–	KM657927	KR006607	KR006636	–	–	–	KT951556	–
<i>Amylocorticium cebennense</i>	CFMR:HHB-2808	USA	GU187505	GU187561	GU187675	–	–	GU187439	GU187770	GU187612
<i>Antrodia tanakae</i>	Cui 9743	China	KR605814	KR605753	KR610743	–	–	–	KR610833	KR605914
<i>Aphanobasidium pseudotsugae</i>	CFMR:HHB-822	USA	GU187509	GU187567	GU187695	–	–	GU187455	GU187781	GU187620
<i>Athelia epiphylla</i>	CFMR:FP-100564	USA	GU187501	GU187558	GU187676	–	–	GU187440	GU187771	GU187613
<i>Boletopsis leucomelaena</i>	AFTOL-ID 1527	USA	DQ484064	DQ154112	GU187763	–	–	GU187494	GU187820	DQ435797
<i>Boletus edulis</i>	HMJAU4637	–	JN563894	KF112455	KF112202	–	–	KF112586	KF112704	–
<i>Bondarzewia</i> sp.	Yu 56	China	KT693203	KT693205	KX066148	–	–	KX066158	KX066165	–
<i>Callistosporium graminicolor</i>	AFTOL-ID 978	USA	DQ484065	AY745702	GU187761	–	–	GU187493	KJ424369	AY752974
<i>Clavulicium macounii</i>	GB:KHL12129	Sweden	KC203494	KC203494	KC203514	–	–	–	–	KC203494
<i>Coriolopsis trogii</i>	RLG4286sp	USA	JN164993	JN164808	JN164898	–	–	JN164820	JN164867	–
<i>Cotylidia</i> sp.	MB5	–	AY854079	AY629317	AY885148	–	–	AY864868	AY883422	AY705958
<i>Daedalea modesta</i>	Cui 10151	China	KP171205	KP171227	KR610716	–	–	–	KR610806	KR605883
<i>Daedaleopsis septentrionalis</i>	H6035	Finland	HG973499	HG973499	HG973507	–	–	–	HG973516	–
<i>Datronia mollis</i>	RLG6304sp	USA	JN165002	JN164791	JN164901	–	–	JN164818	JN164872	–
<i>Datronia stereoides</i>	Holonen	Finland	KC415179	KC415196	–	–	–	–	–	–
<i>Datroniella scutellata</i>	RLG9584T	USA	JN165004	JN164792	JN164902	–	–	JN164817	JN164873	–
<i>Datroniella tropica</i>	Dai 13147	China	KC415181	KC415189	–	–	–	–	KC477838	–
<i>Echinochaete brachypora</i>	TFM:F 24996	Japan	AB462321	AB462309	–	–	–	–	–	–
<i>Echinochaete ruficeps</i>	TFM:F 15716	Japan	AB462310	AB368065	–	–	–	–	AB368123	–
<i>Echinochaete russiceps</i>	TFM:F 24250	Japan	AB462313	AB462301	–	–	–	–	–	–
<i>Favolus acervatus</i>	Cui 11053	China	KU189774	KU189805	KU189920	KU189956	KU189864	KU189889	KU189994	KU189835
<i>Favolus acervatus</i>	Dai 10749b	China	KX548953	KX548979	KX549043	KX549018	KX549033	KX549065	KX549073	KX549000
<i>Favolus philippinensis</i>	Cui 10941	China	KX548976	KX548998	KX549062	KX549032	KX549042	–	–	KX549016

Table 1 Continued.

Species	Specimen No.	Country	GenBank accession No.							
			ITS	nLSU	EF1- α	mtSSU	TUB	RPB1	RPB2	nSSU
<i>Favolus philippinensis</i>	Dai 7959	China	KX548977	KX548999	KX549063	–	–	–	–	KX549017
<i>Favolus brasiliensis</i>	INPA241452	Brazil	AB735953	AB735977	–	–	–	–	–	–
<i>Favolus emerici</i>	Cui 10926	China	KU189776	KU189807	KU189922	–	KU189866	KU189890	KU189995	KU189837
<i>Favolus emerici</i>	Yuan 4410	China	KX548954	KX548980	KX549044	–	KX549034	KX549066	–	KX549001
<i>Favolus niveus</i>	Cui 11129	China	KX548955	KX548981	KX549045	KX549019	KX549035	KX549067	KX549074	KX549002
<i>Favolus niveus</i>	Dai 13276	China	KX548956	KX548982	KX549046	KX549020	KX549036	KX549068	–	KX549003
<i>Favolus pseudobetulinus</i>	TFMF27567	Japan	AB587644	AB587639	–	–	–	–	–	–
<i>Favolus pseudobetulinus</i>	TRTC:51022	Canada	AB587629	AB587620	–	–	–	–	–	–
<i>Favolus pseudoemerici</i>	Cui 11079	China	KX548958	KX548984	KX549048	KX549022	KX549037	KX549069	KX549075	KX549004
<i>Favolus pseudoemerici</i>	Cui 13757	China	KX548959	KX548985	KX549049	KX549023	–	–	–	KX549005
<i>Favolus roseus</i>	TFM:F 20589	Malaysia	AB735975	AB368099	–	–	–	–	AB368156	–
<i>Favolus septatum</i>	Zhou 287	China	KX548968	–	KX549054	KX549024	–	–	–	KX549008
<i>Favolus spathulatus</i>	Cui 8290	China	KX548969	KX548991	KX549055	KX549025	KX549038	–	–	KX549009
<i>Favolus spathulatus</i>	Dai 13615A	China	KU189775	KU189806	KU189921	KU189957	KU189865	–	–	KU189836
<i>Favolus gracilisporus</i>	Cui 4292	China	KX548970	KX548992	KX549056	KX549026	–	–	–	KX549010
<i>Favolus gracilisporus</i>	Li 1938	China	KX548971	KX548993	KX549057	KX549027	KX549039	KX549070	KX549076	KX549011
<i>Favolus</i> sp.	MEL 2382969	Australia	KP012829	KP012829	–	–	–	–	–	–
<i>Fomitopsis pinicola</i>	AFTOL-ID 770	–	AY854083	AY684164	AY885152	–	–	AY864874	AY786056	AY705967
<i>Ganoderma lingzhi</i>	Dai 12574	China	KJ143908	–	JX029977	–	–	JX029985	JX029981	–
<i>Ganoderma tsugae</i>	AFTOL-ID 771	–	DQ206985	AY684163	DQ059048	–	–	–	DQ408116	AY705969
<i>Geastrum recolligens</i>	OSC41996	–	–	DQ218486	DQ219230	–	–	–	DQ219052	–
<i>Gloeophyllum sepiarium</i>	Wilcox-3BB	USA	HM536091	HM536061	HM536110	–	–	–	HM536109	HM536062
<i>Grifola frondosa</i>	AFTOL-ID 701	–	AY854084	AY629318	AY885153	–	–	AY864876	AY786057	AY705960
<i>Grifola sordulenta</i>	AFTOL-ID 562	–	AY854085	AY645050	AY885154	–	–	AY864877	AY786058	AY665780
<i>Hexagonia glabra</i>	Dai 10691	China	JX569733	JX569750	–	–	–	–	KF274649	–
<i>Hexagonia tenuis</i>	Cui 8468	China	JX559277	JX559302	–	–	–	–	JX559311	–
<i>Hydnochaete duportii</i>	AFTOL-ID 666	–	DQ404386	AY635770	DQ435793	–	–	–	–	AY662669
<i>Hyphoderma praetermissum</i>	AFTOL-ID 518	–	AY854081	AY700185	AY885150	–	–	AY864871	AY787221	AY707094
<i>Jaapia argillacea</i>	CBS:252.74	Netherlands	GU187524	GU187581	GU187711	–	–	–	GU187788	–
<i>Lactarius deceptivus</i>	AFTOL-ID 682	USA	AY854089	AY631899	AY885158	–	–	AY864883	AY803749	AY707093
<i>Lentinus arcularius</i>	Cui 10998	China	KX548973	KX548995	KX549059	KX549029	–	KX549071	KX549077	KX549013
<i>Lentinus arcularius</i>	Cui 11398	China	KU189766	KU189797	KU189911	KU189947	–	KU189884	KU189980	KU189826

Table 1 Continued.

Species	Specimen No.	Country	GenBank accession No.								
			ITS	nLSU	EF1- α	mtSSU	TUB	RPB1	RPB2	nSSU	
<i>Lentinus badius</i>	JS0094	Malaysia	KP283478	KP283512	–	–	–	–	KP325691	–	–
<i>Lentinus brumalis</i>	Cui 7188	China	KX851591	KX851646	KX851771	–	–	KX851575	KX851747	KX851758	KX851723
<i>Lentinus brumalis</i>	Cui 10750	China	KU189765	KU189796	KU189910	–	–	KU189857	KU189883	KU189979	KU189825
<i>Lentinus crinitus</i>	DSH92N43C	Costa Rica	KP283495	KP283523	–	–	–	–	KP325687	–	–
<i>Lentinus flexipes</i>	TENN56491	USA	AF516553	AJ488115	–	–	–	–	–	–	–
<i>Lentinus flexipes</i>	TENN56503	USA	AB478884	AB368100	–	–	–	–	–	–	–
<i>Lentinus longiporus</i>	DAOM:229479	Canada	AB478880	LC052217	–	–	–	–	–	–	–
<i>Lentinus longiporus</i>	WD2579	Japan	AB478879	LC052218	–	–	–	–	–	–	–
<i>Lentinus polychrous</i>	KM141387	Thailand	KP283487	KP283514	–	–	–	–	–	–	–
<i>Lentinus sajor-caju</i>	JS0056	Malaysia	KP283494	KP283511	–	–	–	–	KP325679	–	–
<i>Lentinus squarrosulus</i>	BORH0009	Malaysia	KP283484	KP283515	–	–	–	–	KP325681	–	–
<i>Lentinus substrictus</i>	Wei 1582	China	KU189767	KU189798	KU189912	KU189948	KU189858	–	–	KU189981	KU189827
<i>Lentinus substrictus</i>	Wei 1600	China	KC572022	KC572059	–	–	–	–	–	–	–
<i>Lentinus thailandensis</i>	Dai 6722	China	KX851590	KX851645	KX851770	KX851698	–	–	–	KX851757	KX851722
<i>Lentinus thailandensis</i>	MSUT_6734	Thailand	LC052221	LC052219	–	–	–	–	–	–	–
<i>Lentinus tigrinus</i>	MUCL22821	Belgium	AB478881	AB368072	–	–	–	–	–	AB368130	–
<i>Leptosporomyces raunkiaeri</i>	CFMR:HHB-7628	USA	GU187528	GU187588	GU187719	–	–	–	GU187471	GU187791	GU187640
<i>Lignosus rhinocerotis</i>	PEN94	Malaysia	JQ409359	AB368074	–	–	–	–	–	AB368132	–
<i>Microporus affinis</i>	Cui 7714	China	JX569739	JX569746	–	–	–	–	–	KF274661	–
<i>Microporus flabelliformis</i>	Dai 11574	China	JX569740	JX569747	–	–	–	–	–	KF274662	–
<i>Microporus vernicipes</i>	KUC20130711-23	South Korea	KJ668503	KJ668355	–	–	–	–	–	–	–
<i>Microporus xanthopus</i>	Cui 8284	China	JX290074	JX290071	–	–	–	–	–	JX559313	–
<i>Mycobonia flava</i>	CuTENN10256	Costa Rica	AY513570	AJ487934	–	–	–	–	–	–	–
<i>Mycobonia flava</i>	TENN59088	Argentina	AY513571	AJ487933	–	–	–	–	–	–	–
<i>Neodatronia gaoligongensis</i>	Cui 8055	China	JX559269	JX559286	–	–	–	–	–	JX559317	–
<i>Neodatronia sinensis</i>	Dai 11921	China	JX559272	JX559283	–	–	–	–	–	JX559320	–
<i>Neofavolus alveolaris</i>	Cui 9900	China	KX548974	KX548996	KX549060	KX549030	KX549040	KX549072	KX549078	KX549014	–
<i>Neofavolus alveolaris</i>	Dai 11290	China	KU189768	KU189799	KU189913	KU189949	KU189859	KU189885	KU189982	KU189828	–
<i>Neofavolus americanus</i>	Dai 12761	USA	KX900072	KX900186	–	–	–	–	–	–	–

Table 1 Continued.

Species	Specimen No.	Country	GenBank accession No.							
			ITS	nLSU	EF1- α	mtSSU	TUB	RPB1	RPB2	nSSU
<i>Neofavolus cremeoalbidus</i>	Cui 12412	China	KX899982	KX900109	KX900330	KX900201	–	–	–	KX900259
<i>Neofavolus cremeoalbidus</i>	TUMH:50009	Japan	AB735980	AB735957	–	–	–	–	–	–
<i>Neofavolus mikawai</i>	Cui 11152	China	KU189773	KU189804	KU189919	KU189955	KU189863	KU189888	KU189986	KU189834
<i>Neofavolus mikawai</i>	Dai 12361	China	KX548975	KX548997	KX549061	KX549031	KX549041	–	KX549079	KX549015
<i>Neofavolus squamatus</i>	Cui 12175	China	KX900070	KX900184	KX900370	KX900250	KX899942	–	KX900317	KX900295
<i>Neofavolus suavissimus</i>	DSH2011	USA	KP283496	KP283525	–	–	–	KP325693	–	–
<i>Neofavolus suavissimus</i>	LE202237	USA	KM411460	KM411476	KM411491	–	–	–	–	–
<i>Neofavolus</i> sp.	MA672	USA	KP283506	KP283524	–	–	–	KP325696	–	–
<i>Neolentinus adhaerens</i>	DAOM 214911	–	HM536096	HM536071	HM536117	–	–	–	HM536116	HM536072
<i>Panus lecomtei</i>	HHB-11042-Sp	USA	KP135328	KP135233	–	–	–	KP134877	KP134970	–
<i>Phanerochaete chrysosporium</i>	HHB-6251-Sp	USA	KP135094	KP135246	–	–	–	KP134842	KP134954	–
<i>Picipes ailaoshanensis</i>	Cui 12578	China	KX900067	KX900182	KX900368	–	–	–	KX900315	KX900293
<i>Picipes ailaoshanensis</i>	Cui 12585	China	KX900068	KX900183	KX900369	KX900248	–	–	KX900316	KX900294
<i>Picipes americanus</i>	JV 0509-149	USA	KC572002	KC572041	–	–	–	–	–	–
<i>Picipes americanus</i>	JV 0809-104	USA	KC572003	KC572042	–	–	–	–	–	–
<i>Picipes annularius</i>	Cui 10123	China	KX900060	KX900176	KX900363	–	–	–	–	KX900286
<i>Picipes atratus</i>	Cui 11289	China	KX900043	KX900159	–	–	KX899935	KX900384	KX900307	KX900271
<i>Picipes atratus</i>	Dai 13375	China	KX900042	KX900158	–	KX900227	–	KX900383	–	KX900270
<i>Picipes auriculatus</i>	Cui 13616	China	KX900063	KX900179	–	KX900245	–	–	–	KX900289
<i>Picipes auriculatus</i>	Yuan 4221	China	KX900064	KX900180	KX900366	KX900246	–	–	–	KX900290
<i>Picipess austroandinus</i>	MR10472	Argentina	AF516568	AF516568	–	–	–	–	–	–
<i>Picipess austroandinus</i>	MR10701	Argentina	AF516569	AF516569	–	–	–	–	–	–
<i>Picipes badius</i>	Cui 10853	China	KU189780	KU189811	KU189929	KX900198	KU189871	KU189894	KU189894	KU189844
<i>Picipes badius</i>	Cui 11136	China	KU189781	KU189812	KU189930	KU189964	KU189872	KU189895	KU189990	KU189845
<i>Picipes baishanzuensis</i>	Cui 11395	China	KU189763	KU189794	KU189908	KU189946	KU189856	–	KU189978	KU189824
<i>Picipes baishanzuensis</i>	Dai 13418	China	KU189762	KU189793	KU189907	KU189945	KU189855	KU189882	KU189977	KU189823
<i>Picipes brevistipitatus</i>	Cui 11345	China	KX900074	KX900188	KX905085	KX900237	–	–	–	KX900280
<i>Picipes brevistipitatus</i>	Cui 13652	China	KX900075	KX900189	KX905086	KX900238	–	–	–	KX900281
<i>Picipes conifericola</i>	Cui 9950	China	KU189783	KU189814	KU189934	KU189968	KU189875	KU189897	KU189993	KU189848
<i>Picipes conifericola</i>	Dai 11114	China	JX473244	KC572061	KU189935	KU189969	–	–	–	KU189849

Table 1 Continued.

Species	Specimen No.	Country	GenBank accession No.							
			ITS	nLSU	EF1- α	mtSSU	TUB	RPB1	RPB2	nSSU
<i>Picipes cf. dictyopus</i>	Cui 11109	China	KX900025	KX900145	KX900347	KX900220	KX899934	KX900380	KX900303	KX900267
<i>Picipes cf. dictyopus</i>	Cui 11092	China	KX900026	KX900146	KX900348	KX900221	–	KX900381	KX900304	KX900268
<i>Picipes dictyopus</i>	TENN 59385	Belize	AF516561	AJ487945	–	–	–	–	–	–
<i>Picipes fraxinicola</i>	Dai 2494	China	KC572023	KC572062	KU189932	KU189966	–	–	–	–
<i>Picipes fraxinicola</i>	Wei 6025	China	KC572024	KC572063	–	–	–	–	–	–
<i>Picipes melanopus</i>	H 6003449	Finland	JQ964422	KC572064	–	–	–	–	–	–
<i>Picipes melanopus</i>	MJ 372-93	Czech	KC572026	KC572065	–	–	–	–	–	–
<i>Picipes pumilus</i>	Cui 5464	China	KX851628	KX851682	KX851785	KX851710	KX851581	KX851753	KX851765	KX851735
<i>Picipes pumilus</i>	Dai 6705	China	KX851630	KX851684	KX851787	KX851711	–	–	–	KX851737
<i>Picipes rhizophilus</i>	Dai 11599	China	KC572028	KC572067	KU189933	KU189967	KU189874	KU189896	KU189992	KU189847
<i>Picipes rhizophilus</i>	Dai 16082	China	KX851634	KX851687	KX851788	KX851713	–	–	–	KX851738
<i>Picipes nigromarginatus</i>	Cui 8113	China	KX900062	KX900178	KX900365	KX900244	–	–	–	KX900288
<i>Picipes subdictyopus</i>	Cui 11220	China	KX900057	KX900173	KX900360	KX900240	–	KX900390	KX900314	KX900283
<i>Picipes subdictyopus</i>	Cui 12539	China	KX900058	KX900174	KX900361	KX900241	–	–	–	KX900284
<i>Picipes submelanopus</i>	Dai 13294	China	KU189770	KU189801	KU189915	KU189951	KU189860	KU189886	KU189984	KU189830
<i>Picipes submelanopus</i>	Dai 13296	China	KU189771	KU189802	KU189916	KU189952	KU189861	–	–	KU189831
<i>Picipes subtropicus</i>	Cui 2662	China	KU189759	KU189791	KU189905	KU189943	–	–	–	KU189821
<i>Picipes subtropicus</i>	Li 1928	China	KU189758	KU189790	KU189904	KU189942	KU189854	KU189881	KU189976	KU189820
<i>Picipes subtubaeformis</i>	Cui 10793	China	KU189753	KU189785	KU189900	KU189938	KU189851	KU189877	KU189973	KU189816
<i>Picipes subtubaeformis</i>	Dai 11870	China	KU189752	KU189784	KU189899	KU189937	KU189850	KU189876	KU189972	KU189815
<i>Picipes taibaiensis</i>	Dai 5741	China	JX489169	KC572071	–	–	–	–	–	–
<i>Picipes taibaiensis</i>	Dai 5746	China	KX196783	KX196784	KX196785	KX196786	–	–	–	KX196787
<i>Picipes tibeticus</i>	Cui 12215	China	KU189755	KU189787	KU189902	KU189940	KU189853	KU189879	KU189975	KU189818
<i>Picipes tibeticus</i>	Cui 12225	China	KU189756	KU189788	KU189903	KU189941	–	KU189880	–	KU189819
<i>Picipes tubaeformis</i>	Niemela 6855	Finland	KC572036	KC572073	–	–	–	–	–	–
<i>Picipes tubaeformis</i>	JV 0309-1	USA	KC572034	KC572072	–	–	–	–	–	–
<i>Picipes ulleungus</i>	Cui 12410	China	KX900022	KX900142	KX900344	KX900217	KX899932	–	KX900302	KX900266
<i>Picipes virgatus</i>	CulTENN11219	Argentina	AF516581	AJ488122	–	–	–	–	–	–
<i>Picipes virgatus</i>	CulTENN11406	Argentina	AF516582	AJ488122	–	–	–	–	–	–
<i>Picipes wuyishanensis</i>	Dai 7409	China	KX900061	KX900177	KX900364	KX900243	–	–	–	KX900287
<i>Podoserpula ailaoshanensis</i>	ZJL2015015	China	KU324484	KU324487	KU324494	–	–	–	–	KU324491
<i>Polyporus auratus</i>	Dai 13665	China	KX900056	KX900172	KX900359	KX900239	–	–	KX900313	KX900282

Table 1 Continued.

Species	Specimen No.	Country	GenBank accession No.							
			ITS	nLSU	EF1- α	mtSSU	TUB	RPB1	RPB2	nSSU
<i>Polyporus austrosinensis</i>	Cui 11140	China	KX900046	KX900162	KX900352	KX900230	–	KX900386	KX900309	KX900273
<i>Polyporus austrosinensis</i>	Cui 11126	China	KX900045	KX900161	KX900351	KX900229	KX899936	KX900385	KX900308	KX900272
<i>Polyporus cuticulatus</i>	Cui 8637	China	KX851614	KX851668	KX851777	KX851702	—	KX851750	KX851760	KX851728
<i>Polyporus cuticulatus</i>	Dai 13141	China	KX851613	KX851667	KX851776	KX851701	KX851576	KX851749	–	KX851727
<i>Polyporus guianensis</i>	TENN 58404	Venezuela	AF516566	AJ487948	–	–	–	–	–	–
<i>Polyporus guianensis</i>	TENN 59093	Argentina	AF516564	AJ487947	–	–	–	–	–	–
<i>Polyporus hapalopus</i>	Yuan 5809	China	KC297219	KC297220	KU189918	KU189954	–	–	–	KU189833
<i>Polyporus hemicapnodes</i>	Cui 11259	China	KX851625	KX851679	KX851782	KX851707	KX851580	–	KX851763	KX851733
<i>Polyporus hemicapnodes</i>	Dai 13403	China	KX851627	KX851681	KX851784	KX851709	KX851579	–	KX851764	KX851734
<i>Polyporus lamelliporus</i>	Dai 15106	China	KX851623	KX851677	KX851781	KX851706	KX851578	KX851752	KX851762	KX851732
<i>Polyporus lamelliporus</i>	Dai 12327	China	KX851622	KX851676	KX851780	KX851705	KX851577	–	–	KX851731
<i>Polyporus leprieurii</i>	TENN 58579	Costa Rica	AF516567	AJ487949	–	–	–	–	AB368150	–
<i>Polyporus mangshanensis</i>	Dai 15151	China	KX851796	KX851797	KX851802	KX851798	KX851795	KX851800	KX851801	KX851799
<i>Polyporus parvovarius</i>	Yuan 6639	China	KX900049	KX900165	KX900354	KX900232	KX899937	KX900388	KX900311	KX900275
<i>Polyporus parvovarius</i>	Dai 13948	China	KX900050	KX900166	KX900355	KX900233	KX899938	KX900389	KX900312	KX900276
<i>Polyporus radicans</i>	DAOM198916	Canada	AF516584	AJ487955	–	–	–	–	–	–
<i>Polyporus radicans</i>	TENN 58831	USA	AF516585	AJ487956	–	–	–	–	–	–
<i>Polyporus squamosus</i>	Cui 10394	China	KX851635	KX851688	KX851789	KX851714	KX851582	KX851754	KX851766	KX851739
<i>Polyporus squamosus</i>	Cui 10595	China	KU189778	KU189809	KU189925	KU189960	KU189868	KU189892	KU189988	KU189840
<i>Polyporus subvarius</i>	WD2368	Japan	AB587643	AB587638	–	–	–	–	–	–
<i>Polyporus subvarius</i>	Yu 2	China	AB587632	AB587621	KU189924	KU189959	–	–	–	KU189839
<i>Polyporus tuberaster</i>	Dai 11271	China	KU189769	KU189800	KU189914	KU189950	–	–	KU189983	KU189829
<i>Polyporus tuberaster</i>	Dai 12462	China	KU507580	KU507582	KU507590	KU507584	KU507588	–	–	KU507586
<i>Polyporus umbellatus</i>	Pen 13513	China	KU189772	KU189803	KU189917	KU189953	KU189862	KU189887	KU189985	KU189832
<i>Polyporus varius</i>	Cui 12249	China	KU507581	KU507583	KU507591	KU507585	–	KU507589	KU507592	KU507587
<i>Polyporus varius</i>	Dai 13874	China	KU189777	KU189808	KU189923	KU189958	KU189867	KU189891	KU189987	KU189838
<i>Polyporus</i> sp.1	Cui 11071	China	KX851642	KX851695	KX851794	KX851719	KX851584	KX851755	KX851768	KX851744
<i>Polyporus</i> sp.1	Cui 11045	China	KX851643	KX851696	–	KX851720	KX851583	KX851756	KX851769	KX851745

Table 1 Continued.

Species	Specimen No.	Country	GenBank accession No.							
			ITS	nLSU	EF1- α	mtSSU	TUB	RPB1	RPB2	nSSU
<i>Polyporus</i> sp.2	Dai 13585A	China	KX900055	KX900171	KX900358	KX900236	–	–	–	KX900279
<i>Pseudofavolus cucullatus</i>	Dai 13584A	China	KX900071	KX900185	KX900371	KX900251	–	–	–	–
<i>Pseudofavolus cucullatus</i>	WD2157	Japan	AB587637	AB368114	–	–	–	–	AB368170	–
<i>Russula emeticicolor</i>	FH12253	Germany	KT934011	KT933872	–	–	–	KT957382	KT933943	–
<i>Serpula himantoides</i>	MUCL:30528	Belgium	GU187545	GU187600	GU187748	–	–	GU187480	GU187808	GU187651
<i>Schenella pityophilus</i>	OSC59743	–	–	DQ218519	DQ219232	–	–	–	DQ219057	–
<i>Schizophyllum radiatum</i>	AFTOL-ID-516	Panama	AY571060	AY571023	–	–	–	DQ447939	DQ484052	AY705952
<i>Stereopsis radicans</i>	O:KHL15528	Brazil	KC203497	KC203497	KC203517	–	–	–	KC203503	KC203497
<i>Tomentella</i> sp.	AFTOL-ID 1016	USA	DQ835998	DQ835997	–	–	–	–	DQ835999	DQ092920
<i>Trametes conchifer</i>	FP106793sp	USA	JN164924	JN164797	JN164887	–	–	JN164823	JN164849	–
<i>Trametes elegans</i>	FP105679sp	USA	JN164944	JN164799	JN164899	–	–	JN164833	JN164861	–
<i>Trametes polyzona</i>	Cui 11040	China	KR605824	KR605767	KR610760	KR606029	–	–	KR610849	KR605932

Newly generated sequences are shown in black bold.

Fifty-one species of *Polyporus* on the six main clades proposed in our previous study (Zhou et al. 2016a) were added into the multiple DNA data (5.8S+nLSU+EF1- α + RPB1+RPB2+nSSU). Four species of Agaricales viz. *Agaricus campestris* L., *Aphanobasidium pseudotsugae* (Burt) Boidin & Gilles, *Callistosporium graminicolor* Lennox and *Schizophyllum radiatum* Fr. were used to represent the Agaricales clade while *Hydnochaete duportii* Pat., *Hyphoderma praetermissum* (P. Karst.) J. Erikss. & Å. Strid and an undescribed species of *Cotylidia* were used to represent Hymenochaetales clade. Based on the analyses of Zhao et al. (2017), Amylocorticiales was treated as sister clade of Agaricales. Moreover, members of Atheliales, Boletales, Russulales, Thelephorales, Stereopsidales and other three orders were also included in our dataset. Divergence times were estimated by using BEAST v1.8.0 (Drummond et al. 2012).

All the DNA sequences were aligned separately using Clustal Omega (Sievers et al. 2011) and manually adjusted in BioEdit 7.2.5 (Hall 1999). Introns of EF1- α , RPB1 and RPB2 sequences, and poorly aligned regions of nLSU and nSSU were removed from the analysis. The best substitution models were selected by using jModelTest 2.1.7 (Darriba et al. 2012). The XML file was executed in BEAUti v1.8.0. Six DNA datasets were set as different partitions, with substitution and clock models unlinked while the trees linked. The HKY+Gamma+Invariant model was chosen as the substitution model of 5.8S while GTR+Gamma+Invariant was selected for other five genes. The clock model was set to uncorrelated lognormal relaxed clock (Drummond et al. 2006, Lepage et al. 2007). Yule process speciation was used as the tree prior (Gernhard 2008). Gamma priors distribution was used for fossil node calibrations, set shape = 1.0, scale = 50.0, offset = 90.0 for Agaricales clade and 113.0 for Hymenochaetales clade (Sánchez-Ramírez et al. 2014). All the ucl.d.mean parameters for different genes were set to gamma priors distribution, shape = 1.0, scale = 0.001 and

offset = 0.0 (Sánchez-Ramírez et al. 2014). Four independent Markov chain Monte Carlo (MCMC) chains of 100 million generations were conducted and saving trees every 5000th generation. The resulting log file was inspected with Tracer v1.6 (<http://tree.bio.ed.ac.uk/software/tracer/>) to confirm that the estimated effective sample size (ESS) ≥ 200 . 20000 ultrametric trees from each run were summarized using TreeAnnotator v1.8.0 to estimate the 95% credible node intervals referred to as highest posterior densities (HPD), discarding 10% of states as burn-in and setting posterior probability limit 0.80.

Phylogenetic analyses of *Polyporus* and related genera

Trametes conchifer (Schwein.) Pilát, *T. elegans* (Spreng.) Fr. and *T. polyzona* (Pers.) Justo were selected as outgroups in the phylogenies. Totally 735 DNA sequences, which belonging to 122 isolates of *Polyporus* and 28 isolates of allied genera, were used in the phylogenetic analyses, procedures were done as in our previous studies (Zhou et al. 2016a, Zhou & Cui 2017, Zhu et al. 2019).

Eight gene regions were initially aligned separately using Clustal Omega (Sievers et al. 2011) and then manually adjusted to maximize alignment and minimize gaps in BioEdit 7.2.5 (Hall 1999). Sequence alignments were deposited at TreeBase (<http://purl.org/phylo/treebase>; submission ID: 29005).

One thousand partition homogeneity test (PHT) replicates of the combined datasets (ITS+nLSU and ITS+nLSU+EF1- α +mtSSU+RPB1+RPB2+nSSU+TUB) were tested using PAUP 4.0 beta 10 (Swofford 2002) to determine whether the partitions are homogeneous. PHT results revealed that all the DNA sequences displayed congruent phylogenetic signals (P values were 0.866 and 0.994 for ITS+nLSU and the eight-gene dataset, respectively).

The best-fit evolutionary models were selected by hierarchical likelihood ratio tests (hLRT) and Akaike information criterion (AIC) in MrModeltest 2.2 (Nylander 2004) after scoring 24 models of evolution using PAUP 4.0 beta 10. Analyzing results revealed that GTR+I+G was the best-fit model for both ITS+nLSU and the eight-gene dataset.

The best maximum likelihood (ML) topology obtained from 1000 maxtrees was performed using PAUP 4.0 beta 10. All characters were equally weighted and gaps were treated as missing. ML bootstrap values (ML-BS) obtained from 1000 replicates were performed using RAxMLGUI 1.31 (Michalak 2012) with the GTRGAMMA and GTRCAT models to assess the reliability of the nodes.

The maximum parsimony (MP) topology and bootstrap values (MP-BS) obtained from 1000 maxtrees were performed using PAUP 4.0 beta 10. Trees were inferred using the heuristic search option with tree-bisection-reconnection (TBR) branch swapping algorithm and 1000 random sequence additions. Descriptive tree statistics tree length (TL), consistency index (CI), retention index (RI), rescaled consistency index (RC), and homoplasy index (HI) were calculated for each MP tree generated.

Bayesian phylogenetic inference and Bayesian posterior probabilities (BPPs) were performed with MrBayes v3.2 (Ronquist et al. 2012). The analyses were run with four Markov chains for 5 000 000 (ITS+nLSU) and 8 000 000 (eight-gene dataset) generations to make the average standard deviation of split deviation frequencies less than 0.01, and sampled every 100th generation. The first 25 % of the sampled trees were discarded as burn-in and the remaining ones were used to reconstruct a majority rule consensus and calculate BPPs of the clades.

Trees were viewed in FigTree v1.4.2 (<http://tree.bio.ed.ac.uk/software/figtree/>) and edited by using Adobe Illustrator CS5 and Adobe Photoshop CC (Adobe Systems Inc., California, USA). The best topologies from ML analyses were shown in this study with ML-BS (≥ 50), MP-BS (≥ 50) and BPPs (≥ 0.95).

Results

Divergence time estimation

The MCMC tree (Fig. 1) shows that the ancestor of Polyporales evolved during the early Cretaceous, approximately 141.81 Mya (95% HPD = 102.35–191.91Mya), while the mean estimated stem ages of the four main clades of *Polyporales* proposed by Hibbett & Donoghue (2001) and Binder et al. (2013) are between 123.74 and 88.81 Mya. In addition, the mean stem ages of the six major clades of *Polyporus* recognized by Zhou et al. (2016a) are approximately 47–60Mya. Among the six clades, the lentinus clade diverged at 46.9 Mya contained gilled species of *Lentinus* and several poroid species which previously treated as *Polyporus* (*Polyporellus* group), and this clade is sister to *Microporus* P. Beauv. and *Lignosus* Lloyd ex Torrend. The favolus clade and the neofavolus clade grouped together and evolved from the same ancestor dated to 60.01 Mya. The squamosus clade, which dated to 58.09 Mya, contains species of *Polyporus*, *Datronia*, *Neodatronia* B.K. Cui, Hai J. Li & Y.C. Dai, *Datroniella* B.K. Cui, Hai J. Li & Y.C. Dai, *Pseudofavolus* and *Echinochaete*. The core polyporus clade, which including the lectotype of *Polyporus*, is sister to the picipes clade, and both of them diverged at 56.33 Mya but with low support.

Phylogenetic analyses

The ITS+nLSU dataset was composed of 2160 total characters (770 bp ITS and 1390 bp nLSU), of which 1362 characters were constant, 696 variable characters were parsimony-informative. The best ML tree scored 26414.12589 was obtained after trying 518348 rearrangements. Sixty-six equally most parsimonious trees (tree length = 5168, CI = 0.286, RI = 0.756, RC = 0.217, HI = 0.714) were retained after trying 4.2288×10^{10} rearrangements in the MP analyzing. Bayesian analysis had a similar topology with the best ML tree. The ML topology based on the ITS+nLSU sequences was presented in Fig. 2.

In the eight-gene based phylogeny, 7512 total characters (770 bp ITS, 1390 bp nLSU, 607 bp EF1- α , 743 bp mtSSU, 1292 bp RPB1, 1110 bp RPB2, 1118 bp nSSU and 482 bp TUB) were equally weighted. Among these characters, 4521 bp characters were constant and 2651 bp characters were parsimony-informative. The best ML tree scored 81741.75120 was achieved after trying 489289 rearrangements. In the MP analyzing, 56 best parsimonious trees (tree length = 17298, CI = 0.316, RI = 0.721, RC = 0.228, HI = 0.684) were saved after trying 1.5844×10^{10} rearrangements. Bayesian analysis presented essentially the same topology with the best ML tree and the best ML topology was presented along with ML-BS, MP-BS and BPPs in Fig. 3.

In our current study, both ITS+nLSU and the eight-gene dataset analyses support the existence of the six major clades of *Polyporus* proposed in our previous study (Zhou et al. 2016a). Both datasets have the similar topology but with discrepant bootstrap values.

1. The picipes clade is composed of 27 species, which including 7 undescribed ones, with high supports in the eight-gene analyzing (100/98/1.00) but with low supports in the ITS+nLSU analyzing (72/66/-). It reveals that *P. dictyopus* Mont., *P. subdictyopus* H. Lee, N.K. Kim & Y.W. Lim and *P. ulleungus* H. Lee, N.K. Kim & Y.W. Lim has much closer relationships with *Picipes* spp. than other *Polyporus* species. As is shown in Fig. 3, four major lineages are presented in the picipes clade. Twelve species are included in the lineage A and most of them are restricted to the temperate region. Unlike lineage A, species of lineage B are limited in the tropical and subtropical regions. *Picipes submelanopus* (H.J. Xue & L.W. Zhou) J.L. Zhou & B.K. Cui is the only species of lineage C, it is merely collected in temperate and Plateau zones of China. Lineage D includes two subtropical species, *Pi. baishanzuensis* J.L. Zhou & B.K. Cui and *P. ulleungus*, the former one is only reported in Baishanzu Nature Reserve of China (Zhou et al. 2016a), while the later one was originally described from Korea (Tibpromma et al. 2017).

2. The core polyporus clade, which contains the lectotype of *Polyporus* and other five species, is strongly supported in both datasets (94/83/1.00 for ITS+nLSU and 96/96/1.00 for the eight-gene phylogeny). In this clade, *P. tuberaster* is mainly found from temperate zone, but it can also be found in tropical and subtropical regions according to our collections. For other species, *P. umbellatus* is mainly collected from temperate areas, *P. hapalopus* H.J. Xue & L.W. Zhou is limited to subtropical areas, while other three species are restricted to tropical regions.

dataset. Posterior probabilities not less than 0.80 and the mean ages of each node are annotated. The 95 % highest posterior densities of divergence time estimation are marked by horizontal bars.

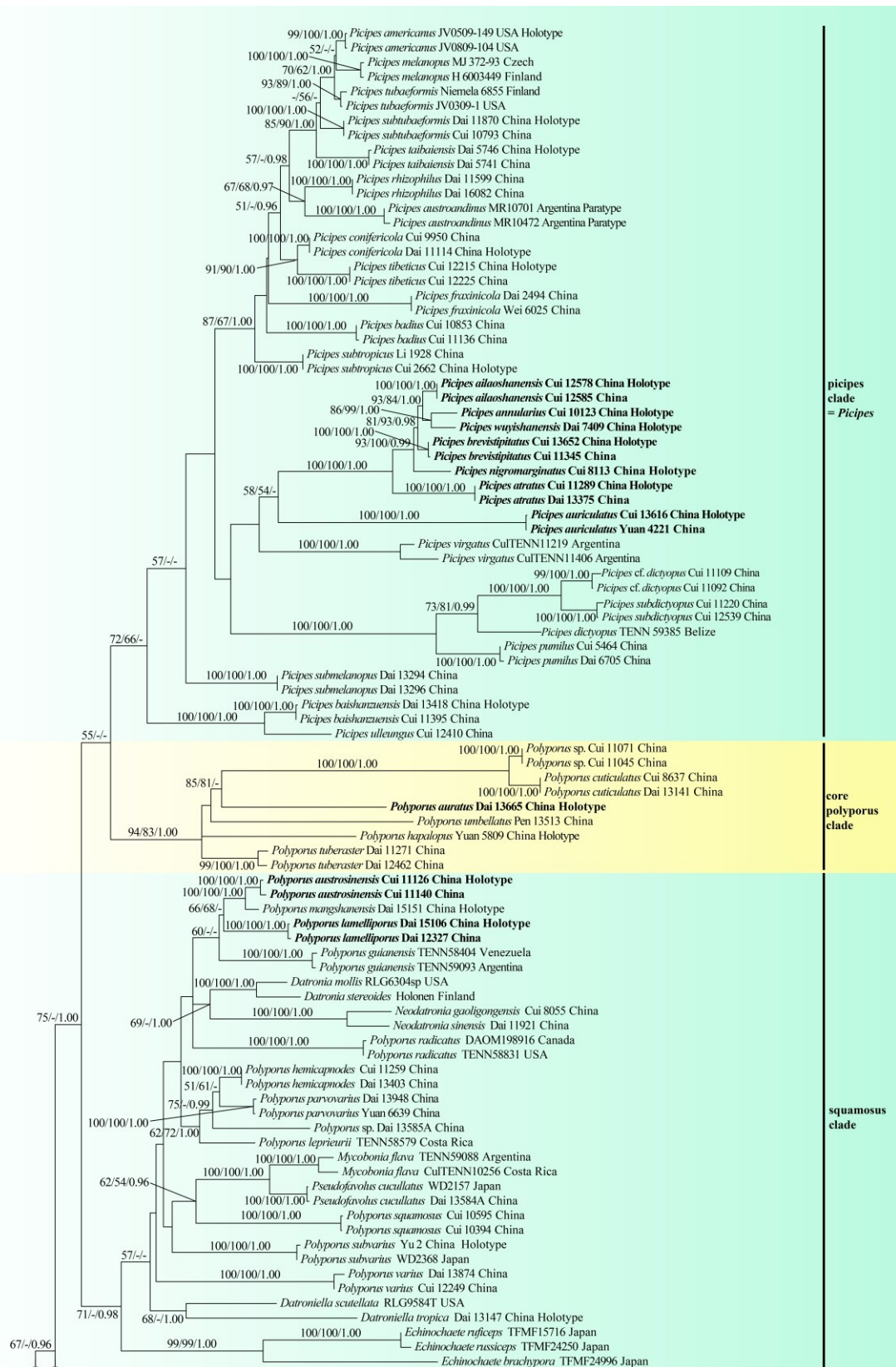


Figure 2 – Phylogeny of *Polyporus* and related genera inferred from ITS+nLSU data. Topology is from ML analysis with maximum likelihood bootstrap support values (≥ 50 , left), parsimony bootstrap support values (≥ 50 , middle) and Bayesian posterior probability values (≥ 0.95 , right). New species are indicated in black bold.

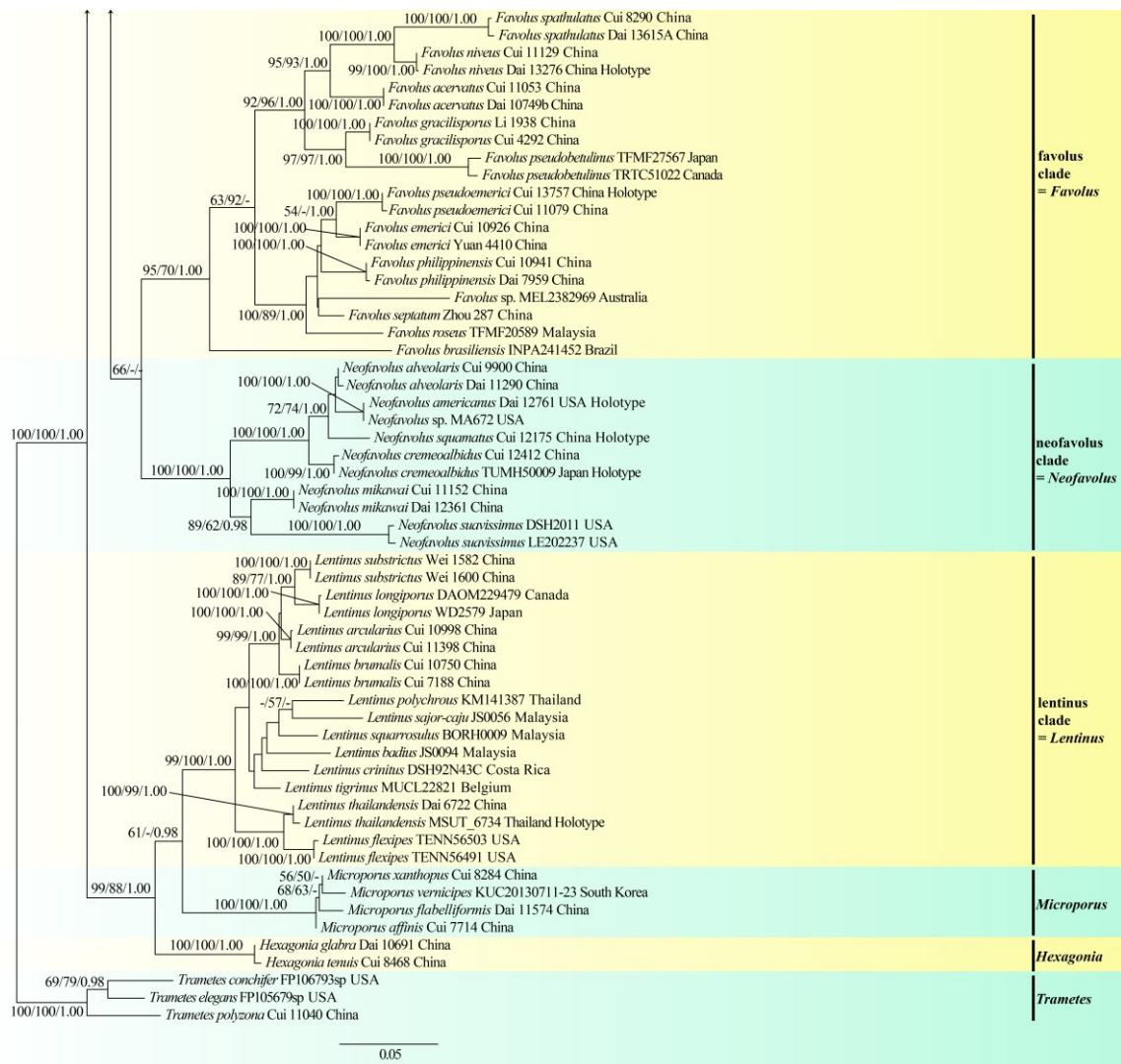


Figure 2 – Continued.

3. Both ITS+nLSU and eight-gene based phylogenies support the division of the squamosus clade. In this clade, twelve *Polyporus* spp. nested with species of *Datronia*, *Datroniella*, *Echinochaete*, *Mycobonia*, *Neodatronia* and *Pseudofavolus*, species in this clade is very diverse in morphology, for the time being, we prefer to remain the different genera names for species in this clade.

4. The favolus clade is comprised of twelve *Favolus* species with high supports in both ITS+nLSU and eight-gene dataset analyses (Figs 2 and 3). Most of these species are distributed in tropical and subtropical areas. However, *F. pseudobetulinus* (Murashk. ex Pilát) Sotome & T. Hatt. has a boreal distribution in northern hemisphere (Sotome et al. 2011). Based on our own collections, few samples of *F. acervatus* (Lloyd) Sotome & T. Hatt. can also be found in temperate areas.

5. Six species are included in the neofavolus clade with high supports (Figs 2, 3). Among these species, *N. squamatus* J.H. Xing, J.L. Zhou & B.K. Cui is only collected in Tibet (plateau zone), *N. americanus* J.H. Xing, J.L. Zhou & B.K. Cui is merely found in the temperate area of America (Xing et al. 2020), while *N. cremeoalbidus* Sotome & T. Hatt. is limited in subtropical regions of China and Japan. *Neofavolus suavissimus* (Fr.) J. S. Seelan, Justo is mainly distributed in warm to cold temperate areas, but several subtropical collections can also be found in Japan (Seelan et al. 2015). Based on our own collections, both *N. alveolaris* and *N. mikawui* (Lloyd) Sotome & T. Hatt. can be collected in temperate, subtropical and tropical regions, the former one mainly distributes in temperate areas while the later mainly in subtropical areas.

6. Six species in group *Polyporellus* of *Polyporus* clustered in the lentinus clade and showed closer relationships with *Hexagonia* Fr., *Lentinus* and *Microporus* than other *Polyporus* spp. This clade is strongly supported in both ITS+nLSU and multi-gene analyses (Figs 2, 3). Three well supported lineages are recognized in the lentinus clade (Fig. 3). Lineage I is composed of four poroid species (*P. arcularius*, *P. brumalis*, *P. ciliatus* Fr. and *P. longiporus* Audet, Boulet & Sirard). These four species mainly distribute in temperate areas though *P. arcularius* and *P. brumalis* can also be found in subtropical, tropical and plateau zones. Lineage II is formed by gilled species of *Lentinus*, and almost all the species in this lineage distribute in the tropical areas. *Polyporus thailandensis* Sotome and *P. tricholoma* Mont. nested in the lineage III are tropical species with poroid hymenophores. All poroid species in the lentinus clade were treated as members of the genus *Lentinus*.

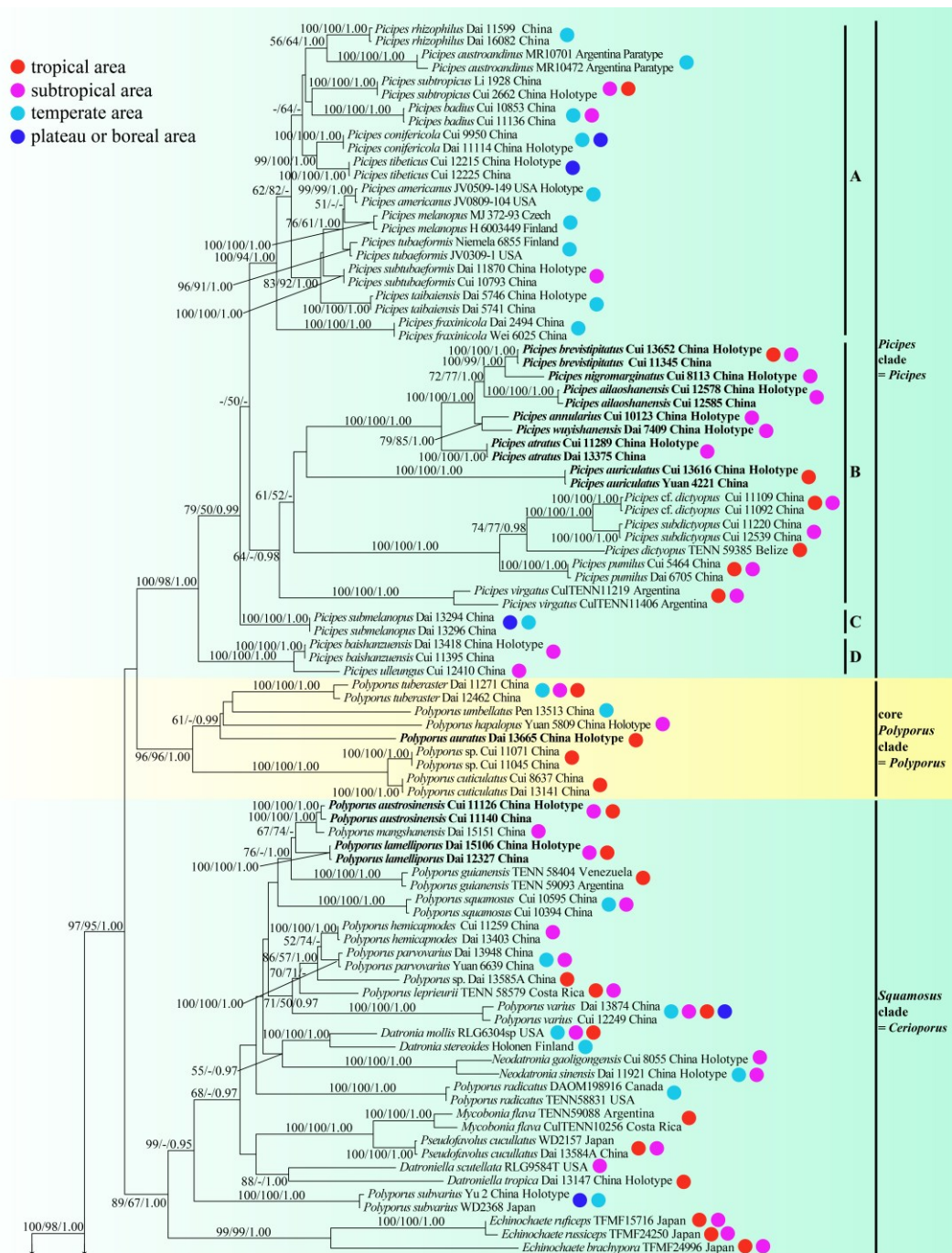


Figure 3 – Phylogeny of *Polyporus* and related genera inferred from the combined dataset ITS+nLSU+EF1- α +mtSSU+TUB+RPB1+RPB2+nSSU. Topology generated by ML analysis with

maximum likelihood bootstrap support values (≥ 50 , left), parsimony bootstrap support values (≥ 50 , middle) and Bayesian posterior probability values (≥ 0.95 , right) are indicated on the nodes. New species are indicated in black bold. The colored dots indicate four different climate zone distributions.

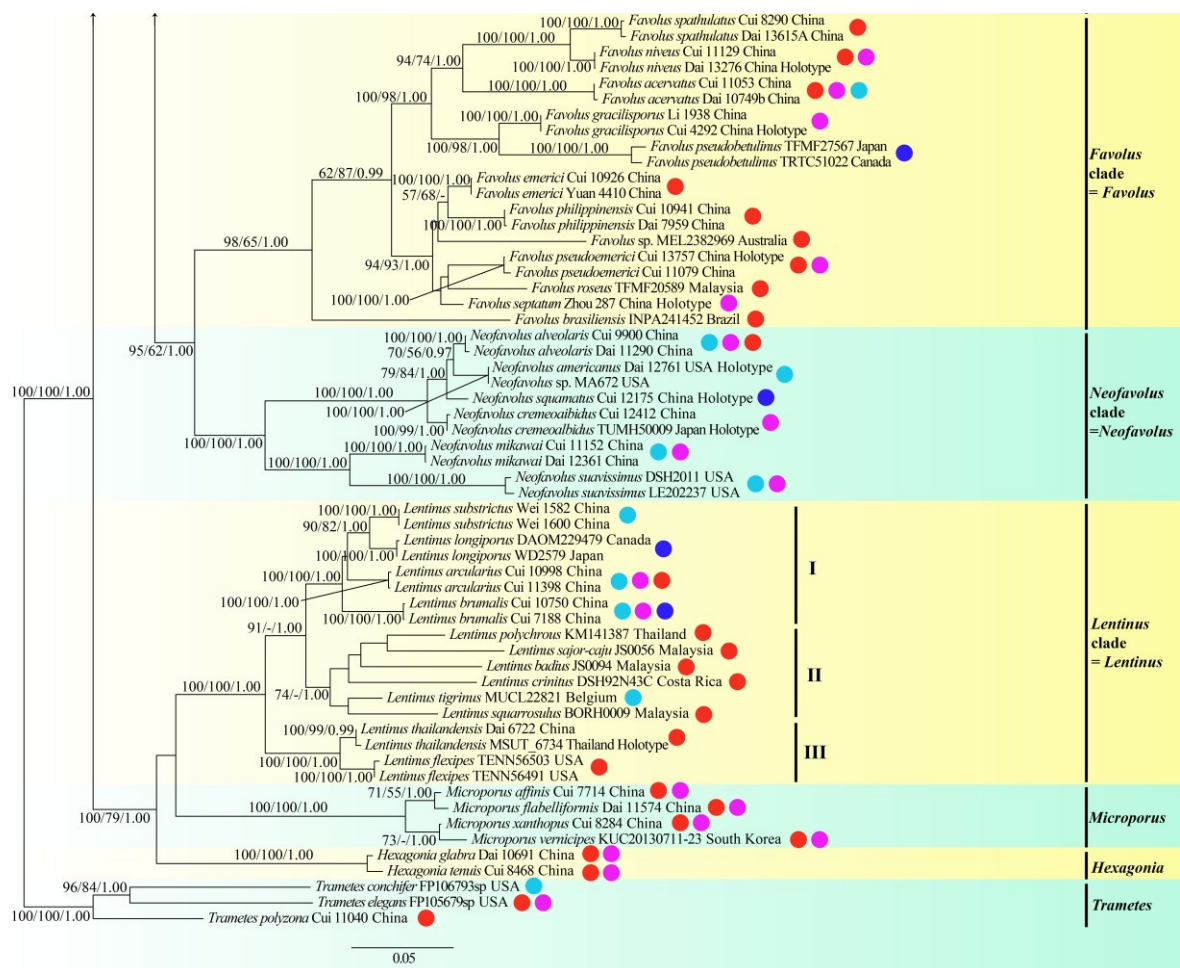


Figure 3 – Continued.

Taxonomy

Picipes ailaoshanensis B.K. Cui, Xing Ji & J.L. Zhou, sp. nov.

Figs 4A, B, 6

Index Fungorum number: IF559395; Facesoffungi number: FoF 10644

Etymology – *ailaoshanensis* (Lat.): referring to the locality (Ailaoshan) of the type specimen.

Basidiomata – Annual, laterally stipitate, solitary, woody hard when dry. Pilei irregularly fan-shaped to semicircular, about 1.6–3.6 cm long, 1.8–5.6 cm wide and up to 5 mm thick at base. Pileal surface yellowish brown to chestnut when dry, glabrous or covered with protuberances towards the stipe, azonate, frequently with radially aligned stripes; margin straight or incurved when dry. Pore surface grey beige when dry; pores angular, 3–7 per mm; dissepiments thin, entire. Context buff to festucine when dry, woody hard upon drying, up to 3.5 mm thick. Tubes concolorous with pore surface, decurrent on one side of the stipe, up to 1.5 mm thick. Stipe short, upper portion concolorous to the pileal surface and bearing a black cuticle at the base, up to 9 mm long and 1.2 cm in diam.

Hyphal structure – Hyphal system dimitic; generative hyphae bearing clamp connections; skeleto-binding hyphae IKI–, CB+; tissues unchanged in KOH.

Context – Generative hyphae frequent, colorless, thin-walled, occasionally branched, 2–8 μm in diam; skeleto-binding hyphae dominant, colorless, thick-walled with a narrow lumen to solid,

frequently branched, strongly interwoven, 1.2–5.5 μm in diam.

Tubes – Generative hyphae frequent, colorless, thin-walled, frequently branched, 1.5–5 μm in diam; skeleto-binding hyphae dominant, colorless, thick-walled with a wide lumen when young and with a narrow lumen to solid when mature, with dendroid branches, strongly interwoven, 1.5–5 μm in diam. Cystidia absent; cystidioles frequent, subulate and clavate with an acerate head, 15.5–20 \times 5–6.8 μm . Basidia not observed.

Stipe – Generative hyphae infrequent, colorless, thin-walled, occasionally branched, 2–4.3 μm in diam; skeleto-binding hyphae dominant, colorless, thick-walled with a narrow lumen to solid, with arboriform branches, strongly interwoven, 1.8–6.1 μm in diam. Hyphae in cuticle with brown inclusion inside, thick-walled with a wide lumen, bearing clamp connections, 2.5–8 μm in diam.

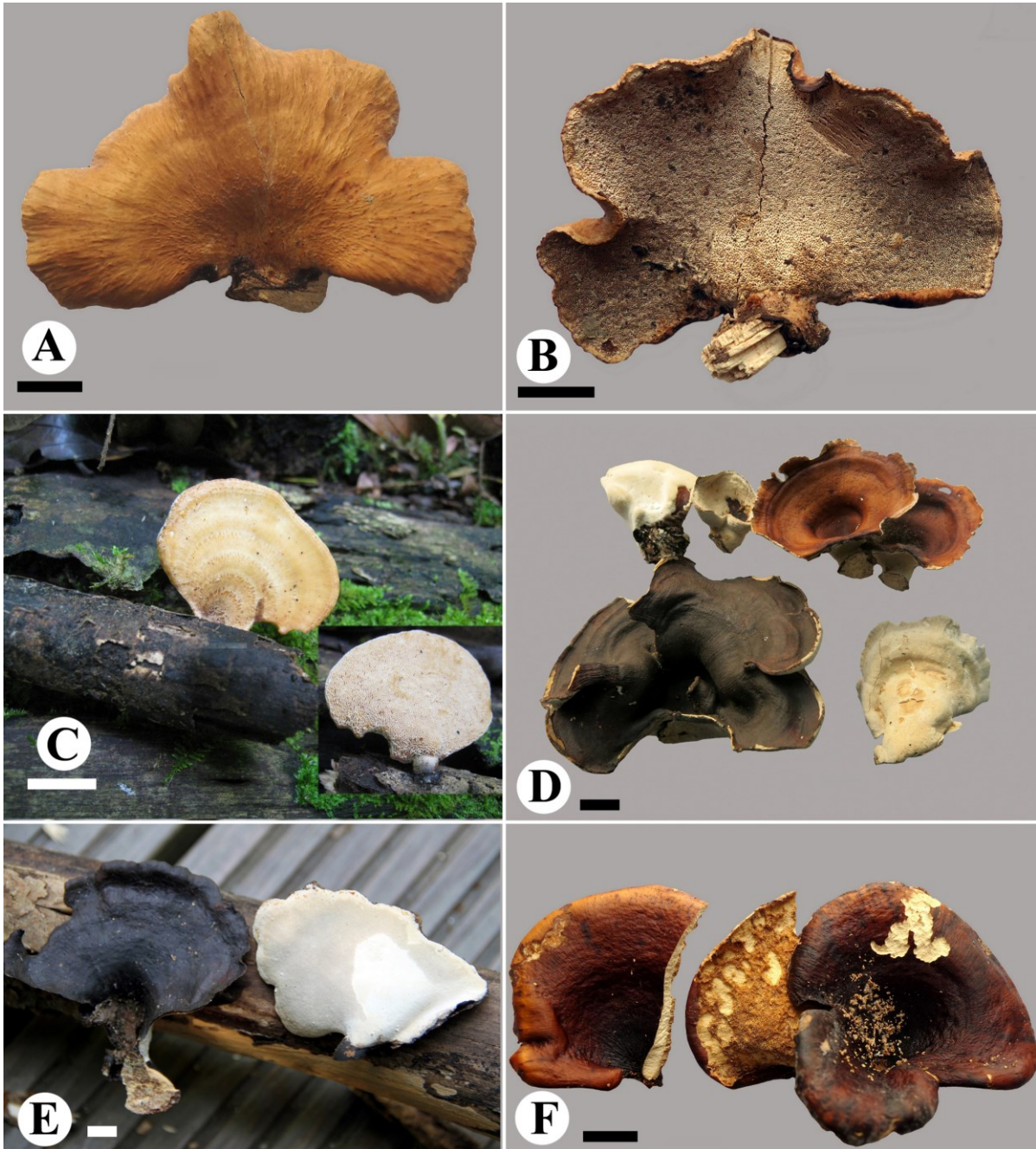


Figure 4 – Basidiomata of four new species: *Picipes ailaoshanensis* (A and B: Cui 12578); *Picipes annularius* (C: Cui 10123); *Picipes atratus* (D: Dai 13375, E: Cui 11289); *Picipes auriculatus* (Cui 13616). Scale bars = 1 cm.

Basidiospores – Basidiospores infrequent, cylindrical, rarely oblong, colorless, thin-walled, smooth, frequently bearing one or more guttules, IKI–, CB–, (5.9–)6–7.3(–8) × (2.5–)2.6–3.6 μm, L = 6.71 ± 0.52 μm, W = 3.06 ± 0.29 μm, Q = 1.91–2.67, Qm = 2.22 ± 0.17 (n = 44/2).

Rot type – A white rot.

Known distribution – Subtropical regions of China.

Materials examined – China, Yunnan Province, Jingdong County, Ailaoshan Nature Reserve, on fallen angiosperm branch, 10 Sep 2015, B.K. Cui, Cui 12578 (BJFC, holotype), Cui 12585 (BJFC, paratype).

Notes – *Picipes ailaoshanensis* is a subtropical species with greyish pore surface, laterally short stipe with a black base, and clavate cystidioles with an acerate head. *Picipes taibaiensis* (Y.C. Dai) J.L. Zhou & B.K. Cui resembles *Pi. ailaoshanensis* by having yellowish brown to chestnut pileus and laterally short stipe, but *Pi. taibaiensis* has brownish pore surface upon drying, larger basidiospores (7.5–10.5 × 3.2–3.8 μm), fusoid cystidioles and temperate distribution (Dai et al. 2009).

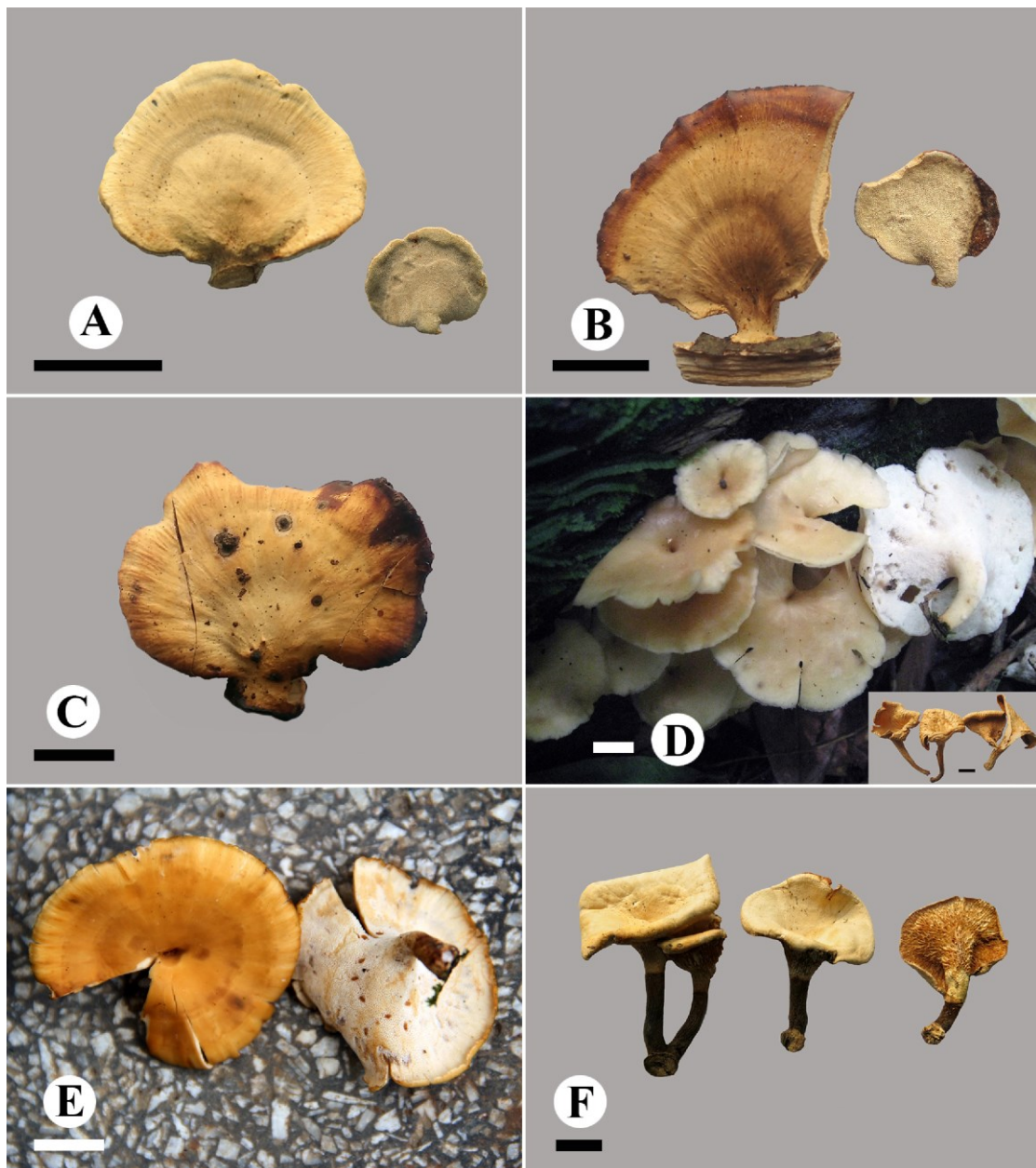


Figure 5 – Basidiomata of six species: *Picipes brevistipitatus* (A: Cui 13652); *Picipes nigromarginatus* (B: Cui 8113); *Picipes wuyishanensis* (C: Dai 7409); *Polyporus auratus* (D: Dai

13665); *Polyporus austrosinensis* (E: Cui 11123); *Polyporus lamelliporus* (F: Dai 15103). Scale bars = 1 cm.

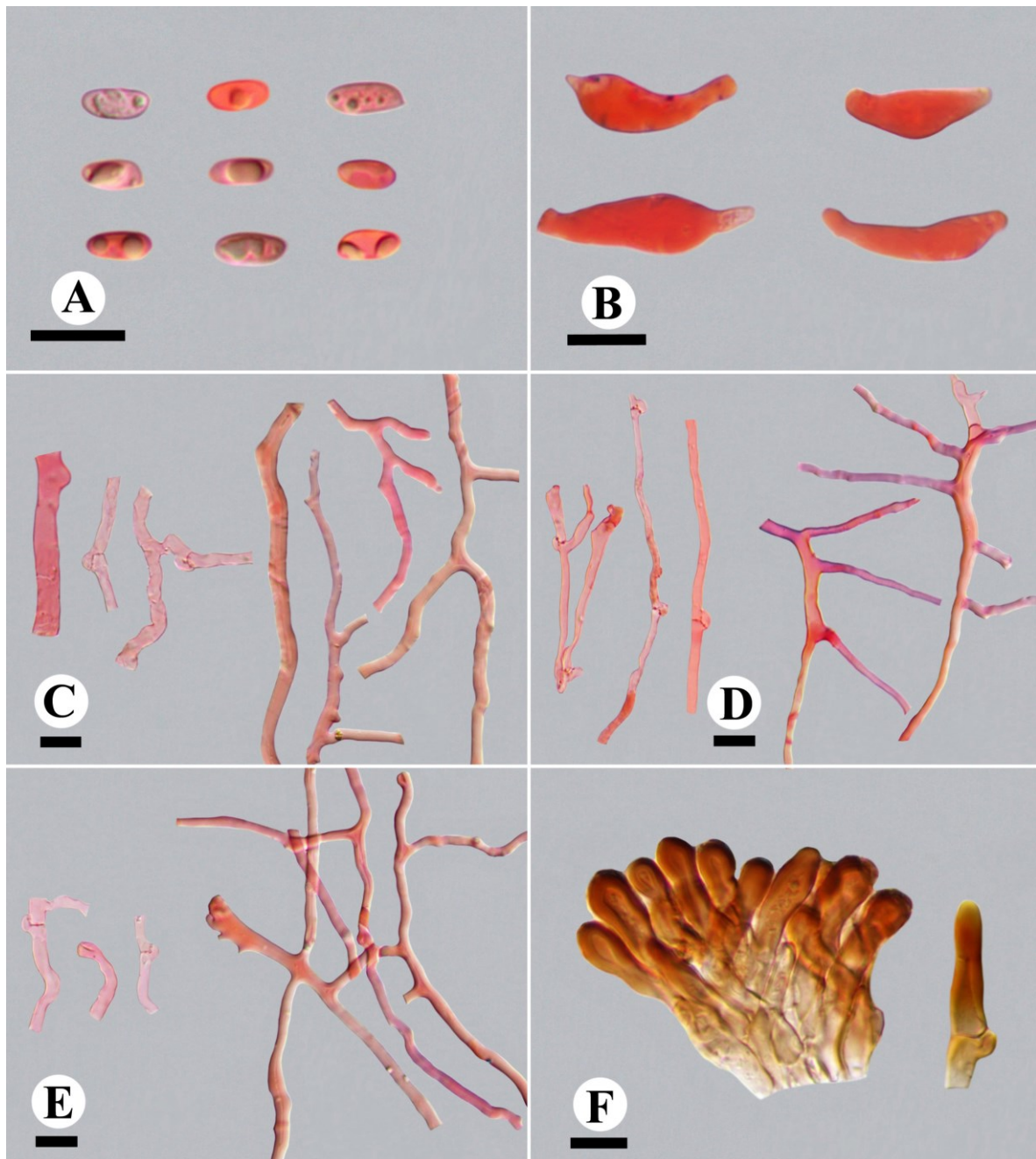


Figure 6 – Microscopic structures of *Picipes ailaoshanensis*. A Basidiospores. B Cystidioles. C Hyphae from context. D Hyphae from trama. E Hyphae from stipe. F Hyphae from cuticle of stipe. Scale bars = 10 µm.

Picipes annularius B.K. Cui, Xing Ji & J.L. Zhou, sp. nov.

Figs 4C, 7

Index Fungorum number: IF559396; Facesoffungi number: FoF 10659

Etymology – *annularius* (Lat.): referring to the annularly arranged squamae on the pileal surface when fresh.

Basidiomata – Annual, laterally stipitate, solitary, coriaceous when fresh and hard when dry. Pilei fan-shaped, projecting up to 1.8 cm long, 2.1 cm wide and 3 mm thick at base. Pileal surface pinkish buff to buff yellow when fresh, becoming buff upon drying, with radially aligned stripes when dry; margin yellowish brown when dry, covered with beige to cinnamon-buff small squamae,

annularly arranged, straight. Pore surface pinkish buff when fresh, becoming buff to yellowish brown when dry; pores angular, 3–5 per mm; dissepiments thin, entire. Context white when fresh, becoming buff to ivory when dry, corky upon drying, up to 1.5 mm thick. Tubes concolorous with pore surface, not decurrent and has an obvious boundary with stipe, up to 2 mm thick. Stipe short, white when fresh and pinkish buff when dry at the upper parts towards the tubes, grey to black when fresh and greyish buff to dark brown when dry at the low parts, tomentose, up to 4 mm long and 3.5 mm in diam.

Hyphal structure – Hyphal system dimitic; generative hyphae bearing clamp connections; skeleto-binding hyphae IKI–, slightly CB+; tissues unchanged in KOH.

Context – Generative hyphae frequent, colorless, thin-walled, rarely branched, 2–5.6 µm in diam; skeleto-binding hyphae dominant, colorless, thick-walled with a narrow lumen, frequently branched, interwoven, 1.2–4.6 µm in diam.

Tubes – Generative hyphae infrequent, colorless, thin-walled, rarely branched, 1.3–3.3 µm in diam; skeleto-binding hyphae dominant, colorless, thick-walled with a narrow lumen, with dendroid branches, strongly interwoven, 1.1–2.9 µm in diam. Cystidia and cystidioles absent. Basidia clavate, with a basal clamp connection and four sterigmata, 13–17 × 7–8.6 µm; basidioles in shape similar to basidia, but slightly smaller.

Stipe – Generative hyphae infrequent, colorless, thin-walled, rarely branched, 3.2–6.9 µm in diam; skeleto-binding hyphae dominant, colorless, thick-walled with a narrow lumen, frequently branched, interwoven, 1.5–4.9 µm in diam.

Basidiospores – Basidiospores cylindrical, rarely oblong, colorless, thin-walled, smooth, occasionally bearing one or two guttules, IKI–, CB–, (5.9–)6.1–7.2(–7.9) × 2.6–3.3(–3.4) µm, L = 6.65 ± 0.46 µm, W = 2.95 ± 0.2 µm, Q = 1.88–2.67, Qm = 2.27 ± 0.2 (n=38/1).

Rot type – A white rot.

Known distribution – Subtropical regions of China.

Materials examined – China, Guangdong Province, Heyuan, Daguishan Forest Park, on fallen angiosperm branch, 18 Aug 2011, B.K. Cui, Cui 10123 (BJFC, holotype), Cui 10120 (BJFC, paratype).

Notes – *Picipes annularius* is a special species has buff pileus covered with annularly arranged beige to cinnamon-buff small squamae and obvious boundary between tubes and stipe. Its buff pileus, cream pore surface and short stipe are similar to those of *P. varius* (Pers.) Fr. But phylogenetically, *P. varius* belongs to the squamosus clade, while *Pi. annularius* clusters with *Picipes* spp. Morphologically, *P. varius* differs in having glabrous pileal surface, smaller pores (5–9 per mm), larger basidiospores (7.5–9 × 2.5–3.3 µm) and basidia (18–30 × 7–9 µm) according to the Chinese specimens.

Picipes atratus B.K. Cui, Xing Ji & J.L. Zhou, sp. nov.

Figs 4D, E, 8

Index Fungorum number: IF559397; Facesoffungi number: FoF 10645

Etymology – *atratus* (Lat.): referring to the black pileal surface when mature.

Basidiomata – Annual, centrally to laterally stipitate, scattered to gregarious, coriaceous to hard leathery when fresh, hard woody when dry. Pilei fan-shaped to irregularly semicircular, occasionally circular with a depressed center, projecting up to 5.8 cm long, 8.7 cm wide and 3 mm thick at base. Pileal surface white when fresh, becoming orange brown and finally black when dry, glabrous, occasionally zonate and with radially aligned stripes; margin straight. Pore surface white when young, becoming white to pale mouse-grey when mature; pores suborbicular, 7–9 per mm; dissepiments thin, entire. Context white when fresh, becoming buff when dry, up to 1 mm thick. Tubes concolorous with pore surface, decurrent on one side of the stipe, up to 2 mm thick. Stipe white with a black base when young, becoming entirely black when mature, bearing a black cuticle, glabrous, up to 1.5 cm long and 1 cm in diam.

Hyphal structure – Hyphal system dimitic; generative hyphae bearing clamp connections; skeleto-binding hyphae IKI–, CB+; tissues unchanged in KOH.

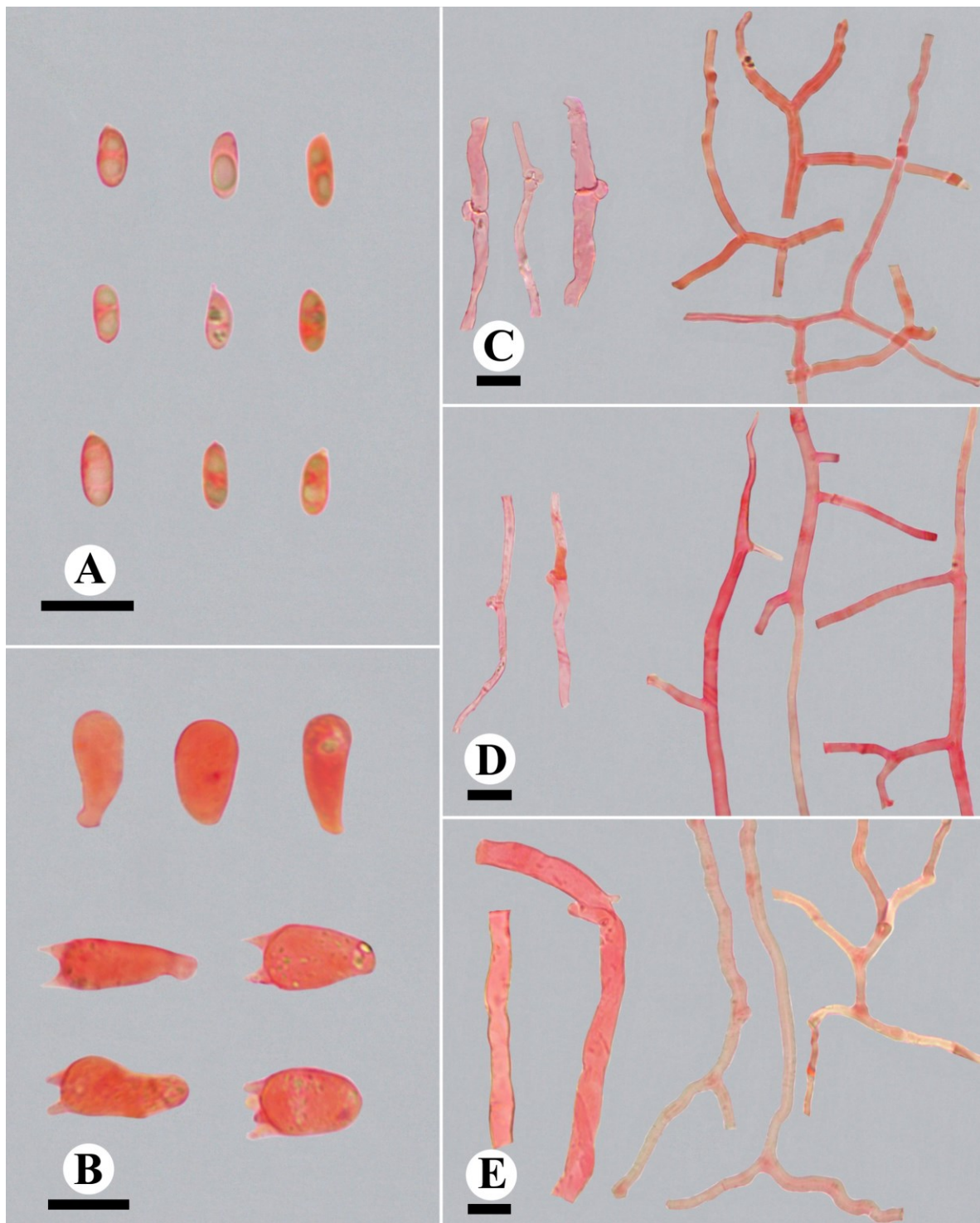


Figure 7 – Microscopic structures of *Picipes annularius*. A Basidiospores. B Basidia and basidioles. C Hyphae from context. D Hyphae from trama. E Hyphae from stipe. Scale bars = 10 μm .

Context – Generative hyphae infrequent, colorless, thin-walled, rarely branched, 1.2–4.3 μm in diam; skeleto-binding hyphae dominant, colorless, thick-walled with a narrow lumen to solid, with arboriform branches, strongly interwoven, 1.5–6.5 μm in diam. Hyphae in cuticle with olivaceous buff to light black inclusion inside, slightly thick-walled with a wide lumen, simple-septate, 3–4.5 μm in diam.

Tubes – Generative hyphae frequent, colorless, thin-walled, frequently branched, 1.5–5.5 μm in diam; skeleto-binding hyphae dominant, colorless, thick-walled with a narrow lumen to solid,

with arboriform branches, strongly interwoven, 1–5 μm in diam. Cystidia absent; cystidioles subulate, 13.5–19.5 \times 4–5 μm . Basidia clavate, with a basal clamp connection and four sterigmata, 11.2–18.5 \times 6.1–8.2 μm ; basidioles in shape similar to basidia, but slightly smaller.

Stipe – Generative hyphae infrequent, colorless, thin-walled, rarely branched, 1–3.7 μm in diam; skeleto-binding hyphae dominant, colorless, thick-walled with a narrow lumen to solid, with arboriform branches, strongly interwoven, 1–5 μm in diam. Hyphae in cuticle with olivaceous buff to light black inclusion inside, slightly thick-walled with a wide lumen, frequently branched, simple-septate, 1–5.6 μm in diam.

Basidiospores – Basidiospores cylindrical, colorless, thin-walled, smooth, frequently bearing one or more guttules, IKI–, CB–, (5.2–)5.6–7(–7.3) \times (2.3–)2.4–3(–3.1) μm , L = 6.21 \pm 0.39 μm , W = 2.74 \pm 0.15 μm , Q = 2–2.63, Qm = 2.27 \pm 0.14 (n=144/2).

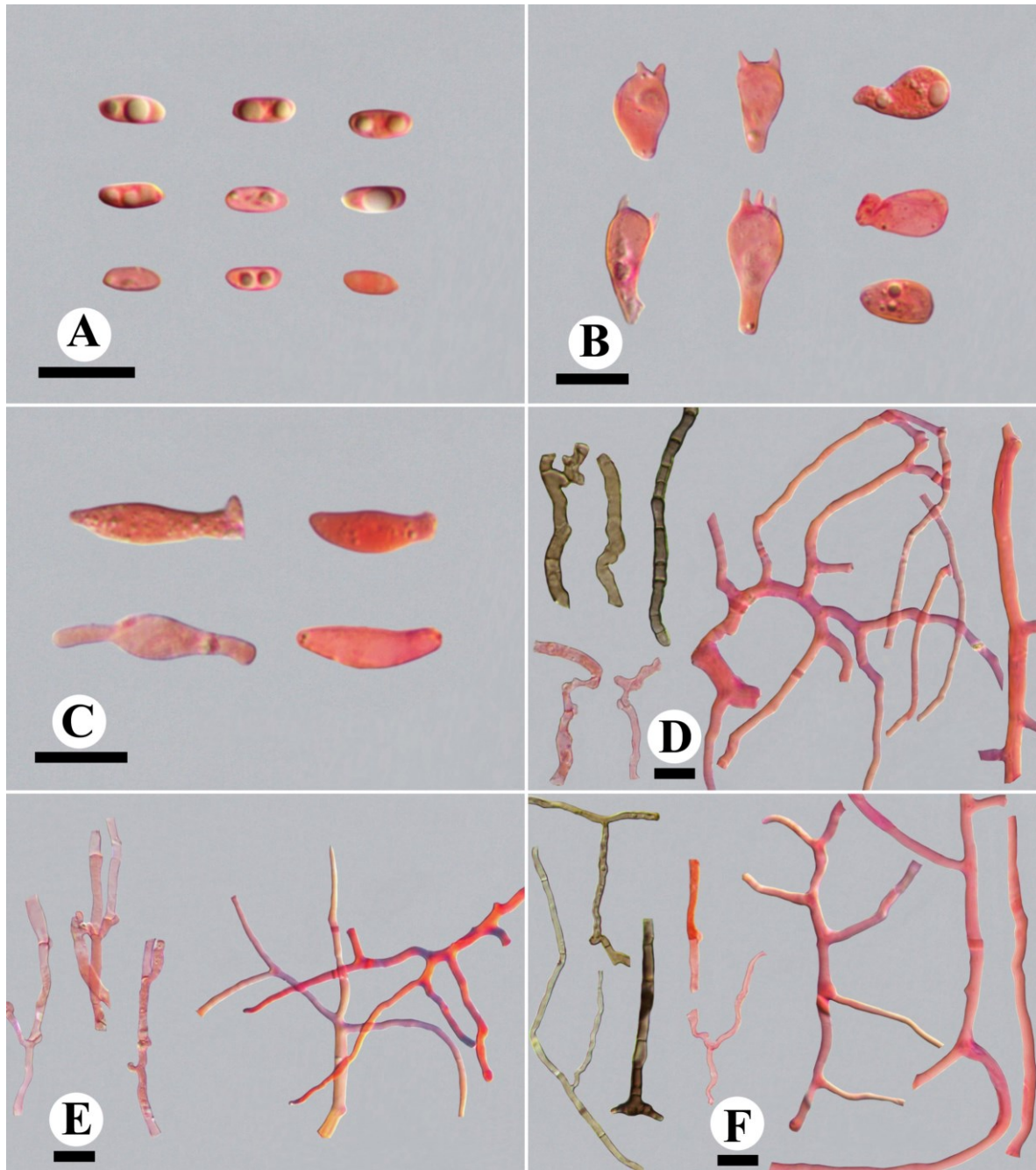


Figure 8 – Microscopic structures of *Picipes atratus*. A Basidiospores. B Basidia and basidioles. C Cystidioles. D Hyphae from context. E Hyphae from trama. F Hyphae from stipe. Scale bars = 10 μm .

Rot type – A white rot.

Known distribution – Subtropical regions of China.

Materials examined – China, Fujian Province, Wuping County, Liangyeshan Nature Reserve, on living angiosperm tree, 25 Oct 2013, B.K. Cui, Cui 11289 (BJFC, holotype); Anhui Province, Qimen County, Guniujiang Nature Reserve, on rotten angiosperm wood, 9 Aug 2013, Y.C. Dai, Dai 13375 (BJFC, paratype).

Notes – *Picipes atratus* is a special subtropical species with a black pileus and stipe in mature specimens. It is morphologically similar to *P. blanchettianus* Berk. & Mont. for the black pileus, black short stipe and similar pore size (7–10 per mm), but the absence of cystidioles, smaller basidia (10–11 × 5–6 µm) and basidiospores (5–6.2 × 2.2–2.5 µm) of *P. blanchettianus* are different from *Pi. atratus* (Ryvarden & Johansen 1980). Based on our own specimens, *Pi. badius* (Pers.) Zmitr. et Kovalenko also has blackish basidiomata when old, but its simple-septate generative hyphae, absence of cystidioles, larger pores (5–6 per mm) and basidia (20–30 × 7–9 µm) are different from *Pi. atratus*.

Picipes auriculatus B.K. Cui, Xing Ji & J.L. Zhou, sp. nov.

Figs 4F, 9

Index Fungorum number: IF559398; Facesoffungi number: FoF 10646

Etymology – *auriculatus* (Lat.): referring to the auricular basidiomata.

Basidiomata – Annual, laterally stipitate, solitary, coriaceous when fresh, woody hard when dry. Pilei auricular to fan-shaped, about 1.7–5 cm long, 1–3 cm wide, and up to 4.5 mm thick at base. Pileal surface blackish red to black towards the stipe when fresh, becoming brownish red to yellowish brown towards the margin when dry, glabrous, with radially aligned stripes; margin incurved upon drying. Pore surface light ivory to honey buff when dry; pores circular to subcircular, 4–6 per mm; dissepiments thin, entire. Context light ivory to buff when dry, woody hard upon drying, up to 3 mm thick. Tubes concolorous with pore surface, up to 1.5 mm thick. Stipe very short or forming a flattened base, bearing a black cuticle, up to 3 mm long and 4.5 mm in diam.

Hyphal structure – Hyphal system dimitic; generative hyphae bearing clamp connections; skeleto-binding hyphae IKI–, CB+; tissues unchanged in KOH.

Context – Generative hyphae infrequent, colorless, thin-walled, occasionally branched, 1.8–6 µm in diam; skeleto-binding hyphae dominant, colorless, thick-walled with a wide to narrow lumen, frequently branched, interwoven, 1.3–8.2 µm in diam, rarely inflated at the branching area. Hyphae in cuticle towards the stipe with buff yellow to reddish brown inclusion inside, thick-walled with a wide lumen, bearing clamp connections, 2.2–7.5 µm in diam.

Tubes – Generative hyphae infrequent, colorless, thin-walled, occasionally branched, 1.3–5.9 µm in diam; skeleto-binding hyphae dominant, colorless, thick-walled with a wide to narrow lumen, with dendroid branches, strongly interwoven, 1.3–7.1 µm in diam. Cystidia and cystidioles absent. Basidia infrequent, clavate, with a basal clamp connection and four sterigmata, 13.3–17.6 × 5.5–7.5 µm; basidioles in shape similar to basidia, but slightly smaller.

Stipe – Generative hyphae infrequent, colorless, thin-walled, occasionally branched, 1.6–4.8 µm in diam; skeleto-binding hyphae dominant, colorless, thick-walled with a narrow lumen, frequently branched, interwoven, 1.6–6 µm in diam. Hyphae in cuticle with buff yellow to brown inclusion inside, thick-walled with a wide lumen, bearing clamp connections, 4–8.8 µm in diam.

Basidiospores – Basidiospores cylindrical, rarely oblong, colorless, thin-walled, smooth, frequently bearing two guttules, IKI–, CB–, (5.4–)5.8–6.8(–7) × (2.4–)2.5–3.2(–3.4) µm, L = 6.27 ± 0.35 µm, W = 2.82 ± 0.21 µm, Q = 1.8–2.69, Qm = 2.24 ± 0.18 (n=72/2).

Rot type – A white rot.

Known distribution – Tropical regions of China.

Materials examined – China, Hainan Province, Baisha County, Yinggeling Nature Reserve, on fallen angiosperm branch, 17 Nov 2015, B.K. Cui, Cui 13616 (BJFC, holotype); Changjiang County, Bawangling Nature Reserve, on fallen angiosperm branch, 12 Nov 2007, H.S. Yuan, Yuan 4221 (IFP, paratype).

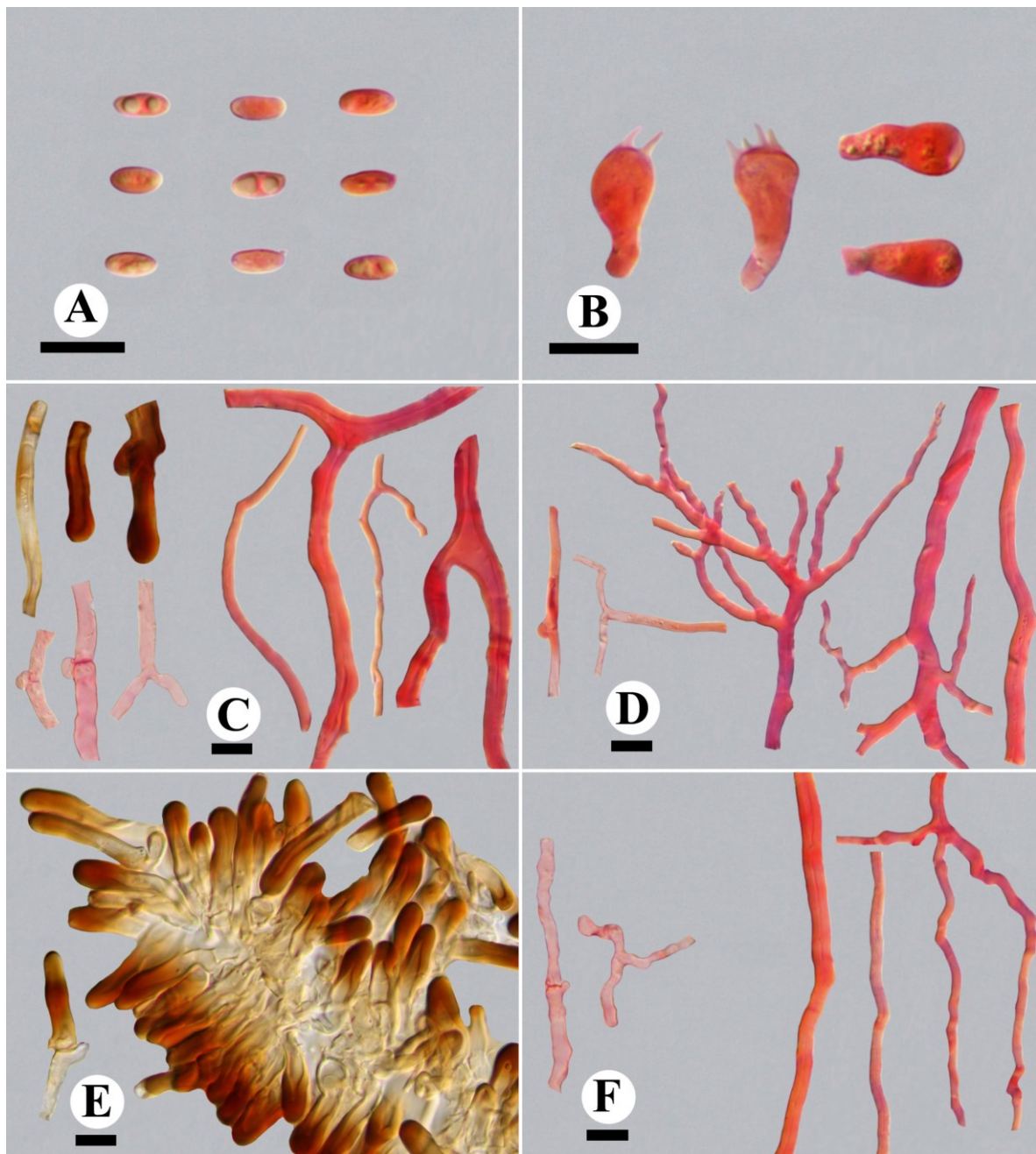


Figure 9 – Microscopic structures of *Picipes auriculatus*. A Basidiospores. B Basidia and basidioles. C Hyphae from context. D Hyphae from trama. E Hyphae from cuticle of stipe. F Hyphae from stipe. Scale bars = 10 μm .

Notes – *Picipes auriculatus* is a tropical species with an auricular basidiomata, yellowish brown to black pileus and a very short black stipe. *Picipes subtubaeformis* J.L. Zhou & B.K. Cui resembles *Pi. auriculatus* by sharing similar pores (4–6 per mm) and basidiospores ($5.7\text{--}6.8 \times 2.7\text{--}3.1 \mu\text{m}$, Zhou et al. 2016a), but its central to lateral stipe, subulate cystidioles, longer basidia ($15.7\text{--}29 \times 5.1\text{--}6.2 \mu\text{m}$) and subtropical distribution are different from *Pi. auriculatus*. *Picipes subtropicus* J.L. Zhou & B.K. Cui also has blackish pileal surface towards the stipe, a very short black stipe, similar basidiospores ($5.1\text{--}6.2 \times 2.2\text{--}2.7 \mu\text{m}$) and subtropical distribution; however, the fan-shaped to semicircle basidiomata and subulate cystidioles (Zhou et al. 2016a) are different from *Pi. auriculatus*.

Picipes brevistipitatus B.K. Cui, Xing Ji & J.L. Zhou, sp. nov.
Index Fungorum number: IF559399; Facesoffungi number: FoF 10647

Figs 5A, 10

Etymology – *brevistipitatus* (Lat.): referring to the basidiomata rising from a very short stipe.

Basidiomata – Annual, laterally stipitate, solitary, woody hard when dry. Pilei fan-shaped to irregularly semicircular, projecting up to 2 cm long, 3.1 cm wide and 4.5 mm thick at base. Pileal surface cream, buff to olivaceous buff when dry, glabrous, occasionally zonate and with radially aligned stripes; margin straight. Pore surface pale mouse-grey when dry; pores suborbicular, 3–6 per mm; dissepiments thin, entire. Context buff when dry, woody hard upon drying, up to 2.5 mm thick. Tubes concolorous with pore surface, decurrent on one side of the stipe, up to 2 mm thick. Stipe very short or forming a flattened base, concolorous with pileal surface, glabrous, up to 4 mm long and 8.5 mm in diam.

Hyphal structure – Hyphal system dimitic; generative hyphae bearing clamp connections; skeleto-binding hyphae IKI–, CB+; tissues unchanged in KOH.

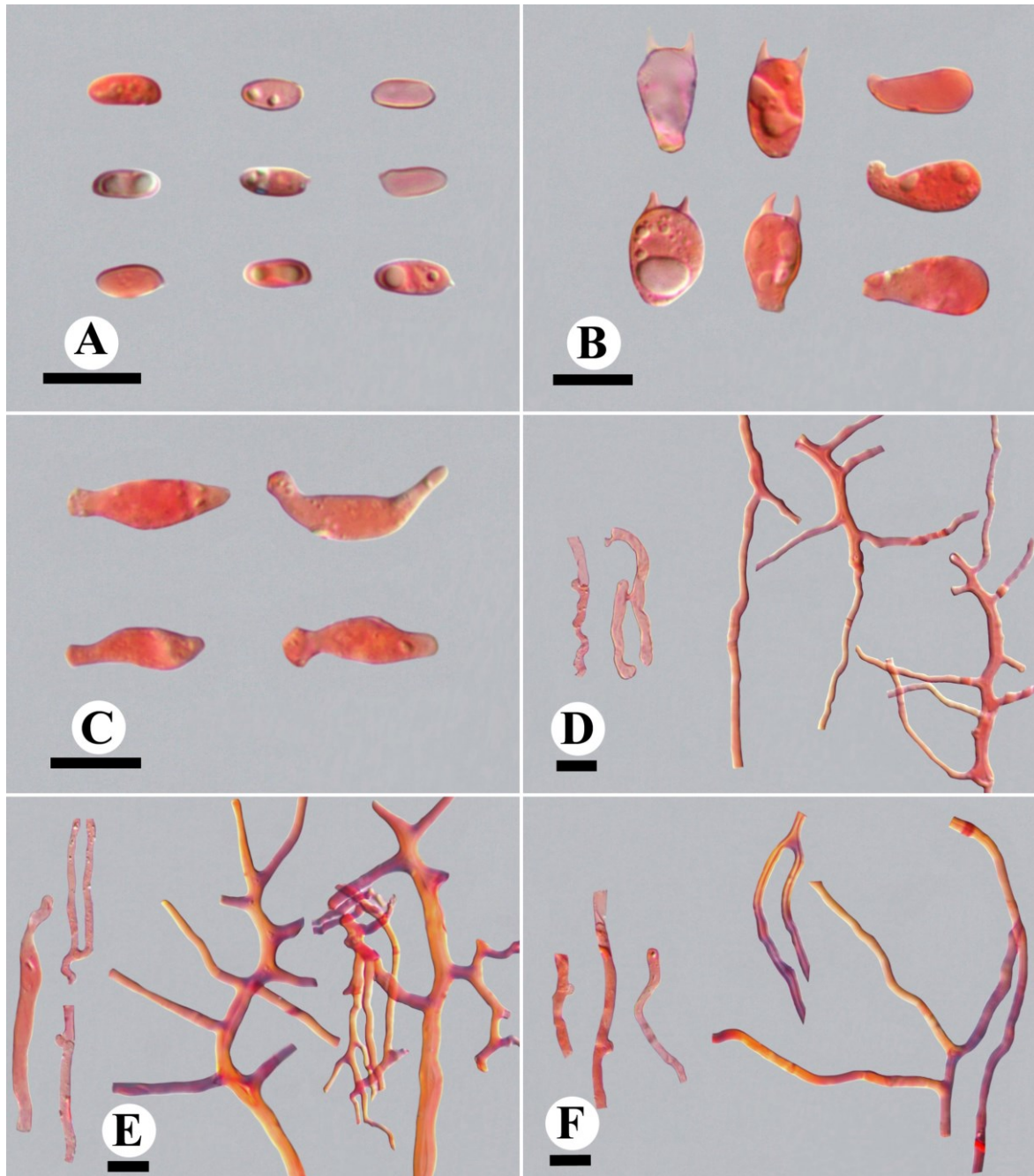


Figure 10 – Microscopic structures of *Picipes brevistipitatus*. A Basidiospores. B Basidia and basidioles. C Cystidioles. D Hyphae from context. E Hyphae from trama. F Hyphae from stipe. Scale bars = 10 μ m.

Context – Generative hyphae infrequent, colorless, thin-walled, occasionally branched, 1.5–3.5 µm in diam; skeleto-binding hyphae dominant, colorless, thick-walled with a wide to narrow lumen or solid, with arboriform branches, strongly interwoven, 1.5–4 µm in diam.

Tubes – Generative hyphae frequent, colorless, thin-walled, occasionally branched, 1.5–5.5 µm in diam; skeleto-binding hyphae dominant, colorless, thick-walled with a wide to narrow lumen or solid, with arboriform branches, strongly interwoven, 1–6 µm in diam. Cystidia absent; cystidioles subulate, 15–25.5 × 4.5–5.8 µm. Basidia oblong to clavate, with a basal clamp connection and four sterigmata, 12.5–15.5 × 4.8–9.6 µm; basidioles clavate, slightly smaller than basidia.

Stipe – Generative hyphae frequent, colorless, thin-walled, rarely branched, 1.5–3.6 µm in diam; skeleto-binding hyphae dominant, colorless, thick-walled with a wide to narrow lumen or solid, moderately branched, interwoven, 1–4.5 µm in diam.

Basidiospores – Basidiospores cylindrical, rarely oblong, colorless, thin-walled, smooth, frequently bearing one or more guttules, IKI–, CB–, (5.7–)5.9–7.1(–7.7) × (2.6–)2.7–3.4(–3.8) µm, L = 6.54 ± 0.39 µm, W = 2.98 ± 0.22 µm, Q = 1.84–2.73, Qm = 2.2 ± 0.15 (n = 85/3).

Rot type – A white rot.

Known distribution – Tropical and subtropical regions of China.

Materials examined – China, Hainan Province, Qiongzong County, Limushan Forest Park, on fallen angiosperm branch, 18 Nov 2015, B.K. Cui, Cui 13652 (BJFC, holotype), Cui 13657 (BJFC, paratype); Fujian Province, Xiamen, Xiamen Botanical Garden, on fallen angiosperm branch, 27 Oct 2013, B.K. Cui, Cui 11345 (BJFC, paratype).

Notes – *Picipes brevistipitatus* is a species collected from subtropical and tropical regions of China, it is characterized by the very short stipe that concolorous with pileus, cream to buff pileal surface with radially aligned stripes and pale mouse-grey pore surface. This species is similar to *Pi. pumilus* (Y.C. Dai & Niemelä) J.L. Zhou & B.K. Cui, both of them have light colored pileus, pale pore surface and similar basidiospores; however, *Pi. pumilus* has smaller pores (8–10 per mm), lacks radially aligned stripes on the pileal surface and absence of cystidioles (Dai et al. 2003). *Polyporus gayanus* Lév. also has a very short stipe, but its larger pores (2–3 per mm), orbicular basidiomata, light brown pileus with dark fibrils towards the margin and larger basidia (17.5–20 × 6.5 µm, Núñez & Ryvarden 1995a) are different from *Pi. brevistipitatus*.

Picipes nigromarginatus B.K. Cui, Xing Ji & J.L. Zhou, sp. nov.

Figs 5B, 11

Index Fungorum number: IF559400; Facesoffungi number: FoF 10648

Etymology – *nigromarginatus* (Lat.): referring to the black margin of the basidiomata when dry.

Basidiomata – Annual, laterally stipitate, solitary, coriaceous when fresh and hard corky when dry. Pilei fan-shaped to semicircular, projecting up to 2.2 cm long, 3.4 cm wide and 3 mm thick at base. Pileal surface festucine to honey-yellow when fresh, becoming reddish brown when dry, glabrous, zonate, with radially aligned stripes; margin black, straight. Pore surface greyish buff when dry; pores subcircular, 7–9 per mm; dissepiments thin, entire. Context buff and woody hard corky upon drying, up to 2 mm thick. Tubes clay brown and hard corky upon drying, less than 1.5 mm thick, decurrent on one side of the stipe. Stipe short, concolorous with pileal surface, glabrous, up to 5 mm long and 4 mm in diam.

Hyphal structure – Hyphal system dimitic; generative hyphae bearing clamp connections; skeleto-binding hyphae IKI–, CB+; tissues unchanged in KOH.

Context – Generative hyphae infrequent, colorless, thin-walled, rarely branched, 2–6.5 µm in diam; skeleto-binding hyphae dominant, colorless, thick-walled with a wide to narrow lumen, moderately branched, interwoven, 1.5–4.8 µm in diam.

Tubes – Generative hyphae frequent, usually present near hymenium, colorless, thin-walled, 1.8–4.2 µm in diam; skeleto-binding hyphae dominant, thick-walled with a wide to narrow lumen, with dendroid branches, strongly interwoven, 1.2–6.6 µm in diam. Cystidia absent; cystidioles

frequent, subulate, $14.2\text{--}17.2 \times 4.7\text{--}5.5 \mu\text{m}$. Basidia clavate, with a basal clamp connection and four sterigmata, $11.4\text{--}18.7 \times 6.2\text{--}7.9 \mu\text{m}$; basidioles in shape similar to basidia, but slightly smaller.

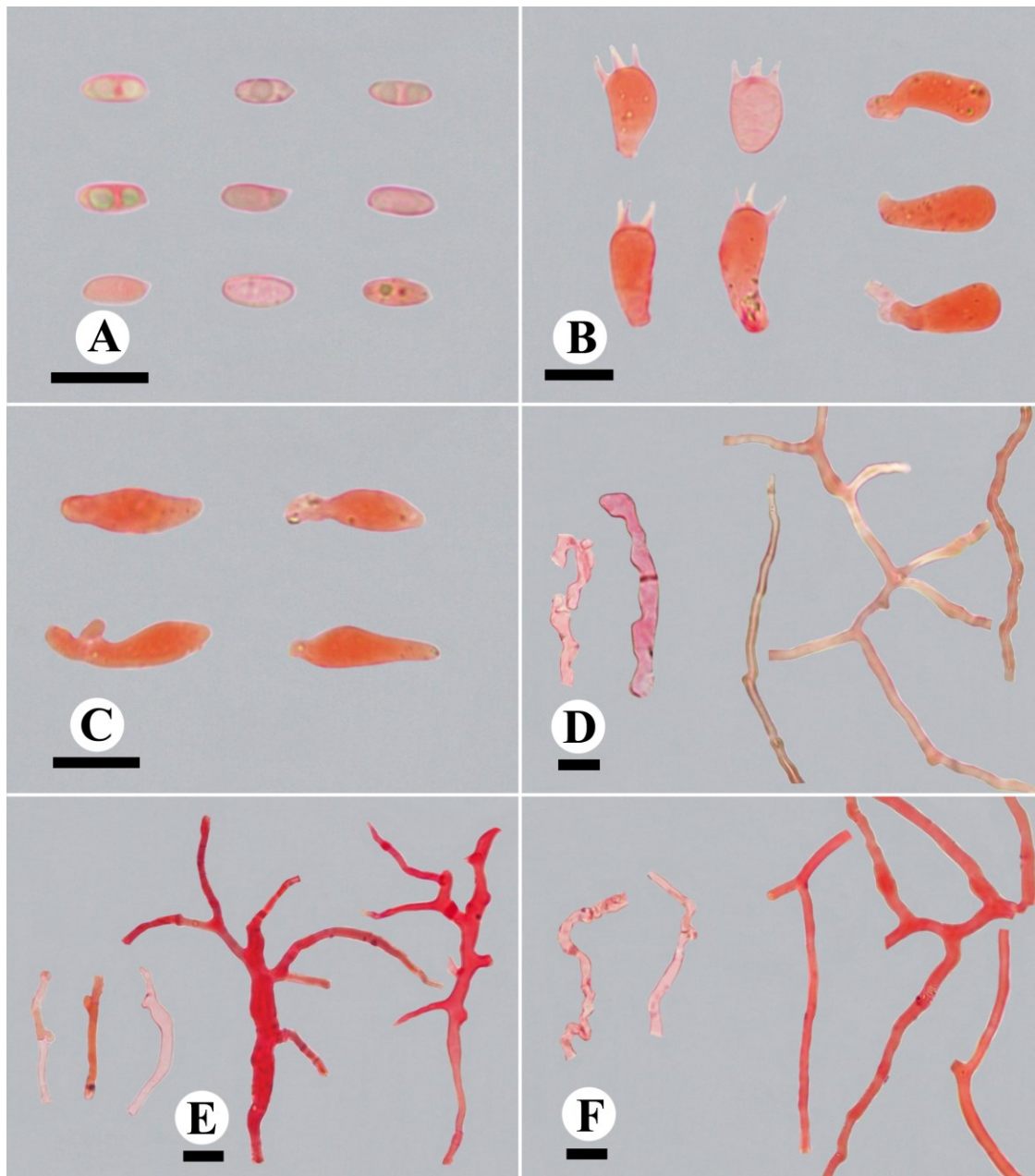


Figure 11 – Microscopic structures of *Picipes nigromarginatus*. A Basidiospores. B Basidia and basidioles. C Cystidioles. D Hyphae from context. E Hyphae from trama. F Hyphae from stipe. Scale bars = 10 μm .

Stipe – Generative hyphae infrequent, colorless, thin-walled, rarely branched, $1.8\text{--}5.1 \mu\text{m}$ in diam; skeleto-binding hyphae dominant, colorless, thick-walled with a narrow lumen to solid, moderately branched, interwoven, $1.3\text{--}5.1 \mu\text{m}$ in diam.

Basidiospores – Basidiospores cylindrical, colorless, thin-walled, smooth, frequently bearing one or two guttules, IKI–, CB– or slightly CB+, $(5.2\text{--})5.6\text{--}6.9(-7.4) \times 2.3\text{--}3(-3.2) \mu\text{m}$, $L = 6.31 \pm 0.55 \mu\text{m}$, $W = 2.64 \pm 0.22 \mu\text{m}$, $Q = 2.03\text{--}2.87$, $Q_m = 2.4 \pm 0.2$ ($n=37/1$).

Rot type – A white rot.

Known distribution – Subtropical regions of China.

Materials examined – China, Yunnan Province, Baoshan, Gaoligongshan Nature Reserve, on fallen angiosperm branch, 25 Oct 2009, B.K. Cui, Cui 8113 (BJFC, holotype), 26 Oct 2009, B.K. Cui, Cui 8191 (BJFC, paratype).

Notes – *Picipes nigromarginatus* is a subtropical species that lacks a brown to black cuticle on the stipe. It can be identified by the reddish brown pileal edge and laterally short stipe. *Picipes nigromarginatus* phylogenetically clustered with *Pi. brevistipitatus* (Figs 2, 3), they sharing similar pileus and basidiospores, but the larger pores (3–6 per mm) and buff pileal margin of *Pi. brevistipitatus* are different from *Pi. nigromarginatus*. *Picipes fraxinicola* (L.W. Zhou & Y.C. Dai) J.L. Zhou & B.K. Cui also has a laterally short stipe without a black cuticle, but it differs from *Pi. nigromarginatus* in the larger pores (2–4 per mm), larger basidiospores ($5-8 \times 2.8-3.7 \mu\text{m}$), absence of cystidioles and temperate distribution (Dai 1999).

Picipes wuyishanensis B.K. Cui, Xing Ji & J.L. Zhou, sp. nov.

Figs 5C, 12

Index Fungorum number: IF559401; Facesoffungi number: FoF 10649

Etymology – *wuyishanensis* (Lat.): referring to the locality (Wuyishan) of the type specimen.

Basidiomata – Annual, laterally stipitate, solitary, hard corky when dry. Pilei semicircular, projecting up to 2.9 cm long, 3.9 cm wide and 6 mm thick at base. Pileal surface buff towards the stipe and darker towards the margin when dry, glabrous; margin brownish red to black, with radially aligned stripes, straight. Pore surface beige grey to pearl beige when dry; pores angular, 3–5 per mm; dissepiments thin, entire. Context buff to buff yellow when dry, hard corky, up to 3 mm thick. Tubes concolorous with pore surface, up to 4 mm thick. Stipe short, concolorous with the pileal surface, bearing a black cuticle at the base, up to 5 mm long and 1 cm in diam.

Hyphal structure – Hyphal system dimitic; generative hyphae bearing clamp connections; skeleto-binding hyphae IKI–, slightly CB+; tissues unchanged in KOH.

Context – Generative hyphae infrequent, colorless, thin-walled, occasionally branched, 2–6.5 μm in diam; skeleto-binding hyphae dominant, colorless, thick-walled with a narrow lumen to solid, frequently branched, strongly interwoven, 1.3–7.4 μm in diam.

Tubes – Generative hyphae infrequent, colorless, thin-walled, occasionally branched, 2–4.2 μm in diam; skeleto-binding hyphae dominant, colorless, thick-walled with a narrow lumen to solid, with dendroid branches, strongly interwoven, 1.5–5.5 μm in diam. Cystidia absent; cystidioles frequent, subulate, 12.3–24 \times 4–6.9 μm . Basidia infrequent, oblong to clavate, with a basal clamp connection and four sterigmata, 11–14.5 \times 6.2–8.9 μm ; basidioles in shape similar to basidia, but slightly smaller.

Stipe – Generative hyphae infrequent, colorless, thin-walled, occasionally branched, 2.5–5 μm in diam; skeleto-binding hyphae dominant, colorless, thick-walled with a wide to narrow lumen, frequently branched, strongly interwoven, 1.5–4.8 μm in diam. Hyphae in cuticle with brown inclusion inside, slightly thick-walled with a wide lumen, simple-septate, 2.2–5.4 μm in diam.

Basidiospores – Basidiospores cylindrical, colorless, thin-walled, smooth, frequently bearing two guttules, IKI–, CB–, (5.6–)6–6.9(–7.4) \times (2.4–)2.5–3(–3.4) μm , $L = 6.42 \pm 0.37 \mu\text{m}$, $W = 2.76 \pm 0.2 \mu\text{m}$, $Q = 2-2.77$, $Q_m = 2.33 \pm 0.17$ ($n = 72/2$).

Rot type. A white rot.

Known distribution – Subtropical regions of China.

Materials examined – China, Fujian Province, Wuyishan, Wuyishan Nature Reserve, on dead angiosperm tree, 22 Oct 2005, Y.C. Dai, Dai 7409 (IFP, holotype), on fallen angiosperm branch, 21 Oct 2013, B.K. Cui, Cui 11246 (BJFC, paratype).

Notes – *Picipes wuyishanensis* is well characterized by its buff pileus with radially aligned stripes, broad and short stipe with a black base. It has a close relationship with *Pi. annularius* according to the phylogenetic analyses (Figs 2, 3). Morphologically, both of them have laterally stipitate basidiomata, similar pore size and basidiospores, but the beige to cinnamon-buff small squamae on pileus and absence of cystidioles in *Pi. annularius* are different from *P. wuyishanensis*.

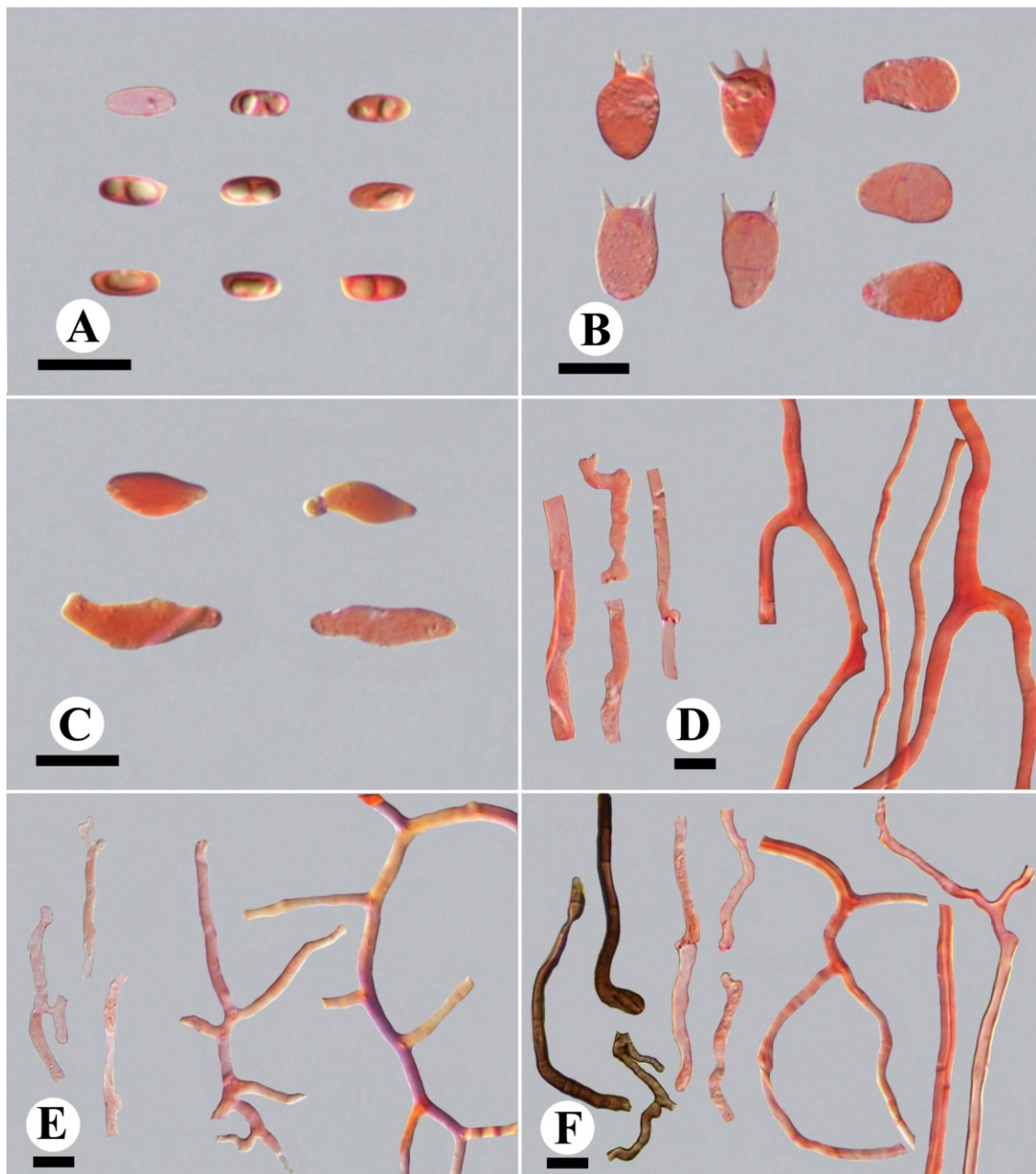


Figure 12 – Microscopic structures of *Picipes wuyishanensis*. A Basidiospores. B Basidia and basidioles. C Cystidioles. D Hyphae from context. E Hyphae from trama. F Hyphae from stipe. Scale bars = 10 μ m.

Polyporus auratus B.K. Cui, Xing Ji & J.L. Zhou, sp. nov.

Figs 5D, 13

Index Fungorum number: IF559402; Facesoffungi number: FoF 10650

Etymology – *auratus* (Lat.): referring to the golden yellow basidiomata when dry.

Basidiomata – Annual, centrally stipitate, gregarious, fleshy when fresh, becoming fragile and light in weight upon drying. Pilei flat with a depressed center when fresh, occasionally becoming infundibuliform upon drying, 1.7–6 cm in diam, up to 4 mm thick. Pileal surface cream to buff when fresh, becoming golden yellow when dry, glabrous, azonate, shining when dry; margin straight when fresh, in-curved upon drying. Pore surface white when fresh, becoming cinnamon when dry; pores angular, 3–4 per mm; dissepiments thin, entire to lacerate. Context white to cream when fresh, becoming buff when dry, up to 3.5 mm thick. Tubes concolorous with pore surface, fragile, decurrent, up to 1 mm thick. Stipe cylindrical, cream when fresh, buff to beige upon drying, up to 4 cm long and 6.5 mm in diam.

Hyphal structure – Hyphal system dimitic in trama and stipe, monomitic in context; generative hyphae bearing clamp connections; skeleto-binding hyphae IKI–, CB+; tissues unchanged in KOH.

Context – Generative hyphae colorless, slightly thick-walled, occasionally branched, with tapering ends, 3.8–12.1 µm in diam, occasionally inflated up to 19 µm in diam.

Tubes – Generative hyphae dominant, colorless, slightly thick-walled, occasionally branched, 1.5–6.8 µm in diam; skeleto-binding hyphae frequent, colorless, thick-walled with a wide lumen, occasionally branched, interwoven, 2–12.1 µm in diam, occasionally inflated up to 18 µm in diam. Cystidia and cystidioles absent. Basidia infrequent, clavate, with a basal clamp connection and four sterigmata, 15.3–26.7 × 6–9.1 µm; basidioles in shape similar to basidia, but slightly smaller.

Stipe – Generative hyphae frequent, colorless, slightly thick-walled, occasionally branched, 3.5–7.8 µm in diam; skeleto-binding hyphae dominant, colorless, thick-walled with a wide to narrow lumen, occasionally branched, interwoven, 2.5–24.5 µm in diam, occasionally inflated up to 34.5 µm in diam.

Basidiospores – Basidiospores cylindrical, rarely oblong, colorless, thin-walled, smooth, frequently bearing two guttules, IKI–, CB–, (6.9–)7.7–10 × 3–3.9 µm, L = 8.66 ± 0.67 µm, W = 3.45 ± 0.24 µm, Q = 2.1–2.93, Qm = 2.52 ± 0.2 (n = 57/1).

Rot type – A white rot.

Known distribution – Tropical regions of China.

Materials examined – China, Hainan Province, Changjiang County, Bawangling Nature Reserve, on rotten angiosperm wood, 16 Jun 2014, Y.C. Dai, Dai 13665 (BJFC, holotype), on fallen angiosperm branch, 18 Jun 2016, B.K. Cui, Cui 13878a (BJFC, paratype).

Notes – *Polyporus auratus* is characterized by its golden yellow and fragile basidiomata in dried condition. According to the phylogenetic analyses (Figs 2, 3), *P. auratus* is strongly clustered in the core polyporus clade with *P. tuberaster* and other four species. Morphologically, *P. auratus* is similar to *P. corylinus* Mauri for their glabrous and cream to buff pileal surface, circular pileus, white to cream pore surface and central stipe, but the later has larger pores (1 per mm; Núñez & Ryvarden 1995a) and smaller basidiospores (6–7.5 × 2–3 µm; Núñez & Ryvarden 1995a). *Polyporus craterellus* Berk. & M.A. Curtis resembles *P. auratus* by sharing centrally stipitate, flat pileus, fragile basidiomata upon drying and inflated skeleto-binding hyphae, but its basidiospores (10–14 × 4–6 µm; Núñez & Ryvarden 1995a) are much larger than *P. auratus*.

Polyporus austrosinensis B.K. Cui, Xing Ji & J.L. Zhou, sp. nov.

Figs 5E, 14

Index Fungorum number: IF559403; Facesoffungi number: FoF 10651

Etymology – *austrosinensis* (Lat.): referring to the species geographically distributed in southern China.

Basidiomata – Annual, centrally stipitate, solitary, fleshy to soft leathery when fresh, becoming fragile when dry. Pilei horn-shaped or flat with a depressed center, up to 6.3 cm in diam and 2 mm thick. Pileal surface cream, beige, buff yellow to orange when fresh, becoming buff to honey yellow when dry, glabrous, usually azonate; margin sharp, straight when fresh, incurved upon drying. Pore surface white when fresh, becoming yellow when bruised, turning to light ivory to buff when dry; pores angular, 4–7 per mm; dissepiments thin, entire. Context white, fleshy to soft leathery when fresh, becoming cream to ivory, fragile when dry, up to 2 mm thick. Tubes concolorous with pore surface or slightly lighter, decurrent, very thin, fragile when dry, less than 0.5 mm. Stipe white to ivory at the upper part and brown at the lower part when fresh, becoming ivory to buff at the upper part and beige brown to brown at the lower part when dry, glabrous, 1.5–3 cm long and 2.5–10 mm in diam.

Hyphal structure – Hyphal system dimitic; generative hyphae bearing clamp connections; skeleto-binding hyphae IKI–, CB+; tissues unchanged in KOH.

Context – Generative hyphae frequent, colorless, thin-walled, frequently branched, 2–8.8 µm in diam, occasionally inflated up to 14.8 µm in diam; skeleto-binding hyphae dominant, colorless,

thick-walled with a wide lumen, moderately branched, interwoven, 1.5–10 μm in diam, occasionally inflated up to 19 μm in diam.

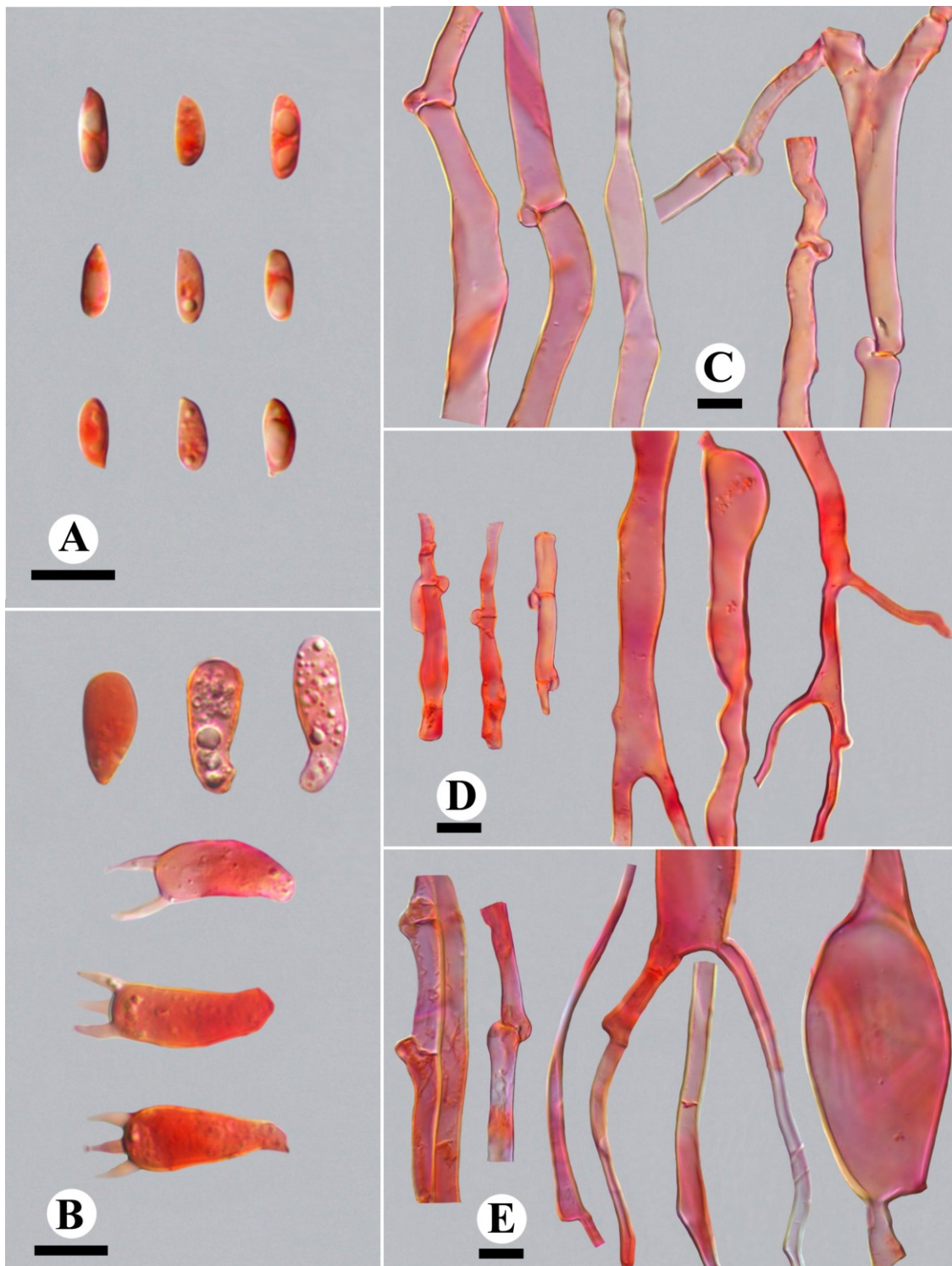


Figure 13 – Microscopic structures of *Polyporus auratus*. A Basidiospores. B Basidia and basidioles. C Hyphae from context. D Hyphae from trama. E Hyphae from stipe. Scale bars = 10 μm .

Tubes – Generative hyphae frequent, colorless, thin-walled, frequently branched, 2–5.5 μm in diam, occasionally inflated up to 8.7 μm in diam; skeleto-binding hyphae dominant, colorless, thick-walled with a wide lumen, moderately branched, interwoven, 1.5–7 μm in diam. Cystidia absent; cystidioles infrequent, bacciliform, 33–45 \times 5.4–6.5 μm . Basidia clavate, with a basal clamp

connection and four sterigmata, $22\text{--}45 \times 7.5\text{--}9.8 \mu\text{m}$; basidioles in shape similar to basidia, but slightly smaller.

Stipe – Generative hyphae frequent, colorless, thin-walled, occasionally branched, $3\text{--}8.5 \mu\text{m}$ in diam; skeleto-binding hyphae dominant, colorless, thick-walled with a wide to narrow lumen, infrequently branched, interwoven, $1.5\text{--}9 \mu\text{m}$ in diam, occasionally inflated up to $12.2 \mu\text{m}$ in diam. Hyphae in cuticle with brown beige to light brown inclusion inside, thick-walled with a wide lumen, bearing clamp connections, $2.3\text{--}5.6 \mu\text{m}$ in diam.

Basidiospores – Basidiospores cylindrical, colorless, thin-walled, smooth, occasionally bearing one small guttule, IKI–, CB–, $(6.7\text{--})7.5\text{--}10.6(\text{--}11.2) \times (2.9\text{--})3.3\text{--}4.4(\text{--}4.9) \mu\text{m}$, $L = 9.05 \pm 0.87 \mu\text{m}$, $W = 3.82 \pm 0.42 \mu\text{m}$, $Q = 2\text{--}2.86$, $Q_m = 2.4 \pm 0.21$ ($n = 69/2$).

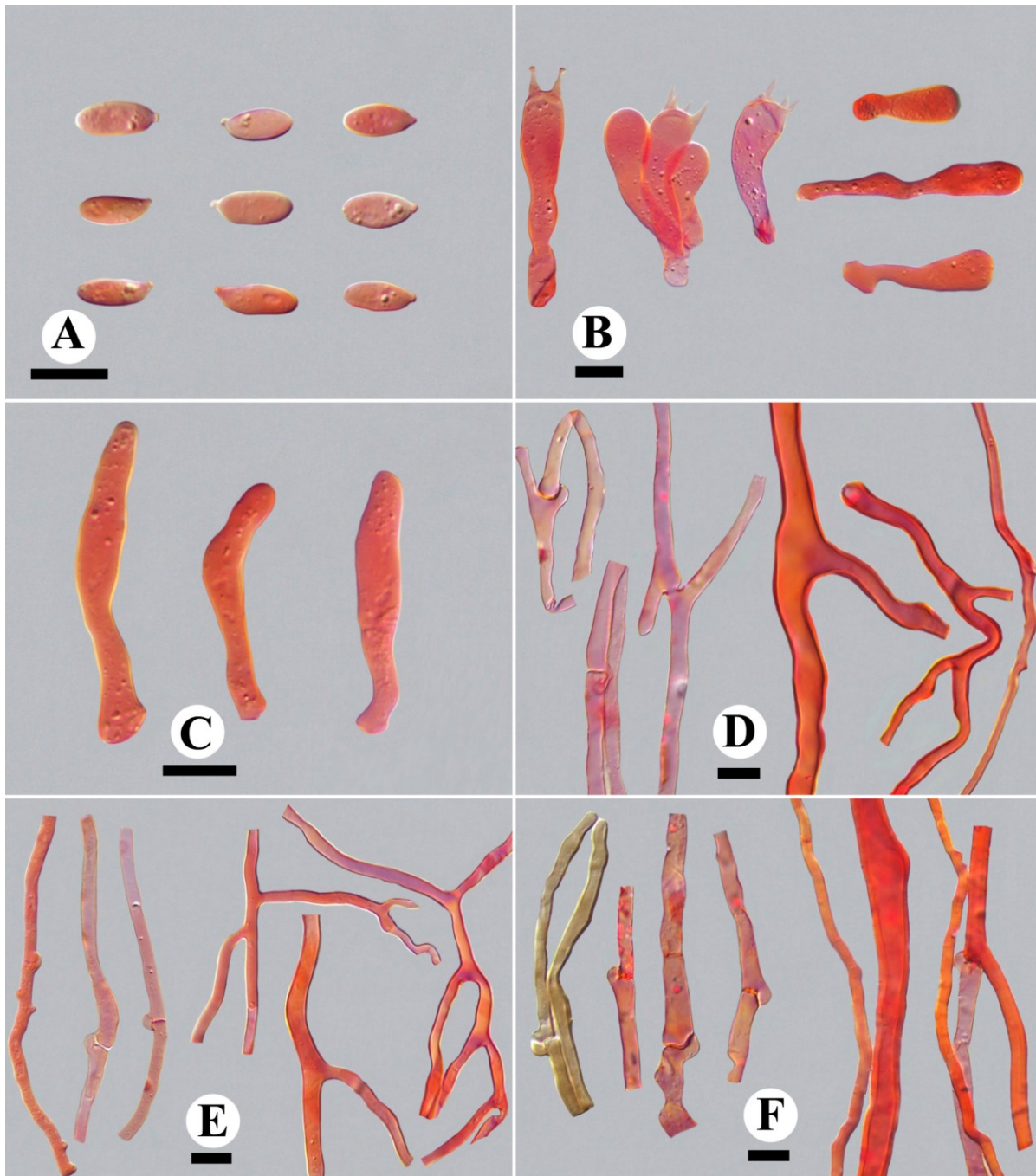


Figure 14 – Microscopic structures of *Polyporus austrosinensis*. A Basidiospores. B Basidia and basidioles. C Cystidioles. D Hyphae from context. E Hyphae from trama. F Hyphae from stipe. Scale bars = $10 \mu\text{m}$.

Rot type – A white rot.

Known distribution – Tropical and subtropical regions of China.

Material examined – China, Yunnan Province, Nanhua County, Dazhongshan Nature Reserve, on fallen angiosperm branch, 15 Jul 2013, B.K. Cui, Cui 11126 (BJFC, holotype), Cui 11123 (BJFC, paratype), Cui 11140 (BJFC, paratype); Hainan Province, Wuzhishan, Wuzhishan Nature Reserve, on angiosperm stump, 19 Nov 2015, B.K. Cui, Cui 13675 (BJFC, paratype).

Notes – *Polyporus austrosinensis* was found in subtropical to tropical regions of China, it is characterized by the fleshy to soft corky basidiomata when fresh, glabrous and cream to orange pileal surface, white pore surface which changed to yellow when bruised. Phylogenetic analyses (Figs 2 and 3) revealed that *P. austrosinensis* has a close relationship with *P. mangshanensis* B.K. Cui, J.L. Zhou & Y.C. Dai; morphologically, *P. austrosinensis* and *P. mangshanensis* share similar basidiospores and pores sizes, brown to dark brown stipe, glabrous pileal surface and inflated hyphae; however, *P. mangshanensis* has both clamped and simple-septate generative hyphae, eccentric to almost lateral stipe, smaller basidia (16.5–24 × 7–10 µm) and corky basidiomata when dry (Hyde et al. 2016). *Polyporus auratus* is similar to *P. austrosinensis* in having similar basidiomata of similar shape, white pore surface, inflated skeleto-binding hyphae, and basidiospores; however, *P. auratus* has larger pores (3–4 per mm), light colored stipe and lacks cystidioles.

Polyporus lamelliporus B.K. Cui, Xing Ji & J.L. Zhou, sp. nov.

Figs 5F, 15

Index Fungorum number: IF559404; Facesoffungi number: FoF 10652

Etymology – *lamelliporus* (Lat.): referring to the pores elongate and lacerate to form a lamellae-shaped structure.

Basidiomata – Annual, centrally stipitate, gregarious or clustered, corky to slightly fragile when dry. Pilei flat with a depressed center or infundibuliform, up to 5.2 cm in diam and 2 mm thick. Pileal surface cream to buff yellow when dry, glabrous and azonate; margin sharp, incurved upon drying. Pore surface buff yellow to light brown when dry; pores angular, usually elongate and lacerate to form lamellae-shaped hymenophores, 0.5–1 per mm, occasionally elongated to 3 mm long and 1.5 mm wide; dissepiments thin, entire to lacerate. Context cream to light ivory when dry, corky upon drying, up to 0.5 mm thick. Tubes lighter than pore surface, fragile when dry, decurrent, up to 1.8 mm thick. Stipe white to cream towards the tubes, brown to black at the lower part, glabrous, 1–3.5 cm long and 2.5–6 mm in diam.

Hyphal structure – Hyphal system dimitic; generative hyphae bearing clamp connections; skeleto-binding hyphae IKI–, slightly CB+; tissues unchanged in KOH.

Context – Generative hyphae frequent, colorless, thin-walled, frequently branched, 2–6 µm in diam, occasionally inflated up to 15.3 µm in diam; skeleto-binding hyphae dominant, colorless, thick-walled with a wide lumen, moderately branched, interwoven, 1.5–8 µm in diam, occasionally inflated up to 19 µm in diam in branching area.

Tubes – Generative hyphae frequent, colorless, thin-walled, frequently branched, 2–5 µm in diam; skeleto-binding hyphae dominant, colorless, thick-walled with a wide to narrow lumen, moderately branched, interwoven, 1.5–5 µm in diam. Cystidia and cystidioles absent. Basidia clavate, with a basal clamp connection and four sterigmata, 27–40 × 8–9.8 µm; basidioles in shape similar to basidia, but slightly smaller.

Stipe – Generative hyphae frequent, colorless, thin-walled, rarely branched, 2–11.5 µm in diam; skeleto-binding hyphae dominant, colorless, thick-walled with a wide to narrow lumen, moderately branched, interwoven, 1.3–8.5 µm in diam, occasionally inflated up to 12 µm in diam in branching area. Hyphae in cuticle with olive yellow to light brown inclusion inside, thick-walled with a wide lumen, bearing both clamp connections and simple-septa, 2.5–8 µm in diam.

Basidiospores – Basidiospores cylindrical, colorless, thin-walled, smooth, frequently bearing one or more guttules, IKI–, CB–, (7.9–)8.4–10.7(–11.5) × (3.3–)3.7–4.7(–4.7) µm, L = 9.42 ± 0.71 µm, W = 4.2 ± 0.25 µm, Q = 2–2.67, Qm = 2.25 ± 0.15 (n = 103/3).

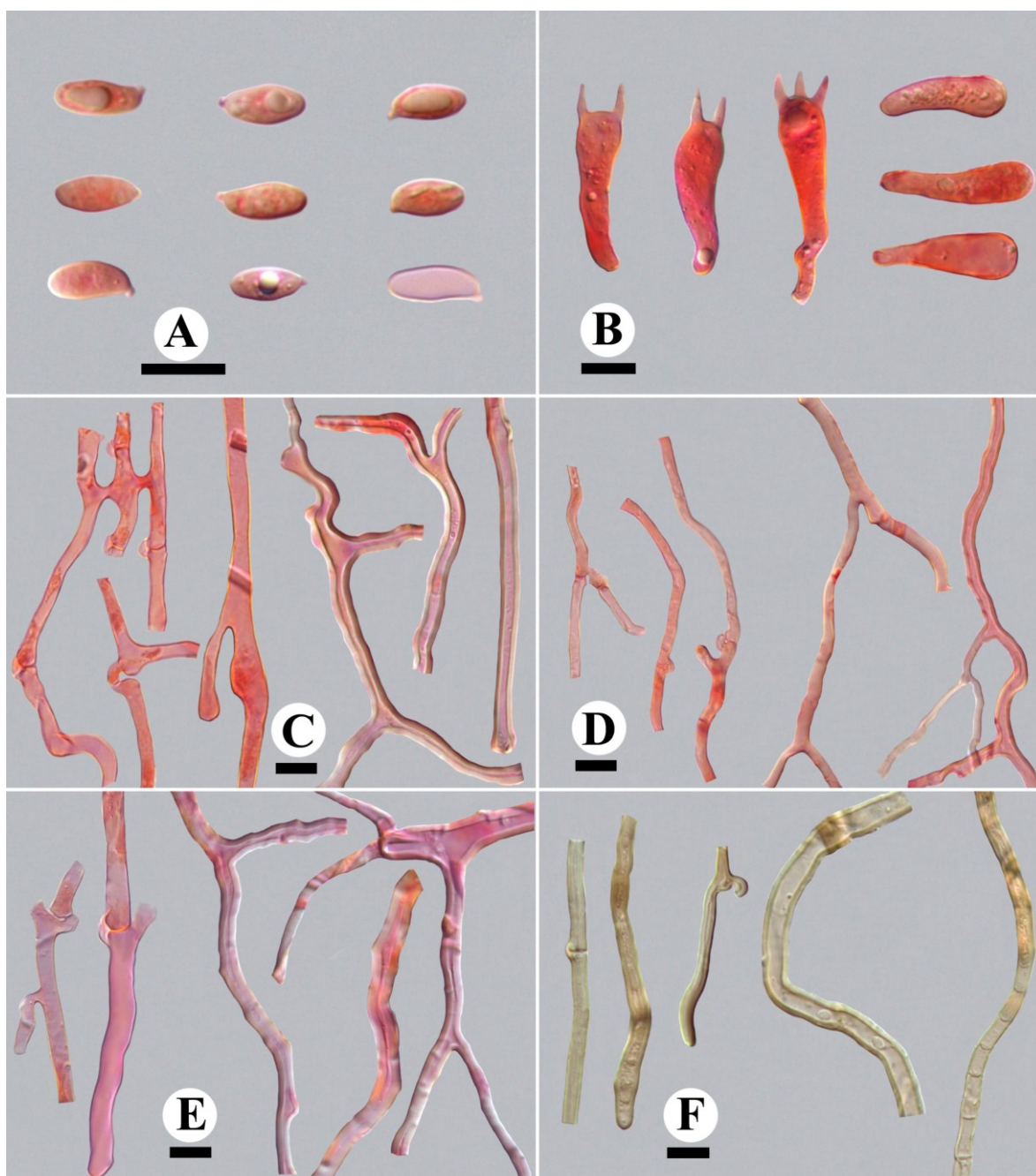


Figure 15 – Microscopic structures of *Polyporus lamelliporus*. A Basidiospores. B Basidia and basidioles. C Hyphae from context. D Hyphae from trama. E Hyphae from stipe. F Hyphae from cuticle of stipe. Scale bars = 10 μm .

Rot type – A white rot.

Known distribution – Tropical and subtropical regions of China.

Material examined – China, Hunan Province, Yizhang County, Mangshan Nature Reserve, on fallen bamboo, 15 Aug 2014, Y.C. Dai, Dai 15106 (BJFC, holotype), Dai 15103 (BJFC, paratype); Yunnan Province, Menghai County, Mangao Nature Reserve, on fallen angiosperm branch, 8 Jun 2011, Y.C. Dai, Dai 12327 (BJFC, paratype).

Notes – *Polyporus lamelliporus* was collected on both bamboo and hardwoods, it is characterized by centrally stipitate basidiomata with light-colored pileus, lamellae-shaped hymenophores, and brown to black stipe. *Polyporus meridionalis* (A. David) H. Jahn is similar to *P. lamelliporus* by sharing central and brown stipe, flat to infundibuliform pileus, large pores and inflated hyphae; but, the white pore surface and ellipsoid to amygdaliform basidiospores ($7\text{--}9 \times$

3.5–4 µm, Núñez & Ryvarden 1995a) are different from *P. lamelliporus*. *Polyporus phyllostachydis* Sotome, T. Hatt. & Kakish. was also collected from bamboo, its central stipitate basidiomata, brown to black stipe, glabrous pileus, and thick-walled skeleto-binding hyphae with a wide to narrow lumen are similar to *P. lamelliporus*; however, the former has both smaller pores (3–4 per mm) and basidiospores (5–7 × 2.5–4 µm), and simple-septate generative hyphae (Sotome et al. 2007). *Polyporus lamelliporus* resembles *P. guianensis* Mont. by sharing black stipe, light brown pore surface and yellowish pileal surface, but the later has somewhat smaller pores (1–2 per mm), shorter basidia (21–27 × 8–10 µm) and solid skeleto-binding hyphae (Núñez & Ryvarden 1995a, b).

New combinations

Picipes dictyopus (Mont.) B.K. Cui, Xing Ji & J.L. Zhou, comb. nov.

Index Fungorum number: IF559405; Facesoffungi number: FoF 10653

Basionym – *Polyporus dictyopus* Mont., Annales des Sciences Naturelles Botanique 3: 349. 1835.

≡ *Melanopus dictyopus* (Mont.) Pat., Essai taxonomique sur les familles et les genres des Hyménomycètes: 80. 1900.

Notes – In our previous study, *Picipes dictyopus* was clustered in the squamosus clade but with low supports (Zhou et al. 2016a). But, after adding more species collected from China, the sequence of *Pi. dictyopus* from type locality (Chile, Palacio et al. 2017) strongly clustered in the picipes clade (Figs 2, 3).

Picipes subdictyopus (H. Lee, N.K. Kim & Y.W. Lim) B.K. Cui, Xing Ji & J.L. Zhou, comb. nov.

Index Fungorum number: IF559406; Facesoffungi number: FoF 10661

Basionym – *Polyporus subdictyopus* H. Lee, N.K. Kim & Y.W. Lim, Fungal Diversity 83: 228. 2017.

Materials examined – China, Shaanxi Province, Zhashui County, Niubeiliang Forest Park, on living tree of *Prunus*, 16 Sep 2013, B.K. Cui, Cui 11220 (BJFC); Yunnan Province, Binchuan County, Jizu Mountain, on fallen angiosperm branch, 8 Sep 2015, B.K. Cui, Cui 12539 (BJFC); Jingdong County, Ailaoshan Nature Reserve, on fallen angiosperm branch, 10 Sep 2015, B.K. Cui, Cui 12593 (BJFC).

Notes – *Polyporus subdictyopus* was originally described from Korea (Tibpromma et al. 2017). Our specimens have almost the same micro-features and ITS sequences with the holotype, SFC20130719-53. However, our specimens have larger pores (4–6 per mm) and slightly shorter basidiospores (6.4–8.1 × 2.4–3.5 µm) than those given in the original description (pores 8–10 per mm, basidiospores 6.8–9.1 × 2.2–2.8 µm, Tibpromma et al. 2017).

Picipes ulleungus (H. Lee, N.K. Kim & Y.W. Lim) B.K. Cui, Xing Ji & J.L. Zhou, comb. nov.

Index Fungorum number: IF559407; Facesoffungi number: FoF 10654

Basionym – *Polyporus ulleungus* H. Lee, N.K. Kim & Y.W. Lim, Fungal Diversity 83: 229. 2017.

Material examined – China, Zhejiang Province, Qingyuan County, Baishanzu Nature Reserve, on fallen branch of *Cyclobalanopsis*, 12 Aug 2015, B.K. Cui, Cui 12410 (BJFC).

Notes – *Polyporus ulleungus* was originally described from Korea (Tibpromma et al. 2017). Our specimen has very similar character and almost the same ITS sequences with the holotype, SFC20120814-41. However, our specimen has larger basidiospores (7.5–9.7 × 3–3.7 µm) than that given in the original description (6.8–8 × 2.3–3.3 µm, Tibpromma et al. 2017).

Lentinus thailandensis (Sotome) B.K. Cui, Xing Ji & J.L. Zhou, comb. nov.

Index Fungorum number: IF559408; Facesoffungi number: FoF 10655

Basionym – *Polyporus thailandensis* Sotome, Mycoscience 57: 86. 2016.

Material examined – China, Yunnan Province, Xishuangbanna, Jinghong, Lvshilin Forest Park, on fallen bamboo, 4 Aug 2005, Y.C. Dai, Dai 6722 (BJFC).

Notes – *Lentinus thailandensis* was originally collected on hardwood from northeast Thailand (Sotome et al. 2016). But the specimen we collected from Xishuangbanna, located in tropical areas of China, grows on fallen bamboo. Our specimen has almost the same macro-features and ITS and nLSU sequences with the holotype, MSUT_6734. However, the basidiospores ($6.3\text{--}7.8 \times 2.9\text{--}4.0 \mu\text{m}$) of our specimen are much smaller than those given in the original description ($7\text{--}10.5 \times 3\text{--}4.5 \mu\text{m}$; Sotome et al. 2016).

Discussion

Divergence times

Because of lacking enough fossils, molecular clocks calibrated by the existing fossils are the only available tools to estimate timing of evolutionary events in fungi (Berbee & Taylor 2010). Based on the calibrations of two fossils of Agaricales and Hymenochaetales, we obtained the diverging relationships between *Polyporus* and its allied genera. Moreover, the divergence times of the main clades of Polyporales were also proved here.

Hibbett & Matheny (2009) considered that the Agaricales is significantly older than the rosids while Boletales appears to be young enough to have been primitively associated with Pinaceae. Previous results confirmed that the origin of crown group rosids ranged from 110 to 93 Mya (Wang et al. 2009) while the crown group Pinaceae diverged 184 or 136 Mya (Gernandt et al. 2008). Our results well conformed to the analyses provided by Hibbett & Matheny (2009).

Hennig (1966) first proposed that taxonomic ranking should represent its geological age. Then, Avise & John (1999) presented a scaling of taxonomic ranks by using the gene-specific molecular clocks, and proposed that each taxonomic genus might signify membership in a clade whose lineages shared a most recent common ancestor in the Pliocene (ca. 2–5 Mya), and each taxonomic order could indicate a clade whose coalescent node fell in the Jurassic (ca. 145–205 Mya). But these scales are not applicable to all the organisms (Zhao et al. 2016). Recently, Zhao et al. (2016, 2017) proposed a series of divergence time scales for different group of fungi.

In the present study, Polyporales is estimated to have a common ancestor evolved during the early Cretaceous. This result matched the divergence time ranges of orders proposed by Zhao et al. (2017). Although there are many species of Polyporales growing on gymnosperm substrates, most members of this order are limited on angiosperms or both on angiosperms and gymnosperms. So, we compared the divergence times of different clades of Polyporales with the originating and diversifying times of angiosperms (Fig. 1). The oldest fossil of angiosperms was dated to 136 Mya, and previously many botanists considered that angiosperms originated during the early Cretaceous (ca. 140–135 Mya; Brenner 1974, Gübeli et al. 1984, Hughes & McDougall 1987, Thusu et al. 1988), and rapidly diversified and dominated in the world during the early to middle Cretaceous (ca. 130–83 Mya; Lidgard & Crane 1988, Crane et al. 1995, Grimaldi 1999). But, based on the analysis of a three-gene dataset, Wikström et al. (2001) proved that the origin of the crown group of extant angiosperms dated to the early to middle Jurassic (ca. 179–158 Mya). Recently, many other botanists also confirmed the crown age for the angiosperms was at least 160 Mya (Moore et al. 2007, Smith et al. 2010, Bell et al. 2010, Magallón 2010, Doyle 2012, Zhang et al. 2012, Magallón et al. 2013, Zeng et al. 2014). According to the analysis of plastid genomes, Moore et al. (2007) confirmed that a rapid diversification of angiosperms occurred between 143.8 and 140.3 Mya. Our analysis indicates that the Polyporales originated at the beginning of the period when angiosperms rapidly diversifying, and then occurred a rapid diversification during the period when angiosperms dominated in the world. The inferred origination and rapid diversification of Polyporales corresponded with the variety and rapid rise of angiosperm-dominated forests may explain why most Polyporales spp. prefer to grow on the angiosperm woods.

As the saprotrophic wood-decay fungi, Polyporales spp. play a key role as decomposers and habitat creators in forest ecosystems (Binder et al. 2013, Norros et al. 2015). The great majority

members of Polyporales can be divided into two major groups: white-rot and brown-rot (Binder et al. 2013). According to our analysis (Fig. 1) based on the 5.8S+nLSU+EF1- α +RPB1+RPB2+nSSU dataset, it seems that species of Polyporales evolved from a common ancestor during the beginning of the Cretaceous, and then parallel diverged into the white-rot group and the brown-rot group at about 124 Mya and the core polyporoid clade, which is now treated as the Polyporaceae (Justo et al. 2017), diverged during the middle Cretaceous.

According to the divergence time estimation of *Polyporus* s. lat. in the current study, the six major clades of *Polyporus* are well supported as allied lineages originated during the early to middle Paleogene period. The divergence times of the picipes clade, the favolus clade, the neofavolus clade and the lentinus clade could effectively support the existence of the four specific genera, *Picipes*, *Favolus*, *Neofavolus* and *Lentinus*. In the squamosus clade, *Datronia* and several other genera are included, while most of them diverged less than 30 Mya. On the basis of the view proposed by Zhao et al. (2016), *Datronia* and other genera should be treated as subgenera of *Cerioporus* for their stem ages ca. 30 Ma. But, species in this clade is not monophyletic taxa and the genera gathered in this clade are morphologically different from each other. Though Zmitrovich & Kovalenko (2016) support the view combine species in squamosus clade into *Cerioporus*, we prefer not to treat this clade as a specific genus before more comprehensive phylogenetic and morphologic evidences are provided.

Phylogenetic analyses

Phylogenetic analyses of the genus *Polyporus* and related genera based on 8-gene loci (ITS, nLSU, nSSU, mtSSU, EF1- α , RPB1, RPB2 and TUB) were reconstructed in this study. The combined datasets of ITS+nLSU and ITS+nLSU+EF1- α +mtSSU+RPB1+RPB2+nSSU+TUB showed similar topologies although the later analysis has higher supports.

Core polyporus clade

Core polyporus clade, which diverged during the early Paleogene, is strongly supported in divergence time estimation, ITS+nLSU and the eight-gene mutiple dataset analyses (Figs 1–3). In this clade, the lectotype of *Polyporus* and five other *Polyporus* spp. are included. Among these species, *P. umbellatus* merely grows from a black sclerotium underground where close to stumps of hardwoods, *P. tuberaster* can grow both on hardwoods and on the ground from a blackish sclerotium (Núñez & Ryvarde 1995a), while others are restricted to hardwoods (Xue & Zhou 2014, Si & Dai 2016). As is shown in Fig. 3, *P. auratus*, *P. cuticulatus* Y.C. Dai, Jing Si & Schigel and an undescribed species are merely collected in the tropical area, *P. hapalopus* only distributes in subtropical region, *P. umbellatus* is limited in circumpolar zone while *P. tuberaster* can be found from temperate to tropical regions.

As the lectotype species of *Polyporus*, *P. tuberaster* was put into group *Polyporus* with *P. austroafricanus* Núñez & Ryvarde, *P. craterellus*, *P. radicans* Schwein., *P. squamosus* and *P. udus* Jungh (Núñez & Ryvarde 1995a). Krüger (2002) proposed that group *Polyporus* is polyphyletic taxa, and this conclusion has been proved by others (Sotome et al. 2008, Dai et al. 2014, Zmitrovich & Kovalenko 2016). In our present study, *P. radicans* has closer relationships with species in squamosus clade. *Polyporus austroafricanus*, *P. craterellus* and *P. udus* are not included in our phylogenetic analyses for lacking enough DNA sequences. But according to the analyses obtained by previous scholars, *P. craterellus* always clustered with *P. umbellatus* (Krüger 2002) while *P. udus* had an unclear phylogenetic position (Sotome et al. 2008). Recently, *P. udus* was combined into genus *Favolus* as *F. udus* (Jungh.) Zmitr. et Kovalenko (Zmitrovich & Kovalenko 2016).

Polyporus umbellatus was morphologically put into group *Dendropolyporus* for its sclerotia (Núñez & Ryvarde 1995a). Sotome et al. (2008) considered *P. umbellatus* as a phylogenetically distinct lineage from other species for its phylogenetic placement was not clarified. Recently, this species was treated as the type species of genus *Cladomeris* Quél. (Zmitrovich & Kovalenko 2016). Based on our analyses, *P. umbellatus* is strongly supported as a member of the core polyporus clade.

The core polyporus clade was treated as a natural group of *Polyporus* (Zhou et al. 2016a). Based on our own specimens collected from China, all species in this clade have fleshy basidiomata when fresh and brittle upon drying, inflated skeleton-binding hyphae, generative hyphae dominant to almost monomitic in trama or context and light-colored stipes (Zhou et al. 2016a). Based on the stem age, phylogenetic relationships and morphological features, here we prefer to treat the core polyporus clade as a specific group, *Polyporus* s. str., and characterize it with the following features: basidiomata annual, centrally to laterally stipitate or substipitate, fleshy when fresh, becoming brittle and light in weight when dry, pore surface white to cream in fresh condition, stipe light colored and without a blackish cuticle, a dimitic hyphal system with generative hyphae and skeleton-binding hyphae, generative hyphae dominant to almost monomitic in trama or context, skeleton-binding hyphae thick walled with a wide lumen and inflated, basidiospores cylindrical, hyaline and thin-walled, on hardwoods or developing from sclerotia buried in the ground, causing a white rot. Based on the above characters, we think *P. craterellus* and *P. udus* should be kept in *Polyporus* s. str. while *P. austroafricanus* and *P. radicans* should not.

Polyporus indigenus I.J. Araujo & M.A. de Sousa, *P. minutosquamosus* Runnel & Ryvar den and *P. sapurema* Möller are not analyzed in our present study for lacking specimens. All the above three species are described from tropical areas of South America, and both *P. indigenus* and *P. sapurema* grow on the ground from a sclerotium while *P. minutosquamosus* grow on dead hard wood (Gomes-Silva et al. 2012, Runnel & Ryvar den 2016). Based on the analyses proposed by Runnel & Ryvar den (2016), *P. minutosquamosus* is phylogenetically closely related to *P. tuberaster* and *P. hapalopus*. Morphologically, according to the description of Gomes-Silva et al. (2012) and Runnel & Ryvar den (2016), we think all the above three species should also be kept in *Polyporus* s. str.

Picipes clade

Picipes clade is sister taxa to the core polyporus clade but with low supports. Twenty-seven species, which include seven new species collected from tropical to subtropical areas of China, are contained in this clade (Figs 2, 3). Several species in this clade were initially treated as members of genus *Melanopus* Pat. for their black stipes (Patouillard 1887), then they were combined into genus *Polyporus* and treated as members of group *Melanopus* (Núñez & Ryvar den 1995a). Recently, this clade was treated as an individual genus according to the phylogenetical and morphological characters (Zmitrovich & Kovalenko 2016, Zhou et al. 2016a). In the present study, the diverged time also support this clade as an individual genus. So, in this article, we follow the views Zmitrovich & Kovalenko (2016) and Zhou et al. (2016a) proposed.

Núñez & Ryvar den (1995a) previously treated *P. centroafricanus* Núñez & Ryvar den, *P. guianensis*, *P. leprieurii* Mont., *P. mikawai* Lloyd, *P. nigrocristatus* Núñez & Ryvar den and *P. varius* as members of group *Melanopus*. But, based on the present analyses, *P. guianensis*, *P. leprieurii* and *P. varius* are strongly clustered in the squamosus clade (Fig. 3). Moreover, *P. mikawai* is now combined into genus *Neofavolus* and treated as *N. mikawai* (Sotome et al. 2013). Because of lacking specimens and DNA sequences, *P. centroafricanus* and *P. nigrocristatus* are not included in our present phylogenetic analyses.

Lineage A of picipes clade is strongly supported by both mutiple genes analyses (Figs 2, 3). This lineage contains twelve species of *Picipes*, including the type species, *Pi. badius*. Among these species, *Pi. badius*, *Pi. subtropicus* and *Pi. subtubaeformis* can be collected from subtropical area or tropical area, while other nine species are restricted to the regions with lower temperature. *Picipes badius* was previously put into *Royoporus* A.B. De (De 1996) for its simple septa, then it was included in the clade /Tubaeformis– “Phaeopodii” with *Pi. melanopus* (Pers.) Zmitr. & Kovalenko and *Pi. tubaeformis* (P. Karst.) Zmitr. & Kovalenko based on ITS+nLSU analysis (Krüger et al. 2006). Recently, Zmitrovich & Kovalenko (2016) defined the genus *Picipes* to substitute this clade, they characterized this genus by lignicolous, numerous branched skeletal with uninflated axial elements, numerous subsolid fibrohyphae in combination with small pores and dark-colored stipe cuticle. But as the *Pi. rhizophilus* (Pat.) J.L. Zhou & B.K. Cui and *Pi. fraxinicola*

were included in phylogenetic analysis, it made the lignicolous and dark-colored stipe not sufficient features to define genus *Picipes* (Zhou et al. 2016a).

Lineage B is tropical to subtropical taxa that merely supported by Bayesian analysis of the eight-gene multiple dataset (Fig. 3). Seven new species and four previously described ones are included in this lineage. Among these species, *Pi. brevistipitatus*, *Pi. nigromarginatus* and *Pi. pumilus* are substipitate and without a black cuticle on the stipe. *Picipes dictyopus* was initially described from temperate forest in Juan Fernández archipelago (Chile) (Pulgarín 2016, Palacio et al. 2017). But in the latest monographic about *Polyporus*, it was reported as a pantropical species (Núñez & Ryvarden 1995a). Based on morphological characters and mating type results, *Pi. dictyopus* was considered as a complex species (Núñez & Ryvarden 1995a, 2001). Recently, on the basis of the specimens collected from South America and the type specimens, Palacio et al. (2017) divided specimens of *Pi. dictyopus* complex into five species: *Atroporus diabolicus* (Berk.) Ryvarden (\equiv *Polyporus diabolicus* Berk.), *Atroporus rufoatratus* (Berk.) Palacio, Reck & Robledo (\equiv *Polyporus rufoatratus* Berk.), *Neodictyopus atlanticus* Palacio, Grassi & Robledo, *Neodictyopus dictyopus* (Mont.) Palacio, Robledo & Drechsler-Santos (\equiv *Polyporus dictyopus* Mont.) and *Neodictyopus gugiottae* Palacio, Robledo, Reck & Drechsler-Santos. Though these species were not added in our phylogenetic analyses, according to the phylogenetic analysis and morphological descriptions Palacio et al. (2017) provided, we think genera *Atroporus* Ryvarden and *Neodictyopus* Palacio, Robledo, Reck & Drechsler-Santos should be treated as synonyms of *Picipes*, and species in the former two genera should be transferred into *Picipes*.

Lineage C merely contains *Pi. submelanopus* in our analyses (Figs 2, 3). *Picipes submelanopus* was originally described from northeast of Qinghai-Tibetan Plateau and reported as a terraneous species that grows on the ground in *Picea* forest (Xue & Zhou 2012). But based on our own specimens, *Pi. submelanopus* can also be found in temperate region of China. Moreover, this species can also be collected both on hardwoods (e.g. *Berberis*) and softwoods (e.g. *Picea*).

Lineage D is well supported by the analyses using ITS+nLSU and the eight-gene multiple datasets (Figs 2, 3). The only two species clustered in this lineage were recently described from China and Korea (Zhou et al. 2016a, Tibpromma et al. 2017), both of them are limited in subtropical region. Morphologically, their black stipe, hard basidiomata in dried condition, uninflated hyphal and strongly branched skeleto-binding hyphae in trama are typical characteristics of *Picipes*.

Favolus clade and neofavolus clade

Favolus clade and neofavolus clade, which were divided from *Polyporus* group *Favolus*, are sister taxa that diverged at about 60 Mya from a common ancestor (Fig. 1). The divergence times can well support the above two clades as specific genera. Núñez & Ryvarden (1995a) initially put *P. alveolaris* (DC.) Bondartsev & Singer, *P. grammocephalus* Berk., *P. philippinensis* Berk. and *P. tenuiculus* (P. Beauv.) Fr. into the group *Favolus* according to morphological analyses. While *P. pseudobetulinus* (Murashk. ex Pilát) Thorn, Kotir. & Niemelä and *P. mikawai* were put into group *Admirabilis* and group *Melanopus*, respectively (Núñez & Ryvarden 1995a). Phylogenetically, it revealed that *P. pseudobetulinus* had closer relationships with *P. grammocephalus* and *P. tenuiculus* while *P. mikawai* closely related to *P. alveolaris* (Krüger 2002, Sotome et al. 2011). Recently, group *Favolus* was divided into two distinct genera viz. *Favolus* and *Neofavolus* based on the morphological studies and phylogenetic analyses of ITS+nLSU (Sotome et al. 2013). Based on the analyses of Sotome et al. (2013), the *P. grammocephalus* complex was divided into two distinct species viz. *F. acervatus* and *F. emerici* (Berk. ex Cooke) Imazeki while *P. tenuiculus* complex was divided into three viz. *F. brasiliensis*, *F. roseus* and *F. spathulatus* (Jungh.) Lév. This conclusion has been widely accepted by subsequent mycologists (Dai et al. 2014, Seelan et al. 2015, Sotome et al. 2016, Zmitrovich & Kovalenko 2016, Zhou et al. 2016a, Tibpromma et al. 2017, Zhou & Cui 2017). In our present study, eleven species and an undescribed one are included in the favolus clade while six species are contained in the neofavolus clade.

Almost all the species in favolus clade are restricted in tropical to subtropical regions except *F. acervatus* and *F. pseudobetulinus*. *Favolus pseudobetulinus* is a temperate species distributed in boreal areas of North America, East Asia and Europe (Thorn et al. 1990, Núñez & Ryvardeen 1995a, Schigel & Toresson 2005, Stome et al. 2011, Dai 2012). It was once treated as a member of *Piptoporus* P. Karst. and then combined into *Polyporus* by Thorn et al. (1990). Later, De (1998) put it into genus *Royoporus* with *P. badius* by the character lacking clamp-connections. But phylogenetic results revealed that the lack of clamp-connections is not a sufficient character to define a genus but can be used only at the species level (Sotome et al. 2011). *Favolus acervatus* was mainly collected from tropical and subtropical areas (Núñez & Ryvardeen 1995a), but it was recently reported in warm-temperate areas of China and Japan (Sotome et al. 2013, Zhou & Cui 2017). Sotome et al. (2013) considered that there may be more additional species of *Favolus* in tropical areas, and this conclusion had been recently proved. Five new species viz. *F. gracilisporus* H. Lee, N.K. Kim & Y.W. Lim, *F. niveus* J.L. Zhou & B.K. Cui, *F. pseudoemericus* J.L. Zhou & B.K. Cui, *F. septatum* J.L. Zhou & B.K. Cui and *F. subtropicus* J.L. Zhou & B.K. Cui collected from tropical and subtropical areas of East Asia were described and illustrated based on the morphological and phylogenetical analyses (Tibpromma et al. 2017, Zhou & Cui 2017). But, after comparing the ITS sequences and morphological descriptions, we find that *F. subtropicus* is a synonym for *F. gracilisporus*. Because the former one was published after the later, so, we should use *F. gracilisporus* as the correct name of this species.

Neofavolus clades is well supported in all trees and contains six species mainly collected from temperate and subtropical areas (Figs 1–3). Sotome et al. (2013) previously considered that all the known species of genus *Neofavolus* are known from temperate regions and unknown from the tropics. However, several samples of *N. mikawai* and *N. alveolaris* distributed in tropical areas of Hainan Province and Yunnan Province of China were collected (Zhou & Cui 2017). *Neofavolus squamatus* collected from Tibet is much different from other *Neofavolus* spp. by its yellowish orange squamae on the pileus and plateau distribution (Xing et al. 2020). For *N. americanus*, a temperate species collected from Connecticut of America, it has larger basidiospores ($10.4\text{--}12 \times 3.8\text{--}4.5 \mu\text{m}$, Xing et al. 2020) than other species in the *Neofavolus* clades. The specimen MA672 collected from Massachusetts state of America has almost the same ITS and nLSU sequences to our present species, but because of lacking its morphological descriptions, we could not confirm whether they are the same species or not. *Neofavolus cremeoalbidus* is a subtropical species originally described from Japan, it is distinct from other *Neofavolus* spp. in its thin and pale-colored basidiomata (Sotome et al. 2013). But when analyzing the samples collected from Zhejiang, located in subtropical areas of China, our specimens has somewhat smaller basidiospores ($8\text{--}10.7 \times 3\text{--}3.8 \mu\text{m}$) than those given in the original description ($8\text{--}12 \times 3\text{--}4 \mu\text{m}$, Sotome et al. 2013). *Neofavolus suavissimus* is a special one with gilled hymenophores. It was previously treated as a member of *Lentinus* and named *L. suavissimus* Fr. for a long time (Pegler 1983, Hibbett & Thorn 1994, Knudsen & Vesterholt 2012). Phylogenetical analyses revealed that it has much closer relationships with *Neofavolus* spp. than *Lentinus* spp. (Seelan et al. 2015, Zmitrovich & Kovalenko 2016, Zhou & Cui 2017).

Lentinus clade

Lentinus clade, evolved during the mid-Paleogene, is well supported in all trees and contains both poroid and gilled species (Figs 1–3). Six polyporoid species, which were previously treated as members of *Polyporus* group *Polyporellus*, and members of genus *Lentinus* are included in this clade (Figs 2, 3). It reveals that species in group *Polyporellus* have much closer relationships with *Lentinus* than other *Polyporus* spp. Krüger (2002) proposed to combine species in the group *Polyporellus* into genus *Lentinus*, but the new combinations were illegally published. Therefore, we accept the names Zmitrovich (2010) and Zmitrovich & Kovalenko (2016) provided.

Phylogenetically, three subclades were presented in the lentinus clade. All the four species clustered in lineage I are with poroid hymenophores. Among these species, *L. brumalis* (Pers.) Zmitr. has circular pores while other three species have angular pores. Geographically, *L.*

longiporus (Audet, Boulet & Sirard) Zmitr. & Kovalenko merely known from boreal areas in Canada and Japan, *L. substrictus* (Bolton) Zmitr. & Kovalenko is widespread in temperate area, *L. brumalis* is common in the Northern Hemisphere while *L. arcularius* (Batsch) Zmitr. is cosmopolitan except for the boreal region (Núñez & Ryvarde 1995a, Sotome et al. 2009). In addition, there are only two tropical species with poroid hymenophores in lineage III, *Lentinus thailandensis* and *L. flexipes*.

Species in lineage II are with lamellate hymenophores and morphologically treated as members of genus *Lentinus*. Among these species, *L. tigrinus* (Bull.) Fr. morphologically has subporoid hymenophore between lamellae and angular pores across the entire width of the pileus, while others are lamellaed (Hibbett et al. 1993, Seelan et al. 2015). *Lentinus* spp. occur from boreal to tropical regions and are widely documented in southeastern Asia (Seelan et al. 2015). Although *L. tigrinus* was reported in tropical areas, Grand et al. (2011) proved *L. tigrinus* merely has a Eurasian and north temperate distribution based on an ITS phylogeny and mating studies. Besides, Seelan et al. (2015) considered *L. tigrinus* as a sister group of *Polyporellus* in their four-gene phylogeny, but with low supports. According to our phylogenetic analyses, *L. tigrinus* reveals closer relationships with other gilled species than polyporoid ones, even though this conclusion is merely supported in the eight-gene phylogeny (Fig. 3).

Morphologically, almost all the species in this clade have central stipe without dark-colored cuticle, dimittic hyphal systems with generative hyphae and skeleto-binding hyphae, inflated hyphae and cylindrical basidiospores (Pegler 1983, Krüger 2002). *Lentinus* was previously considered to be derived from polyporoid species (Pegler 1983, Singer 1986), and this conclusion was subsequently validated according to the phylogenetic analyses (Hibbett & Vilgalys 1993, Hibbett & Donoghue 1995, Ko & Jung 2002, Krüger 2002, Krüger & Gargas 2004). Recently, Seelan et al. (2015) estimated that the ancestral hymenophoral configuration for species of *Lentinus* and *Polyporellus* group is circular pores, with independent transitions to angular pores and lamellae. Based on our present analysis (Fig. 3), the ancestral state for the *Lentinus* clade is estimated to be tropical organisms, with a dissemination to temperate and boreal regions.

Squamosus clade

Species belonging to seven distinct genera viz. *Datronia*, *Datroniella*, *Echinochaete*, *Mycobonia*, *Neodatronia*, *Polyporus* and *Pseudofavolus* are included in the squamosus clade, and this clade is well supported in all trees except parsimony analyses (Figs 1–3). Bayesian evolutionary analysis (Fig. 1) indicates that all these genera are congenetic and have a common ancestor evolved during the early Paleogene. Morphologically, most members in this clade share more or less crustate pileus or stipe although they have various morphologies of basidiomata and distribution patterns (Sotome et al. 2008).

Nine previously described *Polyporus* species and two undescribed ones are contained in this clade (Figs 2, 3). Among these species, *P. hemicapnodes* Berk. & Broome was initially described from Dolosbagey (Sri Lanka) by Berkeley & Broome, and then it was treated as a synonymy of *P. leprieurii* (Núñez & Ryvarde 1995a). Based on our specimens collected from China, though both of them have greyish pore surface, similar pore size and black stipe, *P. leprieurii* has flabelliform to sparhulate pileus, azonate pileal surface, larger basidia (20–30 × 8–10 µm; Núñez & Ryvarde 1995a) and narrower basidiospores (4.5–7 × 2–2.5 µm; Núñez & Ryvarde 1995a), while *P. hemicapnodes* has flat pileus with a depressed center or infundibuliform basidiomata, zonate pileal surface, smaller basidia (17–21 × 6.4–8.8 µm) and rounder basidiospores (5.4–7.6 × 2.9–3.8 µm). *Polyporus guianensis*, *P. leprieurii* and *P. varius* were morphologically put into group *Melanopus* while *P. radicans* and *P. squamosus* were put into group *Polyporus* (Núñez & Ryvarde 1995a). But the phlogenetic analyses reveal that they have much closer relationships with *Datronia* and other five genera than species in core polyporus clade and picipes clade. Morphologically, unlike species in the core polyporus clade, almost all the *Polyporus* species in the squamosus clade have brown to black cuticles on the stipes. Based on our present specimens collected from China,

Polyporus species in squamosus clade have brittle tubes and more or less brittle basidiomata when dry. These features are much different from those of species in the picipes clade.

Datronia was established based on the type species *D. mollis* (Sommerf.) Donk. (Donk 1966). This genus was previously proved to have a close relationship with *Polyporus* (Krüger 2002, Binder et al. 2005, Sotome et al. 2008, Ghobad-Nejhad & Dai 2010, Justo & Hibbett 2011, Sotome et al. 2013, Dai et al. 2014, Seelan et al. 2015, Zmitrovich & Kovalenko 2016). Recently, Li et al. (2014) divided this genus into three distinct genera viz. *Datronia*, *Datroniella* and *Neodatronia* based on the taxonomic and phylogenetic analyses. Although *Datronia*, *Datroniella* and *Neodatronia* produce resupinate to sessile basidiomata, brown context, tissues becoming black in KOH and brownish skeletal hyphae (Li et al. 2014), their dimitic hyphal system with clamped generative hyphae and thick-walled skeleto-binding hyphae, cylindrical basidiospores and white rotting habit are similar to those of *Polyporus* (Núñez & Ryvarden 1995a, 2001, Sotome et al. 2008, Li et al. 2014). Sotome et al. (2008) considered that the presence of the stipe alone might not be a sufficient character to morphologically characterize a phylogenetically differentiated polypore genus.

Pseudofavolus is a distinct genus characterized by the dimidiate basidiomata with a contracted base, tessulate upper surface, thin context, basidiomata becoming hard and brittle upon drying, cylindrical basidiospores longer than 13 µm and tropical distribution (Núñez & Ryvarden 1995a). However, Corner (1984) rejected *Pseudofavolus* as a segregate genus for its dextrinoid hyphae, dendrohyphidia, large basidiospores and thin context could also be found in *Polyporus*. Phylogenetic analyses also revealed *Pseudofavolus* is closely related to *Polyporus* (Krüger 2002, Sotome et al. 2008, Krüger & Gargas 2010). In our present study, *Pseudofavolus* nested in the squamosus clade with moderate support (Figs 2, 3). *Pseudofavolus cucullatus* (Mont.) Patouillard was transferred into *Polyporus* as a variety under *P. miquelii* Mont. (Corner 1984). Krüger (2002) and Krüger & Gargas (2010) also supported the opinion that *Pseudofavolus* should be included in *Polyporus*, but they prefer to choose *Polyporus curtipes* (Berk. & M.A. Curtis) Ryvarden as the valid name for *Ps. cucullatus* in *Polyporus*.

Mycobonia is a genus with hydroid hymenium that established by Patouillard (Jülich 1976). It was previously treated as a member of Thelephoraceae (Donk 1957) and then put into family Polyporaceae (Singer 1986). Corner (1984) considered that *Mycobonia* has a close relationship with *Pseudofavolus* and treated *M. flava* (Sw.) Pat. (the type species of *Mycobonia*) as a variety of *Ps. miquelii* without pores. Krüger & Gargas (2010) proposed that the hymenophore of *M. flava* is reduced to a flat surface as in corticioid and thelephoroid fungi, and the pore walls appear to have become isolated hyphal peg fascicles. While the brittle basidiomata in dried condition, basidiospores and basidia sizes of *M. flava* are similar to those of *P. squamosus* and several other species in squamosus clade (Krüger 2002, Krüger & Gargas 2010). Recently, *M. flava* was transferred into *Polyporus* as a subspecies of *P. curtipes* (Krüger 2002, Krüger & Gargas 2010). But, according to the phylogenetic analyses, *M. flava* seems to be a distinct species far from *Ps. cucullatus*. Hence, we prefer to treat *M. flava* and *Ps. cucullatus* as two different species.

Echinochaete is a genus described by Reid (1963) based on the type species *E. megalopora* (Mont.) Reid (= *E. brachypora* (Mont.) Ryvarden). This genus is characterized by basidiomata with a laterally short stipe-like base, pileus velutinate especially near the attachment, angular to hexagonal pores, dimitic hyphal system with clamped generative hyphae and dextrinoid arboriform skeleto-binding hyphae, spinulose setoid elements on pileal surface and hymenium, cylindrical basidiospores, tropical to subtropical distribution and white rotting habit (Ryvarden & Johansen 1980, Núñez & Ryvarden 1995a, 2001). Phylogenetic analyses proved that *Echinochaete* spp. always cluster with species of *Datronia*, *Mycobonia*, *Polyporus* and *Pseudofavolus* (Krüger 2002, Sotome et al. 2008, Krüger & Gargas 2010, Binder et al. 2013). Morphologically, *Echinochaete* is similar to *Polyporus* with laterally stipitate basidiomata becoming brittle upon drying, similar hyphal characters and cylindrical basidiospores. Both Corner (1984) and Singer (1986) previously treated *Echinochaete* as a synonym of *Polyporus*.

In this study, species in squamosus clade reveals to have a common ancestor and rapidly diversified into different forms of basidiomata with poroid or hydroid hymeniums during Paleogene. Recently, Zmitrovich & Kovalenko (2016) and Zmitrovich (2018) transferred species of *Datronia*, *Datroniella* and *Mycobonia* in squamosus clade into *Cerioporus*, a genus established by Quélet based on the type species *C. squamosus* (Huds.) Quél. They characterized this genus by polyporoid to trametoid hymenium, dimitic hyphal system with inflated axial skeletal and arboriform branching, fusoid basidiospores with navicular or humpbacked tendency (Zmitrovich & Kovalenko 2016). Though the evolutionary time supports the squamosus clade as an individual genus, Zhao et al. (2016, 2017) declared that divergence times should be not used on polyphyletic groups. Moreover, species in this clade are morphologically different from each other. So, in this study, we suggest retaining the genera *Datronia*, *Datroniella*, *Echinochaete*, *Mycobonia* and *Neodatronia* and keeping *Polyporus* species in the squamosus clade in genus *Polyporus* until more evidences are found.

Acknowledgements

This work was financed by the National Natural Science Foundation of China (Nos. U2003211, 31870008), the Scientific and Technological Tackling Plan for the Key Fields of Xinjiang Production and Construction Corps (No. 2021AB004), and Beijing Forestry University Outstanding Young Talent Cultivation Project (No. 2019JQ03016). The authors are very grateful to Dr. Wen-Min Qin (Institute of Applied Ecology, Chinese Academy of Sciences, China) for loan of specimens. Prof. Yu-Cheng Dai (Beijing Forestry University, China), Prof. Hai-Sheng Yuan (Institute of Applied Ecology, Chinese Academy of Sciences, China) are gratefully acknowledged for help in field collections and providing specimens and pictures.

References

- Adanson M. 1763 – Familles des plantes. Vol. 2. Fungi Sect. V. Chez Vincent, Paris.
- Avisé JC, John GC. 1999 – Proposal for a standardized temporal scheme of biological classification for extant species. Proceedings of the National Academy of Sciences of the United States of America 96, 7358–7363. Doi 10.2307/48063
- Bell CD, Soltis DE, Soltis PS. 2010 – The age and diversification of the angiosperms re-revisited. American Journal of Botany 97(8), 1296–1303. Doi 10.3732/ajb.0900346
- Berbee ML, Taylor JW. 2010 – Dating the molecular clock in fungi – how close are we? Fungal Biology Reviews 24, 1–16. Doi 10.1016/j.fbr.2010.03.001
- Binder M, Hibbett DS, Larsson KH, Larsson E et al. 2005 – The phylogenetic distribution of resupinate forms across the major clades of mushroom-forming fungi (Homobasidiomycetes). Systematics and Biodiversity 3(2), 113–157. Doi 10.1017/S1477200005001623
- Binder M, Justo A, Riley R, Salamov A et al. 2013 – Phylogenetic and phylogenomic overview of the Polyporales. Mycologia 105(6), 1350–1373. Doi 10.3852/13-003
- Binder M, Larsson KH, Matheny PB, Hibbett DS. 2010 – Amylocorticiales ord. nov. and Jaapiales ord. nov.: Early diverging clades of Agaricomycetidae dominated by corticioid forms. Mycologia 102(4), 865–880. Doi 10.3852/09-288
- Brenner GJ. 1974 – Palynostratigraphy of the Lower Cretaceous Gevar'am and Talme Yafe Formations in the Gevar'am 2 well (Southern coastal plain Israel). Geological Survey 59, 1–27.
- Buchanan PK, Ryvarden L. 1998 – New Zealand polypore fungi (Aphylophorales): three new species and a new record. New Zealand Journal of Botany 36, 219–231. Doi 10.1080/0028825X.1998.9512563
- Cai Q, Tulloss RE, Tang LP, Tolgor B et al. 2014 – Multi-locus phylogeny of lethal amanitas: implications for species diversity and historical biogeography. BMC Evolutionary Biology 14, 143. Doi 10.1186/1471-2148-14-143

- Chen JJ, Cui BK, Zhou LW, Korhonen K, Dai YC. 2015 – Phylogeny, divergence time estimation, and biogeography of the genus *Heterobasidion* (Basidiomycota, Russulales). *Fungal Diversity* 71(1), 185–200. Doi 10.1007/s13225-014-0317-2
- Clements FE, Shear CL. 1931 – The genera of fungi. The H.W. Wilson Company, New York.
- Corner EJH. 1984 – Ad Polyporaceas II & III. Beihefte zur Nova Hedwigia, Heft 78, 1–222.
- Crane PR, Friis EM, Pedersen KR. 1995 – The origin and early diversification of angiosperms. *Nature* 374, 27–33.
- Cui BK, Li HJ, Ji X, Zhou JL et al. 2019 – Species diversity, taxonomy and phylogeny of Polyporaceae (Basidiomycota) in China. *Fungal Diversity* 97, 137–392. Doi 10.1007/s13225-019-00427-4
- Cunningham GH. 1948 – New Zealand Polyporaceae 3. The genus *Polyporus*. New Zealand Department of Scientific and Industrial Research, Bulletin 74, 1–39.
- Cunningham GH. 1965 – Polyporaceae of New Zealand. New Zealand Department of Scientific and Industrial Research, Bulletin 164, 1–304.
- Dai YC. 1996 – Changbai wood-rotting fungi 5. Study on *Polyporus mongolicus* and *P. tubaeformis*. *Annales Botanici Fennici* 33, 153–163.
- Dai YC. 1999 – Changbai wood-rotting fungi 11. Species of *Polyporus* sensu stricto. *Fungal Science* 14, 67–77.
- Dai YC. 2012 – Polypore diversity in China with an annotated checklist of Chinese polypores. *Mycoscience* 53, 49–80. Doi 10.1007/s10267-011-0134-3
- Dai YC, Härkönen M, Niemelä T. 2003 – Wood-inhabiting fungi in southern China 1. Polypores from Hunan Province. *Annales Botanici Fennici* 40, 381–393.
- Dai YC, Xue HJ, Vlasák J, Rajchenberg M et al. 2014 – Phylogeny and global diversity of *Polyporus* group *Melanopus* (Polyporales, Basidiomycota). *Fungal Diversity* 64, 133–144. Doi 10.1007/s13225-013-0248-3
- Dai YC, Yu CJ, Wang HC. 2007 – Polypores from eastern Xizang (Tibet), western China. *Annales Botanici Fennici* 44, 135–145.
- Dai YC, Yuan HS, Wang HC, Yang F, Wei YL. 2009 – Polypores (Basidiomycota) from Qin Mts. in Shaanxi Province, Central China. *Annales Botanici Fennici* 46, 54–61. Doi 10.5735/085.046.0105
- Darriba D, Taboada GL, Doallo R, Posada D. 2012 – jModelTest 2: more models, new heuristics and parallel computing. *Nature Methods* 9, 772. Doi 10.1038/nmeth.2109
- De AB. 1996 – *Royoporus*—a new genus for *Favolus spathulatus*. *Mycotaxon* 60, 143–148.
- De AB. 1998 – Taxonomy of *Royoporus pseudobetulinus* comb. nov. *Mycotaxon* 69, 137–143.
- Donk MA. 1933 – Revision der Niederländischen Homobasidiomycetes. *Aphyllphoraceae* II. Mededelingen van het Botanisch Museum en Herbarium van de Rijksuniversiteit te Utrecht 9, 1–278.
- Donk MA. 1957 – The generic names proposed for Hymenomycetes VII. “Thelephoraceae” (continuation). *Taxon* 6, 68–85. Doi 10.2307/1217166
- Donk MA. 1966 – Notes on European polypores 1. *Persoonia* 4, 337–343.
- Doyle JA. 2012 – Molecular and fossil evidence on the origin of angiosperms. *Annual Review of Earth and Planetary Sciences* 40, 301–326. Doi 10.1146/annurev-earth-042711-105313
- Drechsler-Santos ER, Ryvarden L, Wartchow F, Cavalcanti MAQ. 2008 – *Polyporus elongoporus* (Aphyllphorales, Poriaceae) sp. nov. *Synopsis Fungorum* 25, 38–43.
- Drummond AJ, Ho SYW, Phillips MJ, Rambaut A. 2006 – Relaxed phylogenetics and dating with confidence. *PLoS Biology* 4(5), e88. Doi: 10.1371/journal.pbio.0040088.
- Drummond AJ, Suchard MA, Xie D, Rambaut A. 2012 – Bayesian phylogenetics with BEAUti and the BEAST 1.7. *Molecular Biology and Evolution* 29, 1969–1973. Doi 10.1093/molbev/mss075
- Eastwood DC, Floudas D, Binder M, Majcherzyk A et al. 2011 – The plant cell wall-decomposing machinery underlies the functional diversity of forest fungi. *Science* 333, 762–765. Doi 10.1126/science.1205411

- Feng B, Xue JP, Wu G, Zeng NK et al. 2012 – DNA sequence analyses reveal abundant diversity, endemism and evidence for Asian origin of the porcini mushrooms. *PLoS ONE* 7(5), e37567. Doi 10.1371/journal.pone.0037567
- Fries EM. 1821 – *Systema Mycologicum*. Vol. 1. Ex Officina Berlingiana, Germany.
- Garcia-Sandoval R, Wang Z, Binder M, Hibbett DS. 2011 – Molecular phylogenetics of the Gloeophyllales and relative ages of clades of Agaricomycotina producing a brown rot. *Mycologia* 103(3), 510–524. Doi 10.3852/10-209
- Gernandt DS, Magallón S, López GG, Flores ZO et al. 2008 – Use of simultaneous analyses to guide fossil-based calibrations of Pinaceae phylogeny. *International Journal of Plant Sciences* 169(8), 1086–1099. Doi 10.1086/590472
- Gernhard T. 2008 – The conditioned reconstructed process. *Journal of Theoretical Biology* 253, 769–778.
- Ghobad-Nejhad M, Dai YC. 2010 – *Diplomitoporus rimosus* is found in Asia and belongs to the Hymenochaetales. *Mycologia* 102, 1510–1517. Doi 10.3852/10-025
- Gilbertson RL, Ryvarde L. 1987 – North American polypores. Vol. 2. Fungiflora, Oslo.
- Glass NL, Donaldson GC. 1995 – Development of primer sets designed for use with the PCR to amplify conserved genes from filamentous ascomycetes. *Applied and Environmental Microbiology* 61(4), 1323–1330.
- Gomes-Silva AC, Ryvarde L, Medeiros PS, Sotão HMP, Gibertoni TB. 2012 – *Polyporus* in the Brazilian Amazonia, with notes on *Polyporus indigenus* I.J. Araujo & M.A. de Sousa and *P. sapurema* A. Møller. *Nova Hedwigia* 94(1–2), 227–238. Doi 10.1127/0029-5035/2012/0094-0227
- Grand EA, Hughes KW, Petersen RH. 2011 – Relationships within *Lentinus* subg. *Lentinus* (Polyporales, Agaricomycetes), with emphasis on sects. *Lentinus* and *Tigrini*. *Mycological Progress* 10, 399–413. Doi 10.1007/s11557-010-0711-4
- Greuter W, McNeill J, Barrie FR, Burdet HM et al. 2000 – International Code of Botanical Nomenclature (Saint Louis Code). Sixteenth International Botanical Congress. Regnum Vegetabile, St Louis.
- Grimaldi D. 1999 – The co-radiations of pollinating insects and angiosperms in the Cretaceous. *Annals of the Missouri Botanical Garden* 86(2), 373–406. Doi 10.2307/2666181
- Gübeli AA, Hochuli PA, Wildi W. 1984 – Lower Cretaceous turbiditic sediments from the Rif chain (Northern Morocco) – palynology, stratigraphy and palaeogeographic setting. *Geologische Rundschau* 73(3), 1081–1114. Doi 10.1007/bf01820889
- Hall TA. 1999 – BioEdit: a user-friendly biological sequence alignment and analysis program for Windows 95/98/NT. *Nucleic Acids Symposium Series* 41, 95–98.
- Hattori T. 2000 – Type studies of the polypores described by E.J.H. Corner from Asia and west Pacific I. Species described in *Polyporus*, *Buglossoporus*, *Melipilus*, *Daedalea*, and *Flabellophora*. *Mycoscience* 41, 339–349.
- Hennig W. 1966 – *Phylogenetic systematics*. University of Illinois Press, Urbana.
- Hibbett DS. 1996 – Phylogenetic evidence for horizontal transmission of group I introns in the nuclear ribosomal DNA of mushroom-forming fungi. *Molecular Biology and Evolution* 13(7), 903–917. Doi 10.1093/oxfordjournals.molbev.a025658
- Hibbett DS, Donoghue MJ. 1995 – Progress toward a phylogenetic classification of the Polyporaceae through parsimony analysis of mitochondrial ribosomal DNA sequences. *Canadian Journal of Botany* 73(Suppl 1), S853–S861. Doi 10.1139/b95-331
- Hibbett DS, Donoghue MJ. 2001 – Analysis of character correlations among wood decay mechanisms, mating systems, and substrate ranges in homobasidiomycetes. *Systematic Biology* 50(2), 215–242. Doi 10.1080/10635150121079
- Hibbett DS, Grimaldi D, Donoghue MJ. 1997 – Fossil mushrooms from Miocene and Cretaceous ambers and the evolution of Homobasidiomycetes. *American Journal of Botany* 84(7), 981–991. Doi 10.2307/2446289

- Hibbett DS, Matheny PB. 2009 – The relative ages of ectomycorrhizal mushrooms and their plant hosts estimated using Bayesian relaxed molecular clock analyses. *BMC Biology* 7, 13. 13–0. Doi 10.1186/1741-7007-7-13
- Hibbett DS, Murakami S, Tsuneda A. 1993 – Hymenophore development and evolution in *Lentinus*. *Mycologia* 85(3), 428–443. Doi 10.2307/3760704
- Hibbett DS, Thorn RG. 1994 – Nematode-trapping in *Pleurotus tuberregium*. *Mycologia* 86, 696–699.
- Hibbett DS, Vilgalys R. 1993 – Phylogenetic relationships of *Lentinus* (Basidiomycotina) inferred from molecular and morphological characters. *Systematic Botany* 18(3), 409–433. Doi 10.2307/2419417
- Hughes N, McDougall A. 1987 – Records of angiospermid pollen entry into the English Early Cretaceous succession. *Review of Palaeobotany and Palynology* 50, 255–272. Doi 10.1016/0034-6667(87)90003-0
- Hyde KD, Hongsanan S, Jeewon R, Bhat DJ et al. 2016 – Fungal diversity notes 367–490: taxonomic and phylogenetic contributions to fungal taxa. *Fungal Diversity* 80, 1–270. Doi 10.1007/s13225-016-0373-x
- Justo A, Hibbett DS. 2011 – Phylogenetic classification of *Trametes* (Polyporales, Basidiomycota) based on a five-marker dataset. *Taxon* 60(6), 1567–1583. Doi 10.1002/tax.606003
- Justo A, Miettinen O, Floudas D, Ortiz-Santana B et al. 2017 – A revised family-level classification of the Polyporales (Basidiomycota). *Fungal Biology* 121, 798–824. Doi 10.1016/j.funbio.2017.05.010
- Jülich W. 1976 – Studies in hydroid fungi-I. On some genera with hyphal pegs. *Persoonia* 8(4), 447–458.
- Knudsen H, Vesterholt J. 2012 – Funga Nordica. Vol. 1. In: Knudsen H, ed. Agaricoid, boletoid, clavarioid, cyphelloid and gasteroid genera. Nordsvamp, Copenhagen.
- Ko KS, Jung HS. 2002 – Phylogenetic evaluation of *Polyporus* s. str. based on molecular sequences. *Mycotaxon* 82, 315–322.
- Kohler A, Kuo A, Nagy LG, Morin E et al. 2015 – Convergent losses of decay mechanisms and rapid turnover of symbiosis genes in mycorrhizal mutualists. *Nature genetics*, 47(4), 410–415. Doi 10.1038/ng.3223
- Krüger D. 2002 – Monographic studies in the genus *Polyporus* (Basidiomycotina) (doctoral dissertation). University of Tennessee, Knoxville, USA.
- Krüger D, Gargas A. 2004 – The basidiomycete genus *Polyporus* – an emendation based on phylogeny and putative secondary structure of ribosomal RNA molecules. *Feddes Repertorium* 115, 530–546.
- Krüger D, Gargas A. 2010 – Unusual polypore fungi – a taxonomic emendation of *Polyporus* (Basidiomycotina) after ribosomal spacer characters. *Cryptogamie Mycologie* 31(4), 389–401.
- Krüger D, Petersen RH, Hughes KW. 2006 – Molecular phylogenies and mating study data in *Polyporus* with special emphasis on group “*Melanopus*” (Basidiomycota). *Mycological Progress* 5, 185–206. Doi 10.1007/s11557-006-0512-y
- Lepage T, Bryant D, Philippe H, Lartillot NA. 2007 – A general comparison of relaxed molecular clock models. *Molecular Biology and Evolution* 24(12), 2669–2680. Doi 10.1093/molbev/msm193
- Li HJ, Cui BK, Dai YC. 2014 – Taxonomy and multi-gene phylogeny of *Datronia* (Polyporales, Basidiomycota). *Persoonia* 32, 170–182. Doi 10.3767/003158514x681828
- Lidgard S, Crane PR. 1988 – Quantitative analyses of the early angiosperm radiation. *Nature* 331, 344–346. 346. Doi 10.1038/331344a0
- Linnaeus C. 1753 – *Species Plantarum*. Laurentius Salvius, Sweden.
- Liu YJ, Whelen S, Hall BD. 1999 – Phylogenetic Relationships Among Ascomycetes: Evidence from an RNA Polymerase II Subunit. *Molecular Biology and Evolution* 16(12), 1799–1808. Doi 10.1093/oxfordjournals.molbev.a026092

- Magallón S. 2010 – Using fossils to break long branches in molecular dating: a comparison of relaxed clocks applied to the origin of angiosperms. *Systematic Biology* 59(4), 384–399. Doi 10.1093/sysbio/syq027
- Magallón S, Hilu KW, Quandt D. 2013 – Land plant evolutionary timeline: gene effects are secondary to fossil constraints in relaxed clock estimation of age and substitution rates. *American Journal of Botany* 100(3), 556–573. Doi 10.3732/ajb.1200416
- Matheny PB. 2005 – Improving phylogenetic inference of mushrooms with RPB1 and RPB2 nucleotide sequences (*Inocybe*; Agaricales). *Molecular Phylogenetics and Evolution* 35, 1–20. Doi 10.1016/j.ympev.2004.11.014
- Matheny PB, Liu YJ, Ammirati JF, Hall BD. 2002 – Using RPB1 sequences to improve phylogenetic inference among mushrooms (*Inocybe*, Agaricales). *American Journal of Botany* 89(4), 688–698. Doi 10.3732/ajb.89.4.688
- Michalak S. 2012 – raxmlGUI: a graphical front-end for RAxML. *Organisms Diversity & Evolution* 12, 335–337. Doi 10.1007/s13127-011-0056-0
- Micheli PA. 1729 – *Nova plantarum genera, iuxta Tournefortii methodum disposita*. Superiorum Permissu, Florence, Italy.
- Moore MJ, Bell CD, Soltis PS, Soltis DE. 2007 – Using plastid genome-scale data to resolve enigmatic relationships among basal angiosperms. *Proceedings of the National Academy of Sciences* 104(49), 19363–19368. Doi 10.1073/pnas.0708072104
- Murrill WA. 1903 – A historical review of the genera of the Polyporaceae. *The Journal of Mycology* 9(2), 87–102.
- Murrill WA. 1904 – The Polyporaceae of North America VI. The genus *Polyporus*. *Bulletin of the Torrey Botanical Club* 31(1), 29–44.
- Niemelä T, Kotiranta H. 1991 – Polypore survey of Finland 5. The genus *Polyporus*. *Karstenia* 31(2), 55–68.
- Norros V, Karhu E, Norden J, Vähätalo AV, Ovaskainen O. 2015 – Spore sensitivity to sunlight and freezing can restrict dispersal in wood-decay fungi. *Ecology and Evolution* 5(16), 3312–3326. Doi 10.1002/ece3.1589
- Núñez M, Ryvarde L. 1995a – *Polyporus* (Basidiomycotina) and related genera. *Fungiflora*, Oslo.
- Núñez M, Ryvarde L. 1995b – Polypores new to Japan 1. Species of *Polyporus*, with a note on *P. hartmanni*. *Mycoscience* 36, 61–65. Doi 10.1007/bf02268574
- Núñez M, Ryvarde L. 2001 – East Asian polypores 2. Polyporaceae s. lato. *Synopsis Fungorum* 14, 165–522.
- Nylander J. 2004 – MrModeltest v2. Program distributed by the author. Evolutionary Biology Centre, Uppsala University, Uppsala.
- Palacio M, Robledo GL, Reck MA, Grassi E et al. 2017 – Decrypting the *Polyporus dictyopus* complex: recovery of *Atroporus* Ryvarde and segregation of *Neodictyopus* gen. nov. (Polyporales, Basidiomycota). *PloS ONE*, 12(10), e0186183. Doi 10.1371/journal.pone.0186183
- Patouillard N. 1887 – *Les Hyménomycètes d'Europe anatomie générale et classification des champignons supérieurs*. Paul Klincksieck, Paris, France.
- Pegler DN. 1983 – *The Genus Lentinus: A World Monograph*. Kew Bulletin Additional Series 10. Her Majesty's Stationary Office, London.
- Petersen JH. 1996 – Farvekort. The Danish Mycological Society's colour-chart. Foreningen til Svampekundskabens Fremme, Greve, Denmark.
- Popoff OF, Wright JE. 1998 – Fungi of Paraguay. 1. Preliminary checklist of wood-inhabiting polypores (Aphyllorphorales, Basidiomycota). *Mycotaxon* 67, 323–340.
- Prieto M, Wedin M. 2017 – Phylogeny, taxonomy and diversification events in the Caliciaceae. *Fungal Diversity* 82(1), 221–238. Doi 10.1007/s13225-016-0372-y
- Pulgarín MP. 2016 – *Estudos taxonômicos e filogenéticos do complexo Polyporus dictyopus mont.* (Polyporaceae, Basidiomycota) (doctoral dissertation). Universidade Federal de Santa Catarina, Florianópolis, Brazil.

- Rehner SA, Buckley E. 2005 – A *Beauveria* phylogeny inferred from nuclear ITS and EF1- α sequences: evidence for cryptic diversification and links to *Cordyceps* teleomorphs. *Mycologia* 97(1), 84–98. Doi 10.3852/mycologia.97.1.84
- Reid DA. 1963 – New or interesting records of Australian Basidiomycetes. V. *Kew Bulletin* 17, 267–308
- Ronquist F, Teslenko M, van der Mark P, Ayres DL et al. 2012 – MrBayes 3.2 efficient Bayesian phylogenetic inference and model choice across a large model space. *Systematic Biology* 61(3), 539–542. Doi 10.1093/sysbio/sys029
- Runnel K, Ryvarden L. 2016 – *Polyporus minutosquamosus* sp. nov. from tropical rainforests in French Guiana with a key to neotropical species of *Polyporus* (Polyporaceae, Basidiomycota). *Nova Hedwigia* 103, 339–347. Doi 10.1127/nova_hedwigia/2016/0354
- Ryvarden L. 1991 – Genera of polypores. Nomenclature and taxonomy. *Fungiflora*, Oslo.
- Ryvarden L, Gilbertson RL. 1994 – European polypores—part 2, Synopsis Fungorum 7. *Fungiflora*, Oslo.
- Ryvarden L, Iturriaga T. 2003 – Studies in neotropical polypores 10. New polypores from Venezuela. *Mycologia* 95(6), 1066–1077. Doi 10.2307/3761913
- Ryvarden L, Johansen I. 1980 – A preliminary polypore flora of East Africa. *Fungiflora*, Oslo.
- Sánchez-Ramírez S, Tulloss RE, Amalfi M, Moncalvo JM. 2014 – Palaeotropical origins, boreotropical distribution and increased rates of diversification in a clade of edible ectomycorrhizal mushrooms (*Amanita* section *Caesareae*). *Journal of Biogeography* 42(2), 351–363. Doi 10.1111/jbi.12402
- Schigel DS, Toresson HG. 2005 – New records of *Polyporus pseudobetulinus*, a rare polypore fungus (Basidiomycota, Aphyllophorales) in Scandinavia, and notes on associated beetles. *Memoranda Societatis pro Fauna et Flora Fennica* 81, 102–107.
- Schwarze FW, Engels J, Mattheck C. 2000 – Fungal strategies of wood decay in trees. Springer-Verlag, Berlin.
- Seelan JS, Justo A, Nagy LG, Grand EA et al. 2015 – Phylogenetic relationships and morphological evolution in *Lentinus*, *Polyporellus* and *Neofavolus*, emphasizing southeastern Asian taxa. *Mycologia* 107(3), 460–474. Doi 10.3852/14-084
- Si J, Dai YC. 2016 – Wood-decaying fungi in eastern Himalayas 5. Polypore diversity. *Mycosystema* 35(3), 252–278. Doi 10.13346/j.mycosystema.140255
- Sievers F, Wilm A, Dineen D, Gibson TJ et al. 2011 – Fast, scalable generation of high-quality protein multiple sequence alignments using Clustal Omega. *Molecular Systems Biology* 7, 539. Doi 10.1038/msb.2011.75
- Singer R. 1986 – The Agaricales in modern taxonomy, 4th ed. Koeltz Scientific Book, Koenigstein.
- Smith SA, Beaulieu JM, Donoghue MJ. 2010 – An uncorrelated relaxed-clock analysis suggests an earlier origin for flowering plants. *Proceedings of the National Academy of Sciences of the United States of America* 107(13), 5897–5902. Doi 10.1073/pnas.1001225107
- Smith SY, Currah RS, Stockey RA. 2004 – Cretaceous and Eocene poroid hymenophores from Vancouver Island, British Columbia. *Mycologia* 96(1), 180–186. Doi 10.2307/3762001
- Song J, Chen JJ, Wang M, Chen YY, Cui BK. 2016 – Phylogeny and biogeography of the remarkable genus *Bondarzewia* (Basidiomycota, Russulales). *Scientific Reports* 6, 34568. Doi 10.1038/srep34568
- Song J, Cui BK. 2017 – Phylogeny, divergence time and historical biogeography of *Laetiporus* (Basidiomycota, Polyporales). *BMC Evolutionary Biology* 17, 102. Doi 10.1186/s12862-017-0948-5
- Sotome K, Akagi Y, Lee SS, Ishikawa NK, Hattori T. 2013 – Taxonomic study of *Favolus* and *Neofavolus* gen. nov. segregated from *Polyporus* (Basidiomycota, Polyporales). *Fungal Diversity* 58, 245–266. Doi 10.1007/s13225-012-0213-6
- Sotome K, Hattori T, Kakishima M. 2007 – *Polyporus phyllostachydis* sp. nov. with notes on other rhizophilic species of *Polyporus*. *Mycoscience* 48, 42–46. Doi 10.1007/s10267-006-0328-2

- Sotome K, Hattori T, Ota Y. 2011 – Taxonomic study on a threatened polypore, *Polyporus pseudobetulinus*, and a morphologically similar species, *P. subvarius*. *Mycoscience* 52, 319–326. Doi 10.1007/s10267-011-0111-x
- Sotome K, Hattori T, Ota Y, Kakishima M. 2009 – Second report of *Polyporus longiporus* and its phylogenetic position. *Mycoscience* 50, 415–420. Doi 10.1007/s10267-009-0506-0
- Sotome K, Hattori T, Ota Y, To-anun C et al. 2008 – Phylogenetic relationships of *Polyporus* and morphologically allied genera. *Mycologia* 100(4), 603–615. Doi 10.3852/07-191R
- Sotome K, Matozaki T, Aimi T, Boonlue S. 2016 – *Polyporus thailandensis*, a new species of group Polyporellus in *Polyporus* (Polyporales, Agaricomycota) from Northeastern Thailand. *Mycoscience* 57(2), 85–89. Doi 10.1016/j.myc.2015.07.006
- Swofford DL. 2002 – PAUP*: phylogenetic analysis using parsimony (*and other methods). Version 4.0b10. Sinauer Associates, Sunderland.
- Thorn RG. 2000 – Some polypores misclassified in *Piptoporus*. *Karstenia* 40, 181–187.
- Thorn G, Kotiranta H, Niemelä T. 1990 – *Polyporus pseudobetulinus* comb. nov.: new records in Europe and North America. *Mycologia* 82, 582–594.
- Thusu B, Van Der Eem JGLA, El-Mehdawi A, Bu-Argoub F. 1988 – Jurassic–Early Cretaceous palynostratigraphy in northeast Libya. In El-Arnauti A, Owens B, Thusu B (eds.) *Subsurface Palynostratigraphy of northeast Libya*. Garyounis University Publications, Libya.
- Tibpromma S, Hyde KD, Jeewon R, Maharachchikumbura SSN et al. 2017 – Fungal diversity notes 491–602: taxonomic and phylogenetic contributions to fungal taxa. *Fungal Diversity* 83, 1–261. Doi 10.1007/s13225-017-0378-0
- Vilgalys R, Hester M. 1990 – Rapid genetic identification and mapping of enzymatically amplified ribosomal DNA from several species of *Cryptococcus*. *Journal of Bacteriology* 172, 4238–4246.
- Wang HC, Moore MJ, Soltis PS, Bell CD et al. 2009 – Rosid radiation and the rapid rise of angiosperm-dominated forests. *Proceedings of the National Academy of Sciences of the United States of America* 106(10), 3853–3858. Doi 10.1073/pnas.0813376106
- White TJ, Bruns TD, Lee S, Taylor JW. 1990 – Amplification and direct sequencing of fungal ribosomal RNA genes for phylogenetics. In: Innis MA, Gelfand DH, Sninsky J, White TJ (eds) *PCR protocols: a guide to methods and applications*. Academic, New York.
- Wikström N, Savolainen V, Chase MW. 2001 – Evolution of the angiosperms: calibrating the family tree. *Proceedings of the Royal Society of London B: Biological Sciences* 268(1482), 2211–2220. Doi 10.1098/rspb.2001.1782
- Xing JH, Zhou JL, Cui BK. 2020 – Two new species of *Neofavolus* (Polyporales, Basidiomycota) based on morphological characters and molecular evidence. *Mycological Progress* 19, 471–480. Doi 10.1007/s11557-020-01574-8
- Xue HJ, Zhou LW. 2012 – *Polyporus submelanopus* sp. nov. (Polyporales, Basidiomycota) from Northwest China. *Mycotaxon* 122, 433–441. Doi 10.5248/122.433
- Xue HJ, Zhou LW. 2014 – *Polyporus hapalopus* sp. nov. (Polyporales, Basidiomycota) from China based on morphological and molecular data. *Mycological Progress* 13, 811–817. Doi 10.1007/s11557-014-0964-4
- Zeng LP, Zhang Q, Sun RR, Kong HZ et al. 2014 – Resolution of deep angiosperm phylogeny using conserved nuclear genes and estimates of early divergence times. *Nature communications* 5, 4956. Doi 10.1038/ncomms5956
- Zhang N, Zeng L, Shan H, Ma H. 2012 – Highly conserved low-copy nuclear genes as effective markers for phylogenetic analyses in angiosperms. *New Phytologist* 195(4), 923–937. Doi 10.1111/j.1469-8137.2012.04212.x
- Zhao RL, Li GJ, Sánchez-Ramírez S, Stata M et al. 2017 – A six-gene phylogenetic overview of Basidiomycota and allied phyla with estimated divergence times of higher taxa and a phyloproteomics perspective. *Fungal Diversity* 84(1), 43–74. Doi 10.1007/s13225-017-0381-5

- Zhao RL, Zhou JL, Chen J, Margaritescu S et al. 2016 – Towards standardizing taxonomic ranks using divergence times – a case study for reconstruction of the *Agaricus* taxonomic system. *Fungal Diversity* 78(1), 239–292. Doi 10.1007/s13225-016-0357-x
- Zheng HD, Liu PG. 2005 – Type studies on *Albatrellus henanensis* and *A. jianfenglingensis*. *Mycotaxon* 95, 257–263.
- Zhou JL, Chen H, Cui BK. 2016b – *Podoserpula ailaoshanensis* sp. nov. (Amylocorticiales, Basidiomycota) from China based on morphological and sequence analyses. *Mycoscience* 57, 295–301. Doi 10.1016/j.myc.2016.04.003
- Zhou JL, Cui BK. 2017 – Phylogeny and taxonomy of *Favolus* (Basidiomycota). *Mycologia* 109(5), 766–779. Doi 10.1080/00275514.2017.1409023
- Zhou JL, Zhu L, Chen H, Cui BK. 2016a – Taxonomy and phylogeny of *Polyporus* group *Melanopus* (Polyporales, Basidiomycota) from China. *PLoS ONE* 11(8), e0159495. Doi 10.1371/journal.pone.0159495
- Zhu L, Song J, Zhou JL, Si J, Cui BK. 2019 – Species diversity, phylogeny, divergence time and biogeography of the genus *Sanghuangporus* (Basidiomycota). *Frontiers in Microbiology* 10, 812. Doi 10.3389/fmicb.2019.00812
- Zmitrovich IV. 2010 – The Taxonomical and nomenclatural characteristics of medicinal mushrooms in some genera of Polyporaceae. *International Journal of Medicinal Mushrooms* 12(1), 87–89.
- Zmitrovich IV. 2018 – Conspectus systematis Polyporacearum v. 1.0. *Folia Cryptogamica Petropolitana* 6, 1–145.
- Zmitrovich IV, Kovalenko AE. 2016 – Lentinoid and polyporoid fungi, two generic conglomerates containing important medicinal mushrooms in molecular perspective. *International Journal of Medicinal Mushrooms* 18, 23–38. Doi 10.1615/intjmedmushrooms.v18.i1.40
- Zmitrovich IV, Volobuev SV, Parmasto IH, Bondartseva MA. 2017 – Re-habilitation of *Cerioporus (Polyporus) rangiferinus*, a sib of *Cerioporus squamosus*. *Nova Hedwigia* 105(3–4), 313–328. Doi 10.1127/nova_hedwigia/2017/0412